

Ministère de l'Enseignement Supérieur et de la Recherche Scientifique

Université Hassiba Benbouali de Chlef



Faculté des Sciences Exactes & Informatiques

Département de Physique



## THÈSE

Présentée pour l'obtention du diplôme de

**DOCTORAT 3<sup>ème</sup> Cycle**

Filière : **PHYSIQUE**

Option : Physique des Matériaux

Par :

**BOUZIDI Fatima**

THÈME:

# Study of Molecules Adsorption onto Solid Surface

Soutenue le 08/01/2024 à 10h devant le jury composé de :

M. Habib RACHED	Professeur (UHB Chlef)	Président
M. Ahmed BOUHEKKA	Professeur (Université de Tissemsilt)	Directeur de thèse
M. Abderrezak BERBRI	Maitre de Conférences -A (UHB Chlef)	Co-directeur de thèse
M. Abdelkader NEBBATI	Maitre de Conférences -A Université d'Ain Témouchent – UBBAT	Examineur
ECH-CHERGUI		
M. Rachid TRAICHE	Maitre de Conférences -A (UHB Chlef)	Examineur
M. Oussama ZEGGAI	Maitre de Conférences -A (UHB Chlef)	Examineur

Année universitaire 2023-2024

## **Abstract**

The adsorption of water on rutile TiO<sub>2</sub> (110) surface controls many chemical processes encountered in nature and industry. The key features of liquid-solid interfaces are the high mobility and often reactivity of the H<sub>2</sub>O molecules and the structural control provided by the solid species.

There are several theoretical and experimental techniques of interest to elucidate the dynamics of water on surfaces. However, in this dissertation, we apply mathematical modelling methods to study these interactions: First, we investigated the behaviour of H<sub>2</sub>O molecules attached on the surface in case of stopping the incoming H<sub>2</sub>O flux before equilibrium, and we show how H<sub>2</sub>O behave under various temperature values and the initial coverage of H<sub>2</sub>O affected. Another point was to study the impact of oxygen vacancies and the amount of H<sub>2</sub>O flux in the dynamics of water on the rutile (110) surface, in the case of steady state, to control and enhance the production of OH. Our results clearly indicate that temperature, oxygen vacancies, the coverage of H<sub>2</sub>O adsorbed on surface and H<sub>2</sub>O flux have a marked effect on the dynamics of water, and it must be taken into account and controlled to achieve the desired applications.

Besides, we are comparing the simple H<sub>2</sub>O molecules behaviour and complex adsorption of bio-molecules like bovine serum albumin (BSA) proteins on TiO<sub>2</sub> surface, where the results demonstrated that the sticking of proteins on surface is accompanied by the expulsion of the adsorbed water and this overbalance to the hydrophobic core inside of the proteins particles which can affect its structure.

Controlling the production of OH is very important in technology applications such as self-cleaning, especially in the purification and decomposition of water besides the splitting of water as well as in biotechnology.

**Keywords:** Surface, Adsorption, Water-rutile TiO<sub>2</sub> (110) interface, Dissociation, Mathematical modeling, Proteins adsorption, OH hydroxyls and FTIR-ATR

## **Résumé**

L'adsorption d'eau sur la surface du rutile  $\text{TiO}_2$  (110) contrôle de nombreux processus chimiques rencontrés dans la nature et l'industrie. Les principales caractéristiques des interfaces liquide-solide sont la grande mobilité et souvent la réactivité des molécules  $\text{H}_2\text{O}$  et le contrôle structurel assuré par les espèces solides.

Il existe plusieurs techniques théoriques et expérimentales d'intérêt pour élucider la dynamique de l'eau sur les surfaces. Cependant, dans cette thèse, nous appliquons des méthodes de modélisation mathématique pour étudier ces interactions: Tout d'abord, nous avons étudié le comportement des molécules  $\text{H}_2\text{O}$  attachées à la surface en cas d'arrêt du flux de  $\text{H}_2\text{O}$  avant l'équilibre, et nous montrons comment  $\text{H}_2\text{O}$  se comporte sous différentes valeurs de température et la couverture initiale de  $\text{H}_2\text{O}$  affectée. Un autre point était d'étudier l'impact des lacunes d'oxygène et de la quantité de flux de  $\text{H}_2\text{O}$  dans la dynamique de l'eau sur la surface de rutile (110), dans le cas de régime stationnaire, pour contrôler et améliorer la production de (OH). Nos résultats indiquent clairement que la température, les lacunes d'oxygène, la couverture de  $\text{H}_2\text{O}$  adsorbée en surface et le flux de  $\text{H}_2\text{O}$  ont un effet marqué sur la dynamique de l'eau, et cela doit être pris en compte et contrôlé pour atteindre les applications souhaitées.

En outre, nous comparons le comportement de simples molécules  $\text{H}_2\text{O}$  et l'adsorption complexe de biomolécules telles que la protéine d'albumine sérique bovine (BSA) sur la surface de  $\text{TiO}_2$ , où les résultats ont démontré que le collage des protéines sur la surface s'accompagne de l'expulsion de l'eau adsorbée et ce déséquilibre du noyau hydrophobe en particule de protéines pouvant affecter sa structure.

Le contrôle de la production de (OH) est très important dans les applications technologiques telles que l'auto-nettoyage, en particulier dans la purification et la décomposition de l'eau en plus de la séparation de l'eau ainsi qu'en biotechnologie.

**Mots clés:** Surface, Adsorption, Eau-rutile  $\text{TiO}_2$  (110) interface, Dissociation, Modélisation mathématique, Adsorption de protéines, OH hydroxyles et FTIR-ATR.

## ملخص

يتحكم ادمصاص الماء على سطح ثاني أكسيد التيتانيوم الروتيل ( $\text{TiO}_2$ ) (110) في العديد من العمليات الكيميائية التي تتم مواجهتها في الطبيعة والصناعة. السمات الرئيسية للواجهات السائلة-الصلبة هي الحركة العالية والتفاعلية في كثير من الأحيان لجزيئات الماء ( $\text{H}_2\text{O}$ ) والتحكم الهيكلي الذي توفره المواد الصلبة.

هناك العديد من التقنيات النظرية والتجريبية ذات الأهمية لتوضيح ديناميكيات الماء على الأسطح. وعليه، في هذه الأطروحة، نطبق النمذجة الرياضية لدراسة هذه التفاعلات: أولاً، قمنا بفحص سلوك جزيئات  $\text{H}_2\text{O}$  الممتزة في حالة إيقاف تدفق  $\text{H}_2\text{O}$  الوارد على السطح قبل التوازن، ثم نوضح كيف يتصرف  $\text{H}_2\text{O}$  تحت قيم درجات الحرارة المختلفة وكذا تأثير التغطية الأولية لـ  $\text{H}_2\text{O}$ . النقطة الأخرى كانت دراسة تأثير شواغر الأكسجين وكمية تدفق  $\text{H}_2\text{O}$  في ديناميكيات الماء على سطح الروتيل (110)، في الحالة المستقرة، للتحكم ولتحسين في كمية إنتاج OH. تشير نتائجنا بوضوح إلى أن درجة الحرارة، شواغر الأكسجين، تغطية  $\text{H}_2\text{O}$  الممتزة على السطح وتدفق  $\text{H}_2\text{O}$  لها تأثير واضح على ديناميكيات الماء، حيث يجب أن تؤخذ بعين الاعتبار والتحكم فيها لتحقيق التطبيقات المرغوبة.

إلى جانب ذلك، نقوم بمقارنة سلوك جزيئات  $\text{H}_2\text{O}$  البسيطة والادمصاص المعقد للجزيئات الحيوية مثل بروتينات ألبومين المصل البقري (BSA) على سطح  $\text{TiO}_2$ ، حيث أظهرت النتائج أن التصاق البروتينات على السطح يترافق مع طرد الماء الممتز وهذا راجع إلى الأجزاء الكارهة للماء التي تكون داخل جزيئات البروتين والتي يمكن أن تؤثر على شكلها.

يعد التحكم في إنتاج OH أمراً مهماً للغاية في التطبيقات التكنولوجية مثل التنظيف الذاتي، خاصة في تنظيف وتقسيم الماء إلى جانب التكنولوجيا الحيوية.

**الكلمات المفتاحية:** السطح، الامتزاز، واجهة الماء – الروتيل ( $\text{TiO}_2$ ) (110)، التفكك، النمذجة الرياضية، امتزاز البروتينات، OH هيدروكسيل و FTIR-ATR

## Acknowledgements

First and foremost, praises and thanks to ALLAH the Almighty for the blessings throughout my life and being to complete this research with success.

While bringing out this thesis to its final form, many people have bestowed upon me their helps and supports in various ways, and they deserve special thanks, it is a pleasure to express my deep gratitude to all of them.

I would like to express my sincere thanks and deepest gratitude to my two supervisors, Prof. A. BOUHEKKA and Dr. A. BERBRI. I am deeply grateful to Prof. A. BOUHEKKA for the long insightful discussions and scientific advice about my research, I would thank him for his constant guidance, and for his patience and support helped me overcome many crisis situations and finish this work, besides he gave me the independence to explore my research, and at the same time guided me when I lost my way. I will never forget that you have reviewed my thesis several times till version X, you were always quietly listening to me and showing me the right direction which helped me in long time to come.

I am also thankful to Dr. A. BERBRI for encouraging the use of correct and consistent notation in my writings and for carefully reading and commenting on countless revisions. More importantly, I am deeply grateful for the understanding, support and encouragement during the whole periods of time. I feel very fortunate for this opportunity to work under two incredible mentors.

I am also thankful to the members of my committee for their time, for their valuable scientific critics and notes that surely will improve our thesis. I would like to thank Prof. H. RACHED from the physics department for giving me the honor of chairing the jury. I respectfully thank Dr. A. NEBBATI ECH-CHERGUI from university of Ain Témouchent who honored me to take part of the defense jury, is an honor for me and I thank him warmly. My sincere thanks go to Dr. R. TRAICHE and Dr. O. ZEGGAI for accepting to examine my work.

I am thankful to all my teachers for guiding and shaping me, especially Prof. M. BELABBAS and Prof. H. KHALFOUN. I have been fortunate to learn from many inspiring teachers over my school career. I also thank all the administration staff of our faculty and university for their help.

I am grateful to my group members each one in his own name for a number of discussions and all the fun times. It was a great experience to work with you all. Many friends have

helped me stay happy and sane through these difficult years. It is difficult to imagine these wonderful years without them. I greatly value their friendship and I deeply appreciate them being there for me.

Most importantly, none of this would have been possible without the love and patience of my parents, brother and sisters. They have been my constant source of love, strength, support and motivation all these years. My parents are my heroes and have sacrificed a lot to bring us up. I can't forget my aunt who welcomed me into her home all this time.

## **List of figures**

**Figure I.1:** The electronic bands structure of materials.

**Figure I.2:** The forbidden band diagram of the electronic structure of insulator, semiconductor and conductor (metal). The position of the Fermi level is when the sample is at absolute zero temperature.

**Figure I.3:** The difference between direct and indirect gap in semiconductors.

**Figure I.4:** The  $\text{TiO}_6$  polyhedra for  $\text{TiO}_2$  phases: a) rutile, b) anatase and c) brookite.

**Figure I.5:** Molecular-orbital bonding structure of  $\text{TiO}_2$ .

**Figure I.6:** The different possible transitions of electrons, (a) excitation, (b) excite electron and decade at low level in conduction band, (c) and (d) are the intraband transition in the presence of impurities, (e) the interaband transition in conduction band.

**Figure I.7:** Schematic presentation of the deferent ways to modify the band structure of  $\text{TiO}_2$ .

**Figure I.8:** Schematic illustrate the various processes occurring after photo excitation of  $\text{TiO}_2$  with UV light.

**Figure I.9:** Dye-sensitized solar cell devises the recombination and electronic transfer processes are indicated with violet arrows and red arrows; the double blue arrow represents the maximum voltage due to the difference between the quasi-Fermi level of the electrons in the conduction band of  $\text{TiO}_2$  and the redox energy of electrolytic mediator.

**Figure I.10:** Photoinduced wettability, (a, b) a hydrophobic  $\text{TiO}_2$  surface convert to a superhydrophilic surface upon irradiation (c, d) Exposure of a hydrophobic  $\text{TiO}_2$ -coated glass to water vapour results antifogging effect induced by UV-illumination.

**Figure I.11:** Schematic of photocatalysis splitting of water onto  $\text{TiO}_2$  surface.

**Figure II.1:** Schematic representative of different reactions occurring on surface.

**Figure II.2:** Simplified schematic of gas –solid adsorption system.

**Figure II.3:** The Lennard-Jones 6-12 potential, which represents the relationship between the distance of two atoms and the energy of system, the equilibrium distance between the interacting atoms are at  $R = R_0$ .

**Figure II.4:** The IUPAC classification of the adsorption isotherms

**Figure II.5:** The faces of rutile: (a) (110); (b) (100); (c) (001).

**Figure II.6:** The structure of rutile (110) (1x1), red (grey) balls are oxygen (titanium) atoms.

**Figure II.7:** The water molecule structure, red (grey) balls are oxygen and hydrogen atoms.

**Figure II.8:** The modification charge of rutile (110) surface depended on the pH factor.

**Figure II.9:** The vibrational modes of isolated water molecule, dashed lines are the bonds of O-H and the arrows represent the relative and displacement direction of the nuclei

**Figure II.10:** Schematic illustrating the interactions of H<sub>2</sub>O molecules on rutile (110) surface.

**Figure II.11:** FTIR-ATR spectrum of water adsorption on TiO<sub>2</sub> surface (dark line), pink line correspond to background. The spectra are kindly provided by Ahmed Bouhekka

**Figure III.1:** The adsorption of molecular water on defect-free (Ti<sub>5c</sub>) sites, dark (light) blue balls hydrogen (oxygen of water) atoms,  $K_1$ ,  $K_2$  are the rates constant of adsorption and desorption respectively.

**Figure III.2:** The dissociative adsorption of water on defect-free (Ti<sub>5c</sub>) sites, where  $K_3$  and  $K_4$  are the rates constant of dissociation and recombination reaction, respectively.

**Figure III.3:** The dissociative adsorption of water on Ti<sub>5c</sub> sites, where  $K_3$  and  $K_4$  are the rates constant of dissociation and recombination reaction, respectively.

**Figure IV.1:** The coverage of Ti, OH, O<sub>b</sub>, O<sub>v</sub>, H<sub>2</sub>O as a function of time, at different values of H<sub>2</sub>O, a)  $\theta_{H_2O} = 0.25$ , b)  $\theta_{H_2O} = 0.2$ . The time starts from the moment where the H<sub>2</sub>O flux is stopped.

**Figure IV.2:** Represent the variation of the surface rate coverage as a function of temperature (K), a) for OH and O<sub>b</sub> and b) for H<sub>2</sub>O.



**Figure IV.3:** The effect of: a) oxygen vacancies, b) H<sub>2</sub>O flux on the behaviour of water on rutile (110) surface.

**Figure IV.4:** Kinetic curves for the OH hydroxyls at rutile TiO<sub>2</sub> (110) surface for various H<sub>2</sub>O flux and concentration of O<sub>v</sub> on the surface.

**Figure IV.5:** The effects of: a) oxygen vacancies and b) H<sub>2</sub>O flux of the variation of oxygen bridging (O<sub>b</sub>).

**Figure IV.6:** The coverage of O<sub>b</sub> as a function of H<sub>2</sub>O flux and O<sub>v</sub> defects on rutile TiO<sub>2</sub> (110) surface.

**Figure IV.7:** The coverage of H<sub>2</sub>O on surface versus H<sub>2</sub>O flux and the coverage of oxygen vacancies O<sub>v</sub>.

**Figure IV.8:** The ratio of ( $\theta_{O_v} / \theta_{H_2O}$ ) on rutile TiO<sub>2</sub> (110) surface versus H<sub>2</sub>O flux.

**Figure IV.9:** The coverage of Ti<sub>5c</sub> on rutile TiO<sub>2</sub> (110) surface as a function of the concentration of oxygen vacancies (O<sub>v</sub>).

**Figure IV.10:** Adsorption spectra of BSA on TiO<sub>2</sub> close to equilibrium situation. Spectra were recorded during flowing BSA solution drop by drop and rinsing with water in between two successive drops.

## **List of tables**

**Table I.1:** The electronic properties of materials

**Table I.2:** The different properties of TiO<sub>2</sub> structure

**Table II.1:** The difference between physisorption and chemisorption

**Table III.1:** Kinetic parameters used in the mathematical models of H<sub>2</sub>O reactions on rutile TiO<sub>2</sub> (110) surface.

**Table III.2:** Nomenclature of the surface coverage

## Table of contents

Abstract	ii
Acknowledgements	v
List of figures	vii
List of tables	x
Table of contents	xi
<b>General introduction</b>	<b>14</b>
<b>References</b>	<b>17</b>
<b>I. Properties, characterizations and applications of Titanium dioxide</b>	<b>18</b>
I.1. Introduction	19
I.2. Crystalline solids	19
I.2.1. Electronic band structure	19
I.2.1.1. Insulators	20
I.2.1.2. Conductors	20
I.2.1.3. Semiconductors	20
I.2.1.3.1. Electronic properties	21
I.2.1.3.2. Intrinsic and extrinsic semi-conductors	21
I.3. Properties and applications of titanium dioxide	24
I.3.1. Titanium dioxide (TiO <sub>2</sub> )	24
I.3.2. Structure of TiO <sub>2</sub>	24
I.3.2.1. Electronic properties of TiO <sub>2</sub>	25
I.3.2.2. Optical properties	26
I.4. Experimental techniques and TiO <sub>2</sub> surface	28
I.4.1. Electrochemical infrared spectroscopy (EC-IR)	28
I.4.2. Fourier transform infrared attenuated total reflection spectroscopy (FTIR-ATR)	29
I.4.3. Scanning tunnelling microscopy (STM)	29
I.5. Applications of TiO <sub>2</sub>	29
I.5.1. Photocatalysis	29
I.5.2. Dye sensitive solar cell	30
I.5.3. Self-cleaning	31
I.5.4. Water splitting	32
I.6. Conclusion	33
<b>References</b>	<b>35</b>

<b>II. Theoretical background of adsorption and dynamics of water on rutile (110) surface</b>	<b>39</b>
II.1. Introduction	40
II.2. Surface phenomenon	40
II.3. Adsorption phenomenon	40
II.3.1. Physical and chemical adsorption	41
II.3.2. Van der Waals forces	42
II.3.2.1. Intermolecular potential	43
II.4. Kinetics and specificity of adsorption	44
II.4.1. Nature of adsorbent	44
II.4.2. Nature of adsorbate	45
II.4.3. Temperature and pressure	45
II.5. Classification of adsorption isotherms	45
II.6. Rutile TiO <sub>2</sub> (110) surface	48
II.7. Water properties	50
II.8. Water adsorption onto rutile TiO <sub>2</sub> (110) surface	50
II.9. Conclusion	54
<b>References</b>	<b>55</b>
<b>III. Mathematical modeling to investigate the dynamics of water adsorption on rutile TiO<sub>2</sub> (110) surface</b>	<b>60</b>
III.1. Introduction	61
III.2. Langmuir model theory	61
III.2.1. Limitation of Langmuir model	63
III.3. Dynamic of water on rutile TiO <sub>2</sub> (110) surface	63
III.3.1. Water adsorption on stoichiometric rutile TiO <sub>2</sub> (110) surface	63
III.3.2. Water adsorption on defective rutile TiO <sub>2</sub> (110) surface	64
III.4. Proposed theoretical model	67
III.5. Numerical methods	69
III.5.1. Euler's method	69
III.5.2. Runge-Kutta-Fehlberg (RKF 45)	70
III.6. Conclusion	71
<b>References</b>	<b>72</b>

<b>IV. Results and discussion</b>	<b>76</b>
IV.1. Introduction	77
IV.2. Water molecules behaviour on rutile (110) surface: Stopping the flux before equilibrium ( $\phi = 0$ )	77
IV.3. Temperature effect	80
IV.4. Effect of oxygen vacancies and H <sub>2</sub> O flux: Steady state case	82
IV.5. Water- proteins interactions on TiO <sub>2</sub> surface	91
IV.6. Conclusion	93
<b>References</b>	<b>95</b>
<b>General conclusion and recommendations</b>	<b>99</b>
<b>Nomenclature</b>	<b>101</b>
<b>List of publications and conferences</b>	<b>103</b>

## General introduction

Energy and health are the most worldwide requirements in life. According to the report from the International Energy Outlook (IEO) published in 2011 by the U.S. Energy information administration expected global energy consumption to increase exponentially, which is estimated to be 53 percent from 2008 to 2035 [1]. Where it's on the rise in light a rapid expansion in industrial activities, there are three types of source for energy generation: nuclear energy, renewable energy and fossil fuels. The main ones being coal, oil and natural gas, supply 78.2 % of energy consumed globally [2, 3] unfortunately, these fuels are non-renewable resulting a pernicious damage including high greenhouse gas emissions, besides the poor infrastructure has led to heavily polluted the ecologic systems with both organic and inorganic materials and these have negative effects on the lives of all beings, but there are wider implications on nature, aquatic organisms, wildlife and farming [4, 5]. This means that relying on fossil fuels for energy generation is unsustainable. Therefore, the development of new materials in order to build low-cost renewable energy technologies is a key challenge for the humanity.

In 1870, according to Jules Verne [6] **who said:** *“I believe that water will one day be employed as fuel, that hydrogen and oxygen which constitute it, used singly or together, will furnish an inexhaustible source of heat and light, of an intensity of which coal is not capable”*. Energy production and environmental remediation are of great importance in current physical-chemistry sciences due to the increasing demand for new energy alternatives to conventional fossil fuels and to meet stringent regulation in environmental protection.

Different chemical and physical procedures are currently used to achieve and reduce these problems, among them adsorption process is the most important that can be carried out for photocatalysis and gas sensor especially in aqueous solutions. The most important are the materials used for the desired performance, which are semiconductors, including germanium (Ge), silicon (Si) and titanium dioxide (TiO<sub>2</sub>).

TiO<sub>2</sub> has been one of the most studied photocatalysis not only for water splitting [7] but also for other reactions such as solar hydrogen production and decomposition of harmful organic and no organic substrates in solution and air [8] as well as particularly promising as some of the most stable, nontoxic and readily available functional materials known today. The heterogeneous photocatalysis based on TiO<sub>2</sub> has increased exponentially especially after the discovery of photoinduced of water splitting reported by Fujishima and Honda [9].

Undoubtedly, the water-TiO<sub>2</sub> interface became partially covered with molecular H<sub>2</sub>O and hydroxyl groups (OH) [10] moderate with different conditions such as the temperature, the coverage of H<sub>2</sub>O molecules and the amount of oxygen vacancies... Unfortunately, this reaction is not yet clear, therefore to enhance the performance of these systems relies on a detailed theoretical understanding of the fundamental reaction mechanisms, understanding of: water chemistry, reactive intermediates and chemical reactions occurring in complex solutions to facilitate the design of more efficient systems [11]. However, there have been many theoretical and experimental means to investigate it.

Thus, the aim of this research has been to contribute in the fundamental understanding of this phenomenon by studying the dynamics of H<sub>2</sub>O molecules adsorption on rutile TiO<sub>2</sub> (110) surface, using a theoretical model of a system of differential coupled equations based on the Langmuir model; the mathematical modeling approaches provide illustrative insight into adsorption processes, which are often difficult to be described experimentally taking into account all ways, different available adsorption sites, of the H<sub>2</sub>O behaviour on the surface.

The overall structure of this thesis takes the form of four chapters, including this general introduction and conclusion. It leads us from brief introduction to the subject and addresses the motivation behind this dissertation.

Chapter I reports an overview of the properties, characterisation and applications of the materials, especially the electronic, optical properties of TiO<sub>2</sub>. Besides this, it contains the techniques that were carried out to study the surface characterisation including STM and FTIR-ATR. At the end, it focused on the most important applications of TiO<sub>2</sub> in modern technology.

Chapter II contains the background information about the surface phenomena including the adsorption process and most factors controlling it and the calculation of isotherms, and it focussed on the detailed description of rutile TiO<sub>2</sub> (110) surface and its interaction with water molecules.

Chapter III describes the theoretical Langmuir model and the proposed mathematical approach, which accumulates all the possibilities way of the dynamics of water on the surface, resulting in a system of nonlinear differential equations, and gives the important numerical methods used to solve this type of equations.

Chapter IV covers the most important results of the factors that affect the adsorption and dynamics of H<sub>2</sub>O molecules on the rutile (110) surface and the formation of OH groups as well as a comparison between the behaviour of the simple water molecule and complex

species such as protein adsorption. The corresponding references are listed at the end of each chapter where the reader may turn for further details.

Finally, the present dissertation is concluded by a general conclusion and recommendations, which contains the most important findings of our research, and then identifies the ideas that merit further investigation in this field.



## **References**

- [1] U.S. Energy Information Administration (EIA), International Energy Outlook 2011, Center for Strategic and International Studies, Howard Gruenspecht, Acting Administrator, September 19, 2011 | Washington, DC.
- [2] Renewables 2013 Global Status Report, Technical report. 19, 29, 34, (2013).
- [3] **H. Ritchie, A. Roser and P. Rosado**, Energy. s.l. Our world in data, (2022).
- [4] **K. Sandhya and S. Sarayu**, Current technologies for biological treatment of textile wastewater-a review, 645–661, s.l. Appl. Biochem. Biotechnol. (2012), Vol. 167.
- [5] **S. Oturan and M.A.Vasudevan**, Electrochemistry: as cause and cure in water pollution-an overview, 97–108, s.l. Environ. Chem. Lett. (2014), Vol. 12.
- [6] **C. Subramaniam**, Designing, manipulation and probing of electrocatalytic interfaces for water splitting, A Chem. Cat. Con. (2020).
- [7] **T. Hisatomi, J. Kubota and K. Domen**, Recent advances in semiconductors for photocatalytic and photoelectrochemical water splitting, 7520-7535, s.l. Chem. Soc. Rev. (2014), Vol. 43.
- [8] **M.S. Hamdy, W.H. Saputera, E.J. Groenen and G. Mul**, A novel TiO<sub>2</sub> composite for photocatalytic waste watertreatment, 75-83, s.l. Catal. ( 2014), Vol. 310.
- [9] **J. Trimboli, M. Mottern, H. Verweij and P.K. Dutta**, Interaction of water with titania: implications for high- temperature gas sensing, 5647-5654, s.l. Phys. Chem. B, (2006), Vol. 110.
- [10] **A. Fujishima and K. Honda**, Electrochemical photolysis of water at a semiconductor electrode, 37-38, s.l. Nat, (1972), Vol. 238.
- [11] **E. Serrano, G. Rus and J.G.Martinez**, Nanotechnology for sustainable energy, 2373–2384 , s.l. Renewable and Sunstainable Energy Reviews, (2009), Vol. 13.

# **Chapter I**

## **Properties, characterizations and applications of titanium dioxide**

The temperature and impurities alter the conductivity of semiconductors. This characteristic gives them a great importance in the fields of electronics and physics. These materials are used in electronic devices and integrated circuits which clearly improved the daily life of human being. In this chapter, we present an overview about the properties and characterization of titanium dioxide and its applications used in our work to study the adsorption of water molecules and their behaviour under varying conditions.

## **I.1. Introduction**

In nature, there are three types of materials conductors, semiconductors and insulators classified according to their band gap or conductivity. Among them semiconductors are technologically the most important class. Therefore, the optical, electronic and chemical properties are unique. However, the surface and interfaces levels play a pivotal role in the most of reactions such as adsorption, absorption, corrosion and catalytic reactions. It is important to understand the different properties of the surface, but it is difficult to analyse and investigate results because the small numbers of atoms at surface are buried on the bulk features. Huge efforts dedicated to develop the analysis techniques which allow extracting precise and sensitive information from the surface. This section covers the different type of materials and their properties plus the most popular and sensitive techniques that can be used for surface and interface analysis [1].

## **I.2. Crystalline solids**

Solids are physical objects constitute of atoms, which firstly postulated by the ancient Greek philosopher Demokritos [2], nevertheless, they are considered one of the greatest bride on the human intellect. These atoms are basically arranged essentially in a perfect periodic array is quite extraordinary in regular 3D periodic pattern regardless of the difference in the elements and their combination. Real solids do not extent to infinity they terminate with surfaces, which represent 2D defects resulting in a small perturbation in physical solid [3]. Indeed, the presence of such defects that makes solids useful, because the defects alter the properties of the ideal crystal, which is in perfect forms would have a limited range of properties [4], according to the space arrangement we can have various types of materials.

### **I.2.1. Electronic band structure**

The electrons in isolated atom filled the atomic orbital's in discrete level, however, when a large number of atoms are brought together around  $10^{23}$  atoms (crystal) the distances between the discrete levels are very small thus forming a band [5]. The highest occupied band (valence band  $E_v$ ) and the lowest unoccupied band (conduction band  $E_c$ ) with the forbidden band (gap band  $E_g$ ) in between as illustrated by the following **Figure I.1** [6]. The forbidden band energy ranges where no electronic states are present and it's given by ( $E_g = E_c - E_v$ ) and represents the minimal energy that is required to excite electron to participate in conduction and it makes the difference between insulators, conductors and semi-conductors.

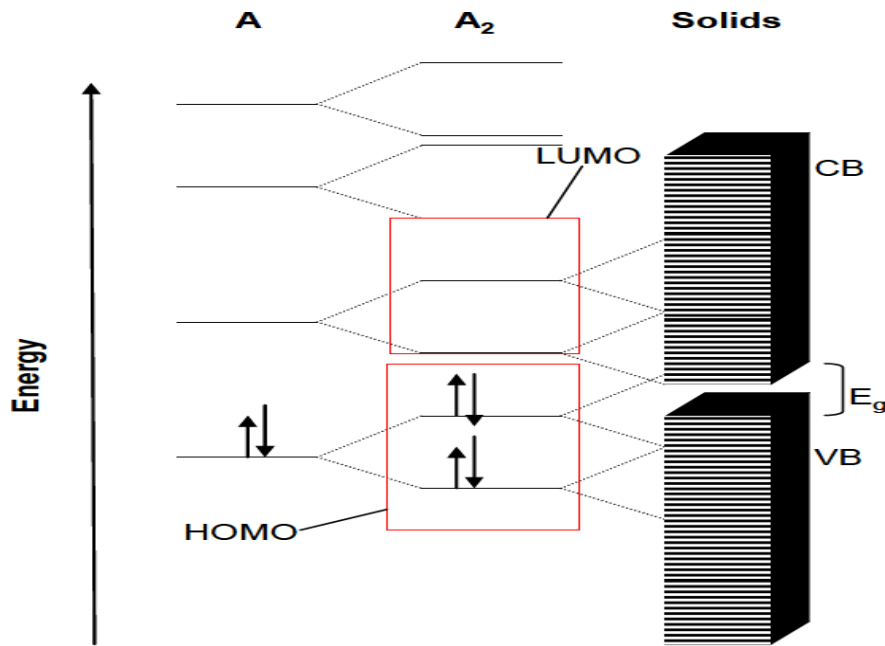


**Figure I.1:** The electronic bands structure of materials [6].

### I.2.1.1. Insulators

In an insulator the valence band is separated from the conduction band by a large gap, where the first is full and the second is empty, only the electrons accept energy more or equal the band gap can be excited to the conduction band including wood. This is the converse of the conductors.

### I.2.1.2. Conductors

The conductors (metals) are solids whose the conduction band overlaps with the valence band (no band gap), thus, they allow the electricity flow through them such as copper, steel and aluminum.

### I.2.1.3. Semiconductors

Semi-conductors are solids with a smaller band gap situated between that of conductors and insulators, where at low temperature the electrons have insufficient energy for moving to the conduction band (insulator). When increasing the temperature, it renders more electrons to have more energy to move to the conduction band leading to increase the conductivity of a semi-conductor, the overall illustration is shown in **Figure I.2**.

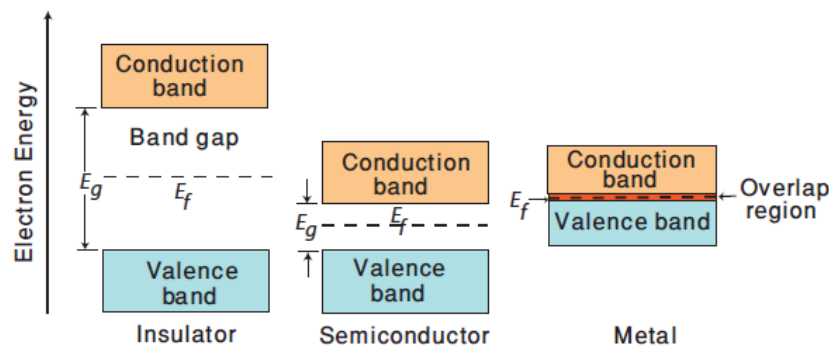


**Figure I.2:** The forbidden band diagram of the electronic structure of insulator, semiconductor and conductor (metal). The position of the Fermi level is when the sample is at absolute zero temperature [7].

**I.2.1.3.1. Electronic properties**

Semi-conductors are materials characterized by a forbidden band ( $E_g$ )  $0 < E_g < 6$  eV which is greater than the insulator and less than the conductor gap. Different properties are classified in following **Table I.1**.

	Conductivity $\sigma$ ( $\Omega \cdot m$ ) <sup>-1</sup>	Resistivity $\rho$ ( $\Omega \cdot m$ )	Band gap (eV)
Conductors	$< 10^6$	10	$\approx 0$
Semi-conductors	$10^{-10} < \sigma < 10^6$	$10^{-2}-10^9$	$0 < E_g < 6$
Insulators	$< 10^{-10}$	$> 10^{14}$	$> 6$

**Table I.1:** The electronic properties of materials [5, 6, 8].

Generally, semi-conductors materials exist in two types; simple and composed; the first one is compound from one element as (Ge, Si...) whereas the second consists of at least two types of elements as ( $Z_n S$ ,  $TiO_2$ ,  $I_n G_a P \dots$ ).

**I.2.1.3.2. Intrinsic and extrinsic semi-conductors**

At temperature equals to 0 K semiconductors behave as insulator, but in thermal agitation at high temperature, randomly they promote transition of electrons to heal the conduction band, however the probability of occupied an energy level is given by Fermi function ( $f(E)$ ) as shown below:

$$f(E) = \frac{1}{1 + e^{\frac{(E-E_f)}{K_B T}}} \quad (\text{I. 1})$$

Where:

$E$ ,  $E_f$ ,  $K_B$  and  $T$  are the energy of reference state, Fermi energy, Boltzmann constant and temperature in Kelvin.

The life time recombination (e-hole) pair generally depends on the direct and indirect gap controlled by the position of the minimal of conduction band and the maximal of valence plus the difference between them as illustrated in the **Figure I.3**, the recombination occurs rapidly in direct gap compared to indirect gap which is due to the variety of optical and electronic properties [8].

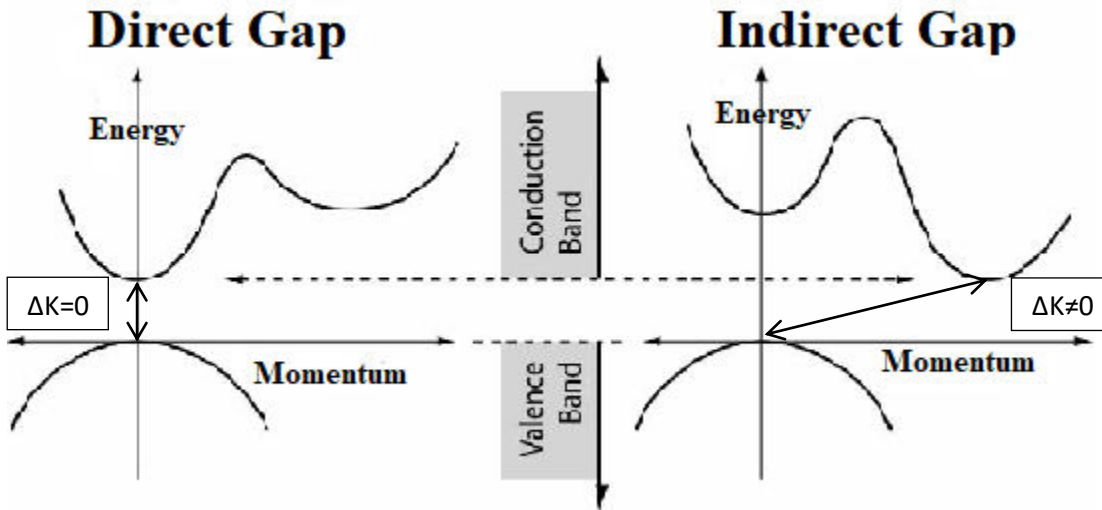


**Figure I.3:** The difference between direct and indirect gap in semiconductors [8].

The semiconductors with no impurities are called intrinsic or pure, however, the number of excited electrons ( $n$ ) (conduction band) and the holes ( $p$ ) in valence band are the same ( $n = p$ ), thus the intrinsic carrier concentration of electrons or holes ( $n_i$ ) is given by the multiplication of probability that a state at energy  $E$  is filled  $f(E)$  and the density of state at that energy  $g(E)$  is given by:

$$n_i = \int_{E_c}^{\infty} f(E)g(E)dE \quad (\text{I. 2})$$

$$n_i = N_c e^{-(E_c-E_f)/K_B T} \quad (\text{I. 3})$$

Where:

$E_c$  and  $E_f$  are conduction band energy and Fermi energy respectively.

The  $N_c$  is the effective density of state at conduction band is given by

$$N_c = 2\left(\frac{2\pi m_e K\beta T}{h^2}\right)^{3/2} \quad (\text{I. 4})$$

The effective density of state at valence band ( $N_v$ ) is:

$$n_i = N_v e^{-(E_f - E_v)/K\beta T} \quad (\text{I. 5})$$

$$N_v = 2\left(\frac{2\pi m_e K\beta T}{h^2}\right)^{3/2} \quad (\text{I. 6})$$

Where:

$E_v$  is the valence band energy,  $m_e$  is noted the mass of electron.

From the equations (I. 3) and (I. 5), it is clear that the forbidden band has an important role in the applications of SCs. At a wide ( $E_g$ ) the material has a fewer mobile carrier. In contrast, the narrow band gap allows the mobility of the charge carriers from the VB to CB, which deals to increase density of charges.

$$n_i = \sqrt{N_v N_c} e^{-E_g/2K\beta T} \quad (\text{I. 7})$$

When doping has been introduced in intrinsic semi-conductor, thus changing the relative number and the type of free charge carriers, this is called doping semiconductor. There are two types, in n-type, the electrons of atoms doped are the majority charge carriers and this increases the conduction charge carriers, whereas, in p-type, the holes are the majority charge carriers. This procedure strongly depends on the atoms used in doping; the number of impurities should be less than the host material to keep on its properties. Therefore, the probability of finding carrier of state is via Fermi function [9],

For electrons donors are:

$$n = N_D e^{-(E_c - E_D)/K\beta T} \quad (\text{I. 8})$$

For holes acceptors are:

$$p = N_A e^{-(E_A - E_v)/K\beta T} \quad (\text{I. 9})$$

Where:  $E_A$ ,  $E_D$  are the acceptors and donor energy,  $N_A$ ,  $N_D$  are the concentration of charge acceptors and donors.

Technologically, semi-conductors become one of the most important materials used in manufacturing the electronic devices including Ge, Si and TiO<sub>2</sub>. Among these, we focus in our work on TiO<sub>2</sub> for several considerations that will be mentioned in next sections.

### **I.3. Properties and applications of titanium dioxide**

#### **I.3.1. Titanium dioxide (TiO<sub>2</sub>)**

Titanium dioxide was discovered in 1791 by the clergyman and William Gregor [10], it has a molecular weight 79.87 g/mole with a chemical formula TiO<sub>2</sub>, titanium dioxide is extracted from the ores in the world which is contained ilmenite and rutile and anatase [11]. Despite, it can be elaborated with variety of methods as spin coating, dip coating... Due to its characteristics abundant, inexpensive, high specific surface area [12] and stable chemically [13] it takes more attention in wide world researchers especially in Asia (china is the leading country), which considered as basic element in deferent technology applications like solar cells, pharmaceutical and medicals, treatment of water...[14-16]. In the following section we will talk in more details about TiO<sub>2</sub> structure.

#### **I.3.2. Structure of TiO<sub>2</sub>**

TiO<sub>2</sub> is a semiconductor composed of two elements Titanium (Ti) and oxygen (O), in nature it exists in three different forms: rutile, anatase and brookite, where the two first have a tetragonal primitive unite cell and brookite has orthorhombic unit cell as shown in the following **Figure I.4**. Both (rutile and anatase bulk) structures can be described regarding the chains of TiO<sub>6</sub> octahedron; means each Ti<sup>4+</sup> ions surrounding with six of O<sup>2-</sup> ions, the difference between them includes in the distortion and the assemble pattern of octahedral chains [17]. Along of this, in rutile each octahedron connecting with ten other octahedron (two sharing edge oxygen pairs and eight sharing corner oxygen atoms), whereas, in anatase the octahedron connecting with eight neighbours octahedrons (four sharing an edge and four sharing a corner) therefore. These distinctions of one to other in lattice structures resulting different mass densities and electronic band structures between the two forms [18] rutile thermodynamically is the most stable whereas anatase is metastable [19-21], anatase and brookite transform irreversibly to rutile under high temperature around (900 K) [22]. Generally, rutile (110) and anatase (101) are the most stable surfaces in TiO<sub>2</sub>. Besides, others properties are surmised in the **Table I.2**. In this works we are focused to study rutile TiO<sub>2</sub> (110) surface.



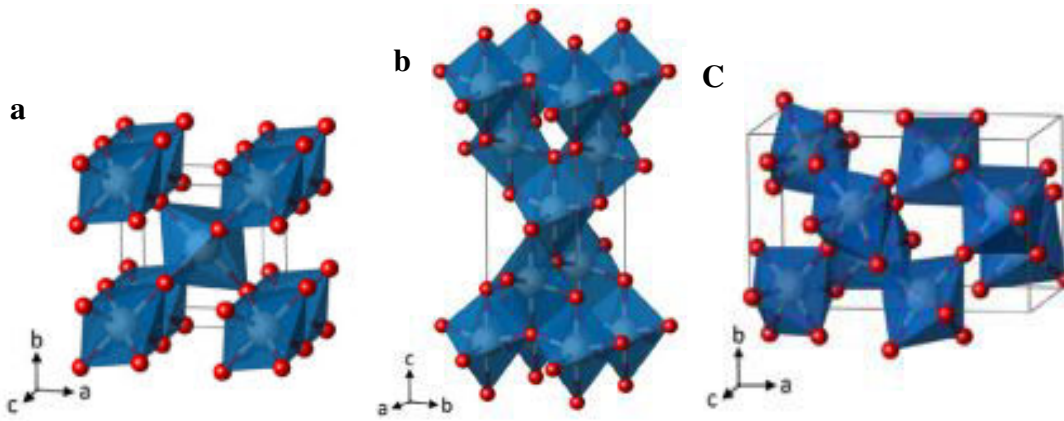


**Figure I.4:** The  $\text{TiO}_6$  polyhedra for  $\text{TiO}_2$  phases: a) rutile, b) anatase and c) brookite [23].

Structure	Rutile	Anatase	brookite
Unit cell	Tetragonal	Tetragonal	orthorombic
Space group	$D_{4h} 19 - P42/mnm$	$D_{4h} 19 - I41/amd$	Pbca
Surface energy(kj/mol)	0	24.75	18.53
Polyhedron type	Octahedron	Octahedron	octahedron
Band gap (eV)	3	3.2	3.32

**Table I.2:** The different properties of  $\text{TiO}_2$  structure ([24] and references therein).

### I.3.2.1. Electronic properties of $\text{TiO}_2$

Several techniques are used to improve the electronic structure such as X-ray absorption, where it's the recombination between the Ti 3d, decomposed onto (Ti  $e_g$ , Ti  $t_{2g}$  ( $d_{yz}$ ,  $d_{zx}$ , and  $d_{xy}$ ),  $O_{2p}$  also decomposed onto (O  $p\sigma$  and O  $p\pi$  orbitals). Therefore, the valence band is subtracting in three regions, first, the  $\sigma$  bonding characterized with low energy contributes to Ti d, the second is  $\pi$  bonding with a middle energy, the higher energy for the O  $p\pi$  bonding due to no contribution with Ti d. The conduction band is decomposed onto  $d_{xy}$  located at the bottom of CB whereas; Ti  $e_g$  and  $t_{2g}$  are anti-bonding with p as the following **Figure I.5** shows the relation between them. The electronic properties are strongly depending on the defects; crystals structure... for example the oxygen vacancy and titanium interstitial play important roles in creating levels in band gap which can enhance the electronic conductivity of the material [25, 26].

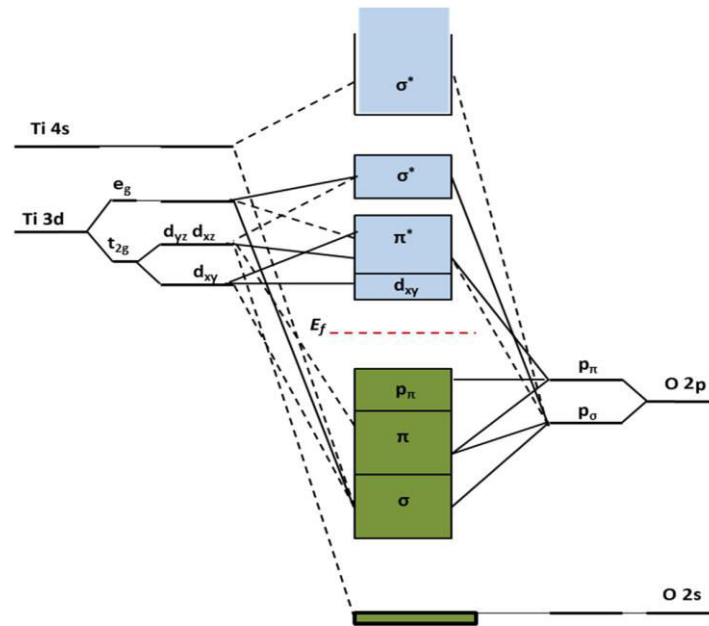


**Figure I.5:** Molecular-orbital bonding structure of TiO<sub>2</sub> [26].

### I.3.2.2. Optical properties

The optical properties of any materials are improved via the absorbance and emission due to excitation of electrons, when the absorbed photons have energy equal or more than band gap, this leads to excite electrons from the valence band to conduction band and leaving behind them holes where dissipate energy and decay to lower levels and also the intraband transition in the small photon energy [27-29]. In addition, in the presence of impurities creates band states in forbidden gap near valence or conduction bands which promotes the intraband transition. TiO<sub>2</sub> has indirect band gap and indirect transitions lead to a lower absorption coefficient compared to direct gap. The indirect transitions are allowed due to a large dipole matrix element and a large density of states for the electron in the valence band. The shortcoming of TiO<sub>2</sub> is high band gap up to 3 eV, which reacts only in UV light (380 nm) meanwhile available around 5 % in solar light [30]. Therefore, many of researchers treated this problem by creating defects and doping TiO<sub>2</sub> with other elements. The defects reduce the band gap and create intraband gap states [31, 32], this enhances the optical and electronic properties, additionally, increases the performance of storage and convert of energy, more details in [29-31], which used in many fields [23, 25, 26]. These states with possible transitions are shown the **Figure I.6**.

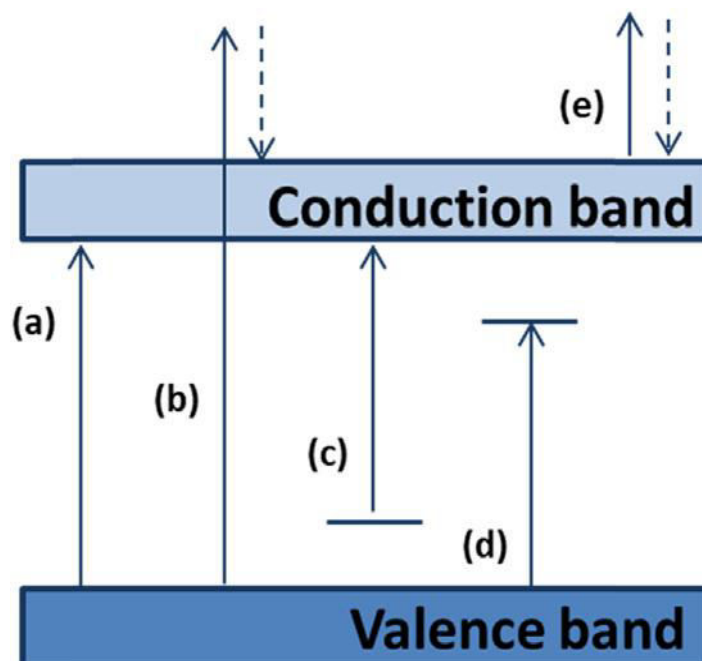


**Figure I.6.** The different possible transitions of electrons, (a) excitation, (b) excite electron and decade at low level in conduction band, (c) and (d) are the intraband transition in the presence of impurities, (e) the interaband transition in conduction band [26].

There are various ways to achieve this purpose either by using intrinsic or extrinsic defects, thus, we attempted to identify the impact of defects on the structural, optical and electronic properties. First, in intrinsic defects by inducing localised like O vacancy or interstitial, Ti vacancy or interstitial, 2D (surface) and 3D (bulk) which perturbs locally the crystal periodicity of semiconductor and leads to create a band state energy in the gap, while, non-localised defects are like (photon and phonon). Second, in extrinsic defects is doping with metals elements such as platinum (Pt). Third, sensitizing  $\text{TiO}_2$ , with other color full inorganic or organic elements can enhance its optical properties in the visible light region [33-35]. Forth, coupling the metal oxide ( $\text{TiO}_2$ ) with others semiconductors can facilitate transfer and exchange of electrons, thus alter its properties, **Figure I.7**, in overall, inducing defects on the surface not only decrease the band gap of semiconductors to enhance the absorption in visible light and near infrared (NIR) regions but also enhance the performance of photocatalytic, In addition, favoured the recombination of majority with minority carriers.

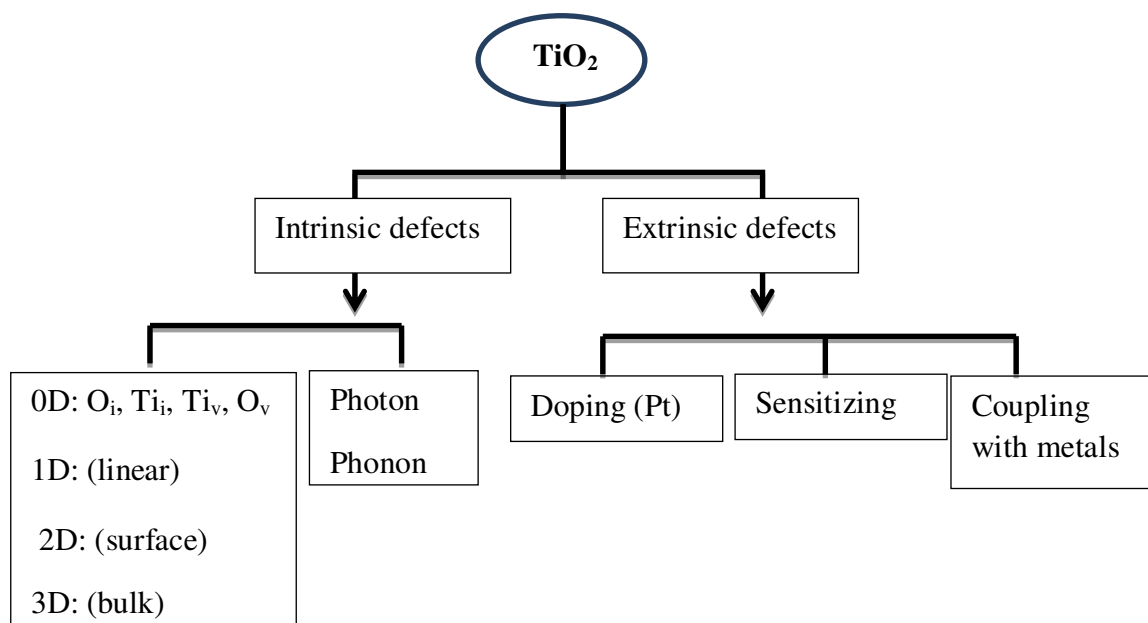


**Figure I.7:** Schematic presentation of the different ways to modify the band structure of TiO<sub>2</sub>.

#### I.4. Experimental techniques and TiO<sub>2</sub> surface

##### I.4.1. Electrochemical infrared spectroscopy (EC-IR)

Electrochemical infrared spectroscopy (EC-IR) and infrared reflection absorption spectroscopy (IRAS) are widely adopted as chemical structure identification techniques on the electrode and solution interface by many groups. This technique is based on the reflection of the infrared beam light from the surface [36], where the s-polarized (electric field perpendicular to the incident plane) radiation becomes active only when the distance from the electrode surface becomes larger and p-polarization (electric field parallel to the incident plane) depends on the incident angle to the surface that means infrared radiation with p-polarization has a strong reaction with the surface molecules. One of the shortcomings of this technique is the infrared attenuated by the electrolyte solution, various researches developed by using surface enhanced infrared absorption (SEIRA) based on an electromagnetic mechanism; however the electric field enters the surface and decreases with the depth of the sample. Therefore, this leads to a higher selectivity of infrared absorption on the surface of the metal nanoparticles. Recently, various groups of researchers are using attenuated total reflection (ATR) where samples are deposited on Si prism [37, 38].

#### **I.4.2. Fourier transform infrared attenuated total reflection spectroscopy (FTIR-ATR)**

Fourier transform infrared attenuated total reflection spectroscopy is based on total reflection of the incident IR radiations at the surface of an internal reflection element (IRE), which is sensitive and popular tool employed for systematic studies of metal / liquid interfaces, especially at very thin films by in situ measurements under different conditions: pH, temperature, concentration and light shining [39-41]. Besides, it can be used for thick films and opaque solution. The goal of this technique is to study of basic issues, such as surface structure; among special features of this technique is the ability to follow the corrosion processes under humid air and liquid conditions [42-44].

#### **I.4.3. Scanning tunnelling microscopy (STM)**

Scanning tunnelling microscopy (STM) was developed by Binnig and Röhrer [45]. For their efforts, they shared the Nobel Prize in physics (1986). Today, STM is a mainstay of modern surface science investigations of atomic manipulation and real-space imaging of surfaces [45-47]. In principle, STM works by allowing electrons to flow from an atomically sharp conductive tip to a conducting sample (or vice versa) through a small gap (potential barrier). This phenomenon is known as the tunnelling effect. Which is helpful tool to obtain detail information on atomic level, local structure of the surface and they are extremely sensitive to height or composition variations on the surface [48, 49], STM is considered as surface science tool.

### **I.5. Applications of TiO<sub>2</sub>**

Since the discovery of photocatalytic splitting of water by Fujishima and Honda in 1972 [50] and the first report nanocrystalline TiO<sub>2</sub> dye sensitized solar cell (DSSC) by O'Regan and Gratzel in 1991[51], these are a milestone in the history of research of TiO<sub>2</sub>. Afterward, TiO<sub>2</sub> has sparked extensive interest in medical, environment and industry fields including photocatalysis, self-cleaning, solar cell and splitting of water.

#### **I.5.1. Photocatalysis**

The photocatalysis is a process that utilizes light to decompose the dirt and other impurities in the presence of catalyst, when exhibits light on surface with energy equal or greater than the band gap, leading to create (electron – holes) pairs see (I. 10) [52] as illustrated in **Figure I.8**. In one hand, the (e<sup>-</sup>) excited to conduction band and left behind (h<sup>+</sup>) in VB which can oxidize the adsorbed water or hydroxyl ions to form hydroxyl radicals OH<sup>•</sup> (I. 12), where these radical groups lead to decompose the organic and non-organic pollutions to CO<sub>2</sub> and H<sub>2</sub>O resulting in the used in several

field as self- cleaning and anti- fogging. In the other hand, the excited electron ( $e^-$ ) reacts with adsorbed compounds and changes oxygen to the superoxide radicals ( $O_2^-$ ) and hydroperoxide radicals ( $HO_2$ ) see (I. 11) and (I. 13) [52], the overall reactions can be summarised below. These reactions are playing a pivotal role in photocatalysis. The pair (e-hole) can get a recombination in the volume or the surface of semiconductor.

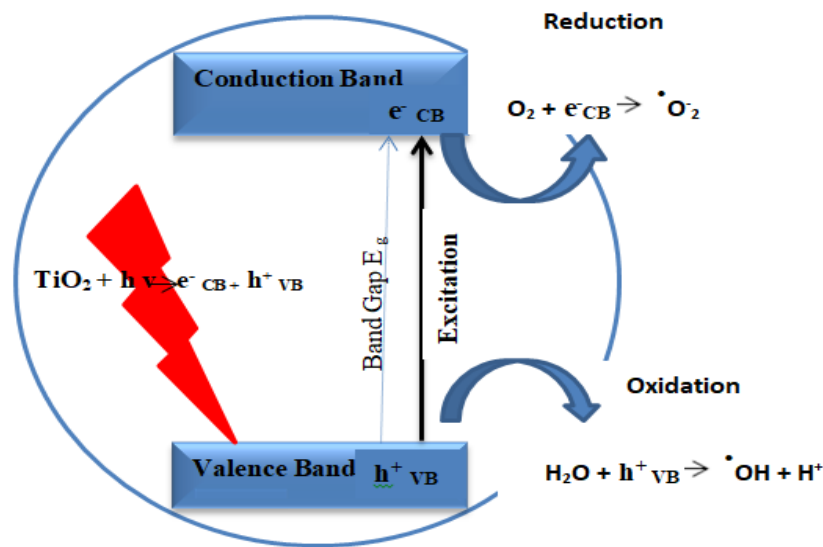
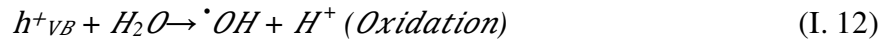
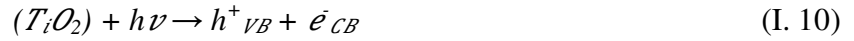


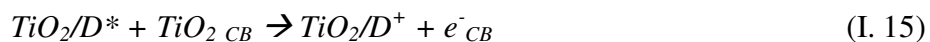
**Figure I.8:** Schematic illustrate the various processes occurring after photo excitation of  $TiO_2$  with UV light.

### I.5.2. Dye sensitive solar cell

Unlike the previous generations of solar cell (first based on the silicon panels and second based on the reduction of the first-generation cells through the use of “thin-film technologies), the third generation (photovoltaic solar cell) theoretically have desirable goals using polymer cells, organic photovoltaic and nanocrystalline cells [53]. When exposing photoanode ( $TiO_2$ /dye) to light irradiation, charges separated at the interfaces and oxidizing the dye  $D^+$ .

The electron reaches to the counter electrode (CE) made from the (FTO/ITO) through electrolyte (placed to ensure the connection) as represented by the reactions equations (I. 14) and (I. 15) below. To permit continuous flow (no stop of reaction), the electron is released to the electrolyte, which contains a redox pair. A reduction reaction then takes place through which the previously oxidized

dye is reduced [54], at the same time,  $I_2$  regenerates the oxidized dye making it ready to receive other photons and place other electrons in the photoelectrochemical circuit of the cell as reactions equations (I. 16) and (I. 17).



To improve the proper functioning of devices, they must be in harmony between them, the dye should not exhibit radiative decay of the excited state and the speed of injection of the electrons toward  $TiO_2/CB$  should be greater, as well as, must ensure the rapid regeneration of the redox pair to reduce the oxidized dye achieve the continue of the reaction as indicating in **Figure I.9**.

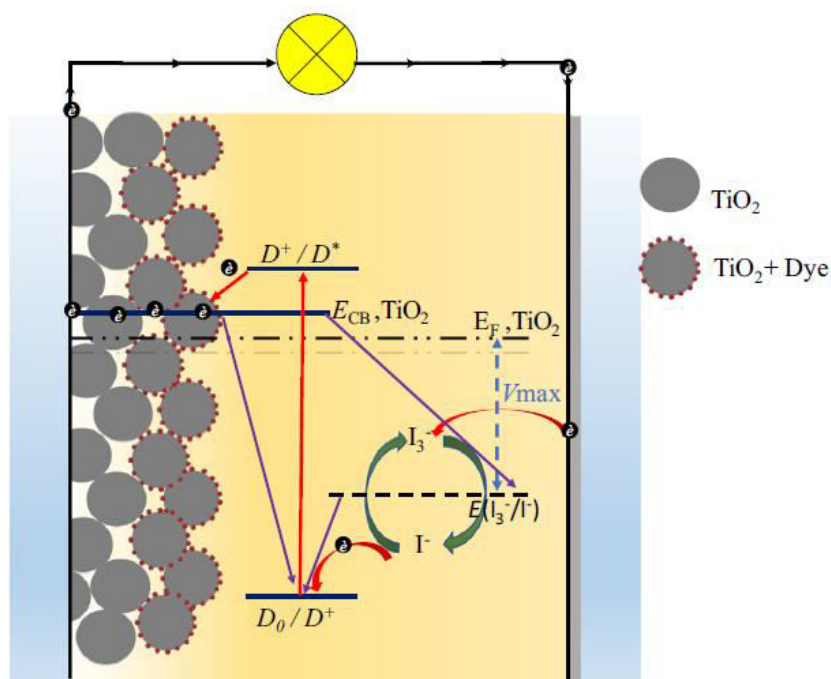


**Figure I.9:** Dye-sensitized solar cell devises the recombination and electronic transfer processes are indicated with violet arrows and red arrows; the double blue arrow represents the maximum voltage due to the difference between the quasi-Fermi level of the electrons in the conduction band of  $TiO_2$  and the redox energy of electrolytic mediator [55].

### I.5.3. Self-cleaning

$TiO_2$  is widespread metal oxides used to remove and cleaning antimicrobial in aqueous and wet environmental even in industrials applications [56], along this way, photocatalytic self-cleaning is divided onto two categories: i) hydrophobic surfaces and ii) hydrophilic surfaces depending on the

surface properties[57, 58]. These types depend to the contact angle between the water droplet and the surface ( $0^\circ < \theta < 90^\circ$  hydrophilic) and ( $\theta > 90^\circ$  hydrophobic) [59] upon the irradiation  $\text{TiO}_2$  surface by UV light the contact angle decreases and approaches to  $\theta \approx 0^\circ$  giving rise to spread the water molecules rapidly on surface and the stain can be effectively taken away, meanwhile in hydrophobic surface the droplet of water split quickly due to water low adhesion on surface thereby remove the pollutants from the surface [60] as illustrated in **Figure I.10**.

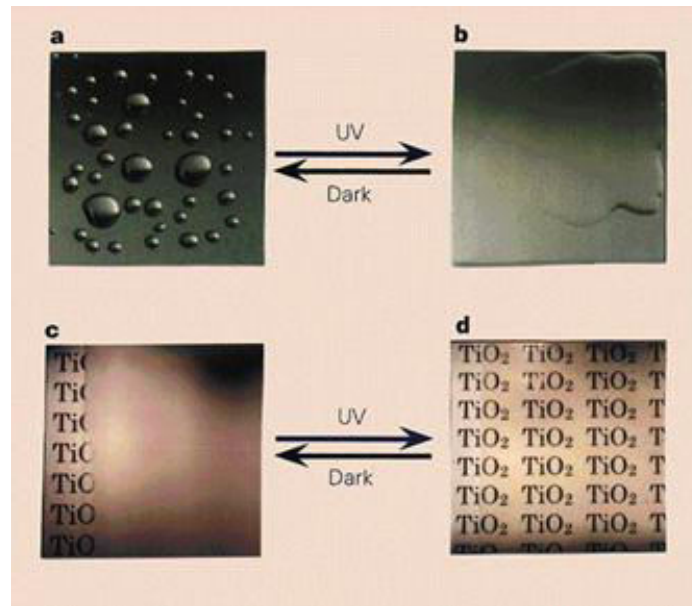


**Figure I.10:** Photoinduced wettability, (a, b) a hydrophobic  $\text{TiO}_2$  surface convert to a superhydrophilic surface upon irradiation (c, d) Exposure of a hydrophobic  $\text{TiO}_2$ -coated glass to water vapour results antifogging effect induced by UV-illumination [32].

#### I.5.4. Water splitting

In light of development and increasing the concern about the global warming, extensive researchers are developed technological strategies to trait these environmental urgent problems of affording renewable energy [61]. Hydrogen can be formed on  $\text{TiO}_2$  – based photocatalysis of water splitting or reforming organics compound through the direct exploitation of sunlight and that considered as environmentally friendly, thus,  $\text{H}_2$  envisaged as an excellent energy to reduce this problem, therefore, worldwide researchers carried out on photocatalysis splitting of water to form  $\text{H}_2$  and  $\text{O}_2$  on  $\text{TiO}_2$  photocatalyst, which intimated by the absorption of photons with energy equal to or greater than the gap form (e- hole) pair as equation (I. 18), the reaction is initiated by electron-transfer-type oxidation of either  $\text{Ti-H}_2\text{O}$  or  $\text{Ti-OH}$  at the surface by photogenerated holes as reaction equation (I. 19)[62] as shown in **Figure I.11**.





These radicals  $\cdot\text{OH}$  and  $(\text{Ti-OH})^+$  have been considered as a key intermediate factors for photocatalytic degradation of organic, non-organic contaminations and for the production of  $\text{H}_2$  fuel generation see (I. 21) and (I. 21), in addition to that the recombination of these hydroxyls producing  $\text{H}_2\text{O}_2$  which may get molecular oxygen and hydrogen via oxidation [63]. To this way, the adsorption of water on  $\text{TiO}_2$  surface is instrumental in furthering the production of OH hydroxyls.

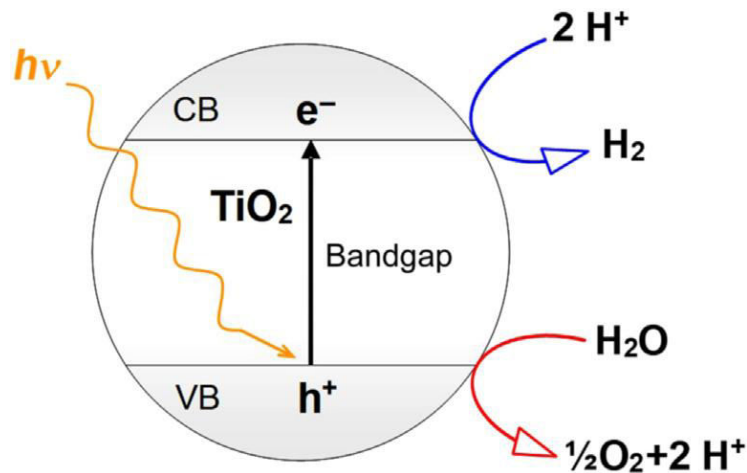
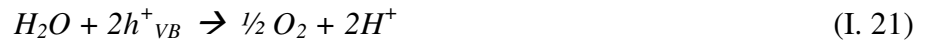


**Figure I.11:** Schematic of photocatalysis splitting of water onto  $\text{TiO}_2$  surface [63].

## I.6. Conclusion

In this chapter, we presented a general idea about the different properties able to classify the materials and their types. However, a lot of techniques are used to identify the optical, thickness and the atomic level of the structure properties such as Fourier transform infrared attenuated total reflection spectroscopy (FTIR-ATR), electrochemical infrared spectroscopy (EC-IR) and scanning tunneling microscopy (STM) which are fairly useful methods and powerful tools to probe interfaces especially using in situ measurements. We focused in these sections deeply on titanium dioxide, this metal oxides has a potential interest in recent years in light of its optical and electrical properties which is considered as a basic devices in different disciplines like photocatalysis, solar

cell and splitting of water as aforementioned, adsorption is considered as an effective method to increase the production of OH hydroxyls under certain conditions.

In the following chapter, more details about the surface phenomena especially the adsorption process besides the dynamics of H<sub>2</sub>O molecules on rutile TiO<sub>2</sub> (110) surface will be discussed.

## References

- [1] **H. Ibach**, Physics of surfaces and interfaces, s.l. Springer, Verlag Heidelberg, Berlin, (2006).
- [2] **N.W. Ashcroft and N.D. Mermin**, Solid state physics, Philadelphia, Saunders College Publishing, (1976).
- [3] **O. Madelung**, Introduction to solid state theory, Berlin, Heidelberg: Springer-Verlag, (1981).
- [4] **A.P. Sutton**, Electronic structure of materials, Oxford : Oxford University Press, (1993).
- [5] **A. Jullien and R. Guinier**, The solid state, Oxford : Oxford University Press, (1989).
- [6] **A.R. J. Herrera**, Preparation, characterization and photocatalytic activity of commercial TiO<sub>2</sub> powders co-doped by N and S, Switzerland, Germany, (2009).
- [7] **S. Amrozia, W. Zia and M.S. Anwar**, Band structure and electrical conductivity in semiconductors, Lahore, Pakistan : LUMS School of Science and Engineering, (2011).
- [8] **A. Bouhekka**, Adsorption of BSA protein on silicon, germanium and titanium dioxide investigated by In Situ ATR-IR spectroscopy, PhD thesis, Es-Senia University of Oran, Algeria, (2013).
- [9] **A. Rockett**, The materials science of semiconductors, s.l. Library of Congress, (2008).
- [10] **J. Singteton**, Band theory and electronic properties of solids, United State, published in United State, (2001).
- [11] **Y. Lan, Y. Lu and Z. Ren**, Mini review on photocatalysis of titanium dioxide nanoparticles and their solar applications, 1031-1045, s.l. Nano Energy (2013), Vol. 2.
- [12] **K. Othmer**, Encyclopedia of chemical technology, 516-541, s.l. John Wiley and Sons, (1998), Vol. 26.
- [13] **W. Zhang, H. He, Y. Tian, H. Li, W. Li, K. Lan, L. Zu, Y. Xia, L. Duan and D. Zhao**, Defect- engineering of mesoporous TiO<sub>2</sub> microspheres with phase junctions for efficient visible light driven fuel production, 104113-104141, s.l. Nano Energy, (2019), Vol. 66.
- [14] **D.C. Cronmeyer**, Electrical and optical properties of rutile single crystals, 876-886, s.l. Phys. Rev. (1952), Vol. 87.
- [15] **A. Fujishima, T.N. Rao and D.A. Tryk**, Titanium dioxide photocatalysis, 1-21, s.l. Photochem. and Photobiol. C: Photochem. Rev. (2000), Vol. 1.
- [16] **T. Prakash**, Review on nanostructured semiconductors for dye sensitized solar cells, 231-243, s.l. Electr. Mater. Lett. (2012), Vol. 8.
- [17] **S. Zhong, S. Wu, X. Chen and K. Xu**, Theory study of H<sub>2</sub>O adsorbed TiO<sub>2</sub> (110) surface: structural and electronic properties, 01058-01062, s.l. Matec. web of conf. (2022), Vol. 358.
- [18] **J.V. Hernandez**, Structural and morphological modification of TiO<sub>2</sub> doped metal ions and investigations of photoinduced charge transfer processes, PhD thesis, university of maine, Mexico, (2018).

- [19] **X. Mao, Z. Wang, X. Lang, Q. Hao, B. Wen, D. Dai, Ch. Zhou, L.-M. Liu and X. Yang**, Effect of surface structure on the photoreactivity of TiO<sub>2</sub>, 6121–6127, s.l. *Phys. Chem. C*, (2015), Vol. 119.
- [20] **S.J. Boyd, D. O’Carroll, Y. Krishnan, R. Long and N. English**, Self- diffusion of individual adsorbed water molecules at rutile (110) and anatase (101) TiO<sub>2</sub> interfaces from molecular dynamics, 398-414, s.l. *Cryst.* (2022), Vol. 12.
- [21] **F. Amano, A. Yamamoto and J. Kumagai**, Highly active rutile TiO<sub>2</sub> for photocatalysis under violet light irradiation at 405 nm, 1079 -1090, s.l. *Catal.* (2022), Vol. 12.
- [22] **K. Cao**, Surface science study of water and hydrogen adsorbed on rutile TiO<sub>2</sub> (110)-(1×1), Peking University, Liuzhou, China, thesis, (2011).
- [23] **M. Asama and K. Shirasaki**, Compact optical isolator for fibers using birefringent wedges, 4296–4299, s.l. *Appl. Optics.* (1982), Vol. 21.
- [24] **M. Landmann, E. Rauls and W.G. Schmidt**, The electronic structure and optical response of rutile, anatase and brookite TiO<sub>2</sub>, 195503-195509, s.l. *Phys. Condens. Matter.* (2012), Vol. 24.
- [25] **U. Diebold**, The surface science of titanium dioxide, 53-229, s.l. *Surf. Sci. Rep.* (2003), Vol. 48.
- [26] **M. Ramamoorthy, D. Vanderbilt and R.D. King-Smith**, First principles calculations of the energetics of stoichiometric TiO<sub>2</sub> surfaces, 16721-16727, s.l. *Phys. Rev. B*, (1994), Vol. 49.
- [27] **X. Chen and S.S.Mao**, Titanium dioxide nanomaterials: synthesis, properties, modifications and applications, 2891-2959, s.l. *Chem. Rev.* (2007), Vol. 107.
- [28] **X. Chen**, Titanium dioxide nanomaterials and their energy applications, 839-851, s.l. *China. J. Catal.* (2009), Vol. 8.
- [29] **K. Bourikas, C. Kordulis and A. Lycourghiotis**, Titanium dioxide (anatase and rutile): surface chemistry, liquid–solid interface chemistry, and scientific synthesis of supported catalysts, 9754-9823, s.l. *Chem. Rev.* (2014), Vol. 114.
- [30] **M.A. Barakat and R. Kumar**, Photocatalytic activity enhancement of titanium dioxide nanoparticles, in photocatalytic activity enhancement of titanium dioxide nanoparticles, 1-29, s.l. Springer, Cham (2016).
- [31] **J.M. Coronado, F. Fresno, M.D. Hernández-Alonso and R. Portela**, Design of advanced photocatalytic materials for energy and environmental applications, London, Springer, (2013).
- [32] **M.A. Shaheed and F.H. Hussein**, Preparation and applications of titanium dioxide and zinc oxide nanoparticles, 2380-2391, s.l. *Environ. Anal. Chem.* (2014), Vol. 2.
- [33] **S. Banerjee, D.D. Dionyioou and S.C. Pillai**, Self- cleaning applications of TiO<sub>2</sub> by photo-induced hydrophilicity and photocatalysis, 396-428, s.l. *Appl. catal. B: Environ.* (2015), Vol. 176.

- [34] **D. Eisenberg and W. Kauzmann**, The structure and the properties of water, New York, Oxford, (1969).
- [35] **L. Theodore, R. Dupont and K. Ganesan**, Unit operations in environmental engineering, s.l. SALEM, MA: Scrivener-Wiley, (2017).
- [36] **L. Theodore**, Chemical engineering: the essential reference, New York: McGraw-Hill, (2016).
- [37] **R.G. Greenler**, IR study of adsorbed molecules on metal surfaces by reflection techniques, 310–315, s.l. Chem. Phys. (1966), Vol. 44.
- [38] **M. Osawa**, Dynamic processes in electrochemical reactions studied by surface-enhanced infrared absorption spectroscopy (SEIRAS), 2861–2880, s.l. Bull. Chem. Soc. Japan. (1997), Vol. 70.
- [39] **M. Osawa**, In-situ surface-enhanced infrared spectroscopy of the electrode/solution interface, 269–314, s.l. Adv. Electrochem. Sci. Engergy, (2006), Vol. 9.
- [40] **N.J. Harrick**, Internal reflection spectroscopy and supplement, Harrick Scientific Corporation, New York, (1985).
- [41] **J.D.E. McIntyre**, Specular reflection spectroscopy of the electrode-solution interphase in: optical techniques in electrochemistry, 61-165, s.l. John Wiley & Sons, (1973), Vol. 9.
- [42] **N.J. Harrick and F.M. Mirabella**, Internal reflection spectroscopy: review and supplement, scientific corp. Ossinig, (1985).
- [43] **F. Zhou, X. Zhang, D. Persson and D. Thierry**, In situ infrared reflection absorption spectroscopy studies of confined zinc surfaces exposed under periodic wet-dry conditions, B19-B22, s.l. Electrochem. and Solid-State Lett. (2001), Vol. 4.
- [44] **D. Persson, S. Axelsen and D. Thierry**, In situ studies of the corrosion during drying of confined zinc surfaces, B7-B10, s.l. Electrochim. and Solid-State Lett. (2001), Vol. 4.
- [45] **H. Rohrer and G. Binnig**, Scanning tunneling microscopy, 355- 369, s.l. IBM Journal of Res. and Development, (1986), Vol. 30.
- [46] **H. Rohrer and G. Binnig**, Scanning tunneling microscopy, 236-244, New York: Surf. Sci. (1983), Vol. 126.
- [47] **H. Rohrer and G. Binnig**, Scanning tunneling microscopy, 726-735, s.l. Helvetica Phys. Acta, (1982), Vol. 55.
- [48] **H. Rohrer and G. Binnig**, Scanning tunneling microscopy - from birth to adolescence, 615-625, s.l. Rev. of Mod. Phys. (1987), Vol. 59.
- [49] **G. Binnig, H. Rohrer, C. Gerber and E. Weibel**, Tunneling through a controllable vacuum gap, 178-180, s.l. Appl. Phys. Lett. (1982), Vol. 40.
- [50] **A. Fujishima and K. Honda**, Electrochemical photocatalysis of water at a semiconductor electrode, 5358-5359, s.l. Nat. (1972), Vol. 238.

- [51] **B. Li, S. Wu and X. Gao**, Theoretical calculation of a TiO<sub>2</sub>- based photocatalyst in the field of water splitting: a review, 1080-1103, s.l. Nanotechnol. Rev. (2020) , Vol. 9.
- [52] **S. Banerjee, S.C. Pillai, P.Falaras, D.D. Dionyioou, K.E. O'shea and J.A. Byrne**, New insight into the mechanism of visible light photocatalysis, 2543-2554, s.l. Phys. Chem. Lett. (2014), Vol. 5.
- [53] **M.K. Nazeeruddin, A. Kay, I. Rodicio, R. Humphry-Baker, E. Muller and P. Liska**, Conversion of light to electricity by cis-X<sub>2</sub>bis (2,20-bipyridyl-4, 40-dicarboxylate) ruthenium, 6382-6390, s.l. Am. Chem. Soc. (1993), Vol. 115.
- [54] **K. Kalyanasundaram and M. Grätzel**, Applications of functionalized transition metalcomplexes in photonic and optoelectronic devices, 347-414, s.l. Coord. Chem. Rev. (1998), Vol. 177.
- [55] **G. Di. Marco and N. Genitori**, Synthetic, natural and bioinspired dyes as TiO<sub>2</sub> sensitizers in sustainable solar cells, Messina, Italy : Elsevier Inc, (2021).
- [56] **I.P. Parkin and R.G. Palgrave**, Self-cleaning coatings, 1689-1695, s.l. Mater. Chem. (2005), Vol. 15.
- [57] **L. Zhang, R. Dillert, D. Bahnemann and M. Vormoor**, Photo-induced hydrophilicity and self-cleaning: models and reality, 7491-7507, s.l. Energy Environ. Sci. (2012), Vol. 5.
- [58] **S. Nishimoto and B. Bhushan**, Bioinspired self-cleaning surfaces with superhydrophobicity, superoleophobicity, and superhydrophilicity, 671-690, s.l. RSC Adv. (2013), Vol. 3.
- [59] **F.Ç. Cebeci, Z. Wu, L. Zhai, R.E. Cohen and M.F. Rubner**, Nanoporosity-driven superhydrophilicity: a means to create multifunctional antifogging coatings, 2856-2862, s.l. Langmuir, (2006), Vol. 22.
- [60] **G.D. Bixler and B. Bhushan**, Rice and butterfly wing effect inspired low drag and antifouling surfaces: a review, 1-37, s.l. Solid State Mater. Sci. (2014), Vol. 40.
- [61] **A.L. Linsebigler, G. Lu and J.T. Yates**, Photocatalysis on TiO<sub>2</sub> surfaces: principles, mechanisms, and selected results, 735-758, s.l. Chem. Rev. (1995), Vol. 95.
- [62] **M. Ni, M.K.H. Leung, D.Y.C. Leung and K. Sumathy**, A review and recent developments in photocatalytic water-splitting using TiO<sub>2</sub> for hydrogen production, 401-425, s.l. Renew. Sustain. Energy Rev. (2007), Vol. 11.
- [63] **E. Selli and M.V. Dozzi**, TiO<sub>2</sub>-based materials for photocatalytic hydrogen production, Milan, Italy, Elsevier Inc. (2021).

## **Chapter II**

# **Theoretical background of adsorption and dynamics of water on rutile (110) surface**

In this part, we will discuss in more details in general the adsorption phenomenon taking into account the different types and the forces that can take place at the interface adsorbent-adsorbate. Then water molecules-TiO<sub>2</sub> interactions will be presented where the rutile (110) surface is discussed plus the properties of H<sub>2</sub>O. This section is very important because it will be helpful when modeling water adsorption in the third chapter of this manuscript.

## II.1. Introduction

The objective of this chapter is describing separately the structure of rutile (110) surface and isolated water molecule ( $\text{H}_2\text{O}$ ) moving to their mutual interactions. We will start off by presenting in general the adsorption process as a special case from the surface phenomena with basic notation about the types of adsorption and interactions, also we will describe the most important factors affecting the adsorption and the isotherms used to quantify it. To this end, we used this information to investigate the behaviour of  $\text{H}_2\text{O}$  on the rutile (110) surface.

## II.2. Surface phenomenon

The surface of any material is a special case from the bulk because the discontinuity of the periodicity creates dangling bonds on the surface, which are promoted to external species (molecules, atoms and ions) that react with it [1, 2]. The physical boundary resulting from this contact is called interface; according to the nature of phases, there exist five types of interfaces: gas-liquid, gas-solid, liquid-liquid, liquid-solid, solid-solid. Many phenomena and processes occur at these interfaces, such as sorption (adsorption, absorption), desorption, diffusion and dissociation as illustrated schematically in **Figure II.1** [3-5].

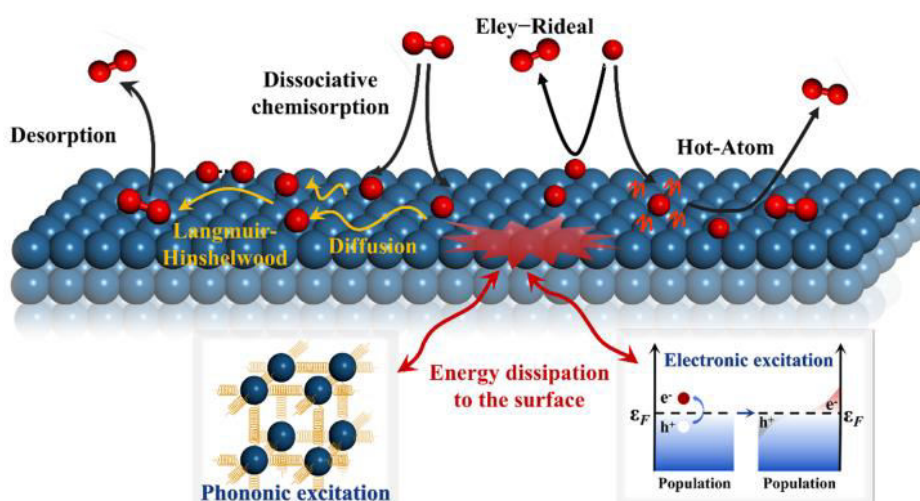


**Figure II.1:** Schematic representative of different reactions occurring on surface [6].

## II.3. Adsorption phenomenon

Adsorption is considered a complementary technique to conventional purification water and waste water processes in particular to remove dissolved impurity substances due to its advantages such as simplicity, low price, easy maintenance and high efficiency [7]. To explain the adsorption phenomenon in the simplest way using the simplified system, this reaction was held under fixed temperature and pressure [8]. The adsorption is the sticking of molecules, ions or atoms from



liquids, gases or solids called (adsorbate) onto the surface called (adsorbent) [9] as summarised in the following **Figure II.2**. Adsorption is distinguished from absorption which refers to molecules penetrated in bulk. The molecules adsorbed onto the surface in one of two ways elastically or inelastically depending on the exchange of energy between the adsorbate and the adsorbent. In elastics, the molecules booming on a surface remain in space with no interaction, or its dearth energy the desertion from the surface, its outcome adsorbed in a short time and desorbed. Desorption is the inverse process of sorption (adsorption, absorption). In inelastic, the molecules adsorbed on the surface in shallow and deep potential. The shallow potential wells, a weak energy corresponding to this reaction summarised in van der Waals forces is called (physical adsorption) or strong interactions with covalent, ionic bonds under name of (chemical adsorption) [10-12], the adsorption and desorption rates investigate the equilibrium on the surface.

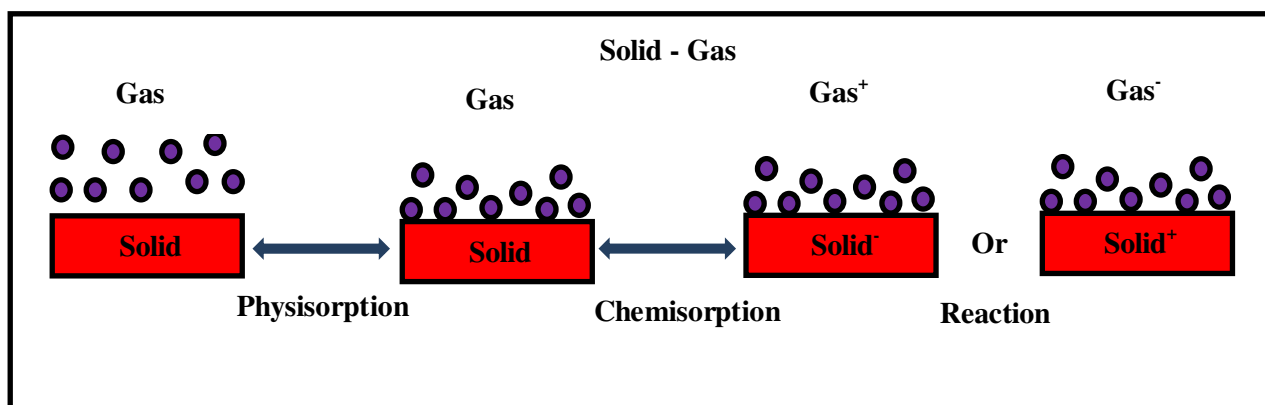


**Figure II.2:** Simplified schematic of gas –solid adsorption system.

### II.3.1. Physical and chemical adsorption

The interaction bonds between the adsorbate and adsorbent are physical adsorption (physisorption) rather than chemical adsorption (chemisorption) [13-14]. The first, characterised with: low adsorption energy ranging from 10 to 40 KJ/mole, the molecules heal the adsorbent surface by a weak bond called van der Waals forces, subsequently, the molecules still relatively free on surface and diffuse with no electron transfer from surface and molecules (aqueous) or the inverse at low temperature, to relatively at high temperature, the molecules approaches on the surface linked by strong bonds (covalent, ionic and metallic) with high adsorption energy ranging from 100 to 400 KJ/mole, which lead to exchange of electrons between adsorbate and adsorbent [15]. Generally, the most important in these types of reactions is the amount of molecules adsorbed on surface; it is often expressed with a graph as function of pressure at constant temperature and is

expressed by adsorption isotherm. The adsorption isotherm is the curve describing the relationship between the mobility of adsorbate in aqueous space to surface (adsorbent) at constant temperature and pH [16]; different scientists have developed different kinds of adsorption isotherms. The following **Table II.1** summarised the difference between physical and chemical adsorption.

<b>Properties</b>	<b>Chemisorption</b>	<b>Physisorption</b>
Specificity	High- specific	Non- specific
Activation energy	Does not require high activation energy	Require high activation energy.
Heat of adsorption	100 to 400 Kj/mole	10 to 40 Kj/mole
Nature de liaison Chimique	Strong (covalent or ionic bond )	Weak (Van der Waals)
Desorption	Difficult	More or less perfect
Adsorption kinetic	Slow	Fast
State of surface	Maximum monolayer	Formation of multilayer

**Table II.1:** The difference between physisorption and chemisorption [17] and references therein.

In the presence of physisorption several forces bring in including dispersion forces, repulsive forces, electrostatic (columbic) which are responsible for the adsorption of polar molecules or by surfaces with a permanent dipole where both interactions. There are under van der Waals forces (named so for their Dutch physicist Johannes Diderik van der Waals).

### **II.3.2. Van der Waals forces**

The ideal law description is extracted from myriad approaches. In 1834; Emile Claperon is combined between the Boyle's and Charles laws to express the elegant linear relationship between volume and temperature as the equation below indicates for ideal gas (17):

$$P.V = n.R.T \quad (\text{II. 1})$$

Where:

$P$ ,  $V$ ,  $n$ ,  $R$  and  $T$  are the pressure of gas (Pa), volume ( $\text{m}^3$ ), amount of substance (mole), ideal gas constant ( $\text{J K}^{-1} \text{mol}^{-1}$ ) (which is the link between microscopic energy and macroscopic temperature) and temperature (K), respectively [18].

For more accurately in the real gasses the van der Waals equation is given bellow:

$$p = \frac{n R T}{(v-n b)} - a \frac{n^2}{v^2} \quad (\text{II. 2})$$

Where:

$a$  and  $b$  are constants corresponds to the attractive forces and extended volume, respectively.

### II.3.2.1. Intermolecular Potential

The van der Waals' forces interaction were predicted to be of molecular scale but the form of the intermolecular potential between the two atoms or molecules as a function of distance  $U(R)$ , was unknown, with the long efforts to determine this potential, a noteworthy advance after the description of the potential energy between two interacting molecules used  $\eta = 6$  and item 12 correspond to repulsive force [19, 20] as indicating in equation (II. 3)

$$U(R) = 4 \varepsilon \left[ \left( \frac{\sigma}{R} \right)^{12} - \left( \frac{\sigma}{R} \right)^6 \right] \quad (\text{II. 3})$$

Where:

$\varepsilon$  and  $\sigma$  are the depth of the potential well (dispersion energy) and the distance at which the particle –particle potential energy is zero (the size of the particle).

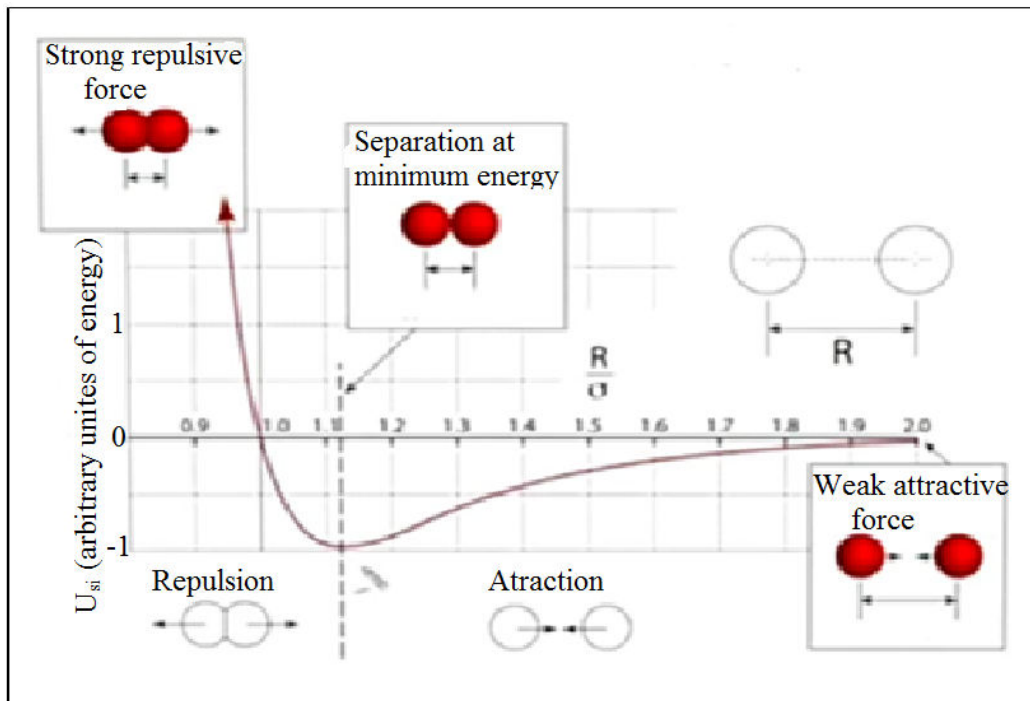


**Figure II.3:** The Lennard-Jones 6-12 potential, which represents the relationship between the distance of two atoms and the energy of system, the equilibrium distance between the interacting atoms are at  $R = R_0$  [21].

The favourable species become spontaneously closer together ( $R = R_0$ ). Corresponds to the random collision), contrary is unfavourable for the distance is very short (long) from  $R_0$  because at  $R \approx$  infinity the potential energy go to zero deal to weak attraction force, whereas at  $R \approx 0$  the potential energy go to infinity this correspond to strong repulsive force, a representative plot of this potential is shown in **Figure II.3**.

## **II.4. Kinetics and specificity of adsorption**

Adsorption kinetics is a curve that allow to describe the rate of adsorption at gas or aqueous species, this kinetics is governed by many factors including the residence time of molecules on surface and the speed of reaction, the nature of adsorbate and adsorbent, rough and porous medium [22, 23] and this appears clearly in some solids that have a good adsorbent properties unlike others.

### **II.4.1. Nature of adsorbent**

The potential of a wide range of solid materials as adsorbents have been investigated so far, therefore, these adsorbents are either natural or engineered materials. Various researchers are classified its by many groups including a) naturally occurring materials (e.g. diatomaceous earth, clay), (b) activated natural materials for intended applications (e.g. activated carbon), (c) synthetic materials (e.g. polymers, zeolites), (d) agricultural solids and industrial (e.g. rice husk, wheat bran, orange peels) and (e) biosorbents (e.g. chitosan bacterial biomasses) [24-26], however, the adsorption depends strongly on the nature of the adsorbent, where different solids adsorb different amounts of the same liquid (gas) even under similar conditions, because each adsorbent has unique characteristics, thus, it moderates the adsorption capacity and dynamics of the adsorbate including the particles size, surface area, wettability, pore size distribution, pore structure, bulk density including the hydrophobic and hydrophilic behaviour and defects [27]. Therefore, the rough, finely divided and porous surface of the adsorbent leads to large adsorption, whereas a smooth or fine surface reaches the equilibrium shortly. In addition, increases in surface area result in greater adsorption. Besides, when a liquid approaching the solid surface, many processes may happen: this liquid can spread onto all the surface corresponding to  $0^\circ$  contact angle, in inverse the surface can repel the liquid to the droplet form corresponding to  $180^\circ$  contact angle and this is the other possibility, the molecules are moving on surface at certain contact angle its stopped, however, the determination of wettability is very important in many disciplines including adhesion, lubrication, friction, coating operations, catalysis and in chemical, mechanical, mineral, microelectronics, biomedical and biological industries [28].

#### **II.4.2. Nature of adsorbate**

The determination properties of the adsorbate are not less interest compared with the adsorbent, because it plays a pivotal role in the adsorption. For example: the particle size of the adsorbate should be comparable with the pore and rough size of the adsorbent and the molecules that make up the surface. In spite of this, a general rule, the neutral surface adsorbs only neutral solution and the polarisation surface adsorbs the polarisation of molecules [29, 30]. In addition, the saturate molecules are low adsorbed on surface. The most molecules adsorbed on the surfaces are classified from fort to low adsorption: acids and bases > alcohols and thiols > aldehydes and ketone > derives halogens and esters > hydrocarbons no saturates > hydrocarbons saturates.

#### **II.4.3. Temperature and pressure**

Temperature and pressure are considered as key parameters in the adsorption dynamics, where initially the adsorption increases by increasing pressure till the equilibrium has no effects on it, as well as the adsorption extended decreases with increasing the temperature.

The reaction kinetics includes how the conditions influence the speed of reaction and resulting information about the reaction mechanism.

#### **II.5. Classification of adsorption isotherms**

The adsorption isotherms describe the interaction pathway between the adsorbate and the adsorbent by some equations that can quantify the amount adsorbed on the surface at fixed temperature. According to the shapes of isotherms, the international union of pure and advanced chemistry (IUPAC) [31] convention have been divided the adsorption isotherms into eight main types, as illustrated in **Figure II.4**.

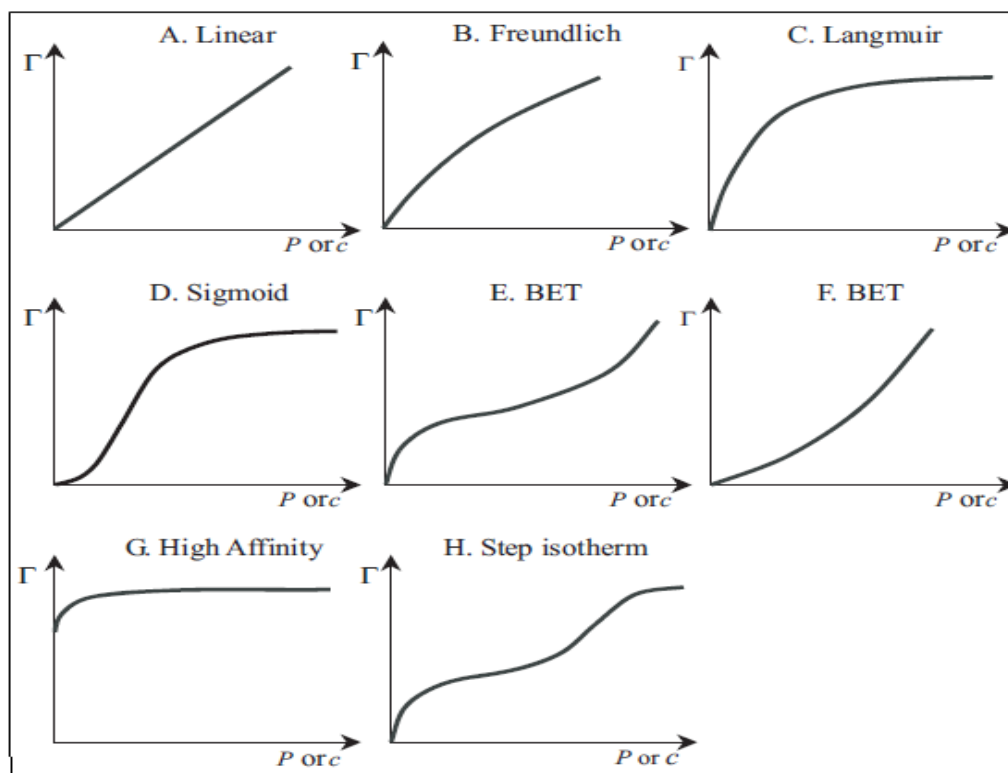


**Figure II.4:** The IUPAC classification of the adsorption isotherms [30]

**Type A (Linear):** The amount of adsorbed molecules increase linearly as function of pressure or concentration at constant T, this type described as the Henry adsorption isotherm [30-32], the linear isotherm is not obvious for presenting reaction mechanism [33].

$$\Theta = K_H P \quad (\text{II. 4})$$

Where:

$K_H$ ,  $P$  and  $\Theta$  are a constant ( $\text{mole m}^{-2} \text{Pa}^{-1}$ ) for gases and ( $\text{L/m}^2$ ) for solutions, pressure and the amount of adsorbed molecules on surface, respectively.

**Type B (Freundlich):** Is the most popular isotherm because unrestricted monolayer- multilayer adsorption, thereby, is often taken to indicate at which the monolayer is complete and the multilayer about to begin. Which is described by the equation of Freundlich (where  $q < 1$ ) [34]:

$$\Theta = K_F P^q \quad (\text{II. 5})$$

Where:

$K_F$  and  $q$  are constants.

**Type C (Langmuir):** Is called Langmuir adsorption isotherm according to Langmuir adsorption equation:

$$\theta = \frac{K_L P}{(1 + K_L P)} \quad (\text{II. 6})$$

Where:

$\theta$  and  $K_L$  are the coverage of surface and the constant of Langmuir.

This type is considered as useful isotherm by several researchers for not substantially large porous size of solids and for reversible reactions, especially when interest to study only the reaction in monolayer [35], thus it characterized the microporous adsorbents [36].

**Type D (sigmoid):** This model used to indicate the lateral interaction between adsorbed molecules; that means before the monolayer is saturated the molecules accumulate to create multilayer and this balance the changes in the direction.

**Type E and F (BET):** These isotherms models are most used widely to describe multilayers (physical adsorption), which encountered to the steps in the **Figure II.** (4E and 4F).

**Type G (high affinity):** This type is an extended case of Langmuir curve where the adsorbate has extremely high affinity for the adsorbent especially at low temperature; the adsorbate is almost completely adsorbed [37].

**Type H (step isotherm):** This isotherm encountered a porous medium, which leads to a small interactions between adsorbate and adsorbent, thus, the knees indicate the completion of monolayer [38-40].

We extend our description to study the behaviour of water molecules on rutile  $\text{TiO}_2$  (110) surface, as consequence rutile (110) has become the most exciting model system owing to its outstanding in wide disciplines like catalysis, electric devices and earth sciences due its photostability, chemical inertness, nontoxicity, low cost oxide [41] and high stability under (UHV) conditions and strong photocatalytic activity [42] besides, in the laboratory is a very useful sample because it can be elaborated by no expensive techniques like spin coating and physical vapor deposition (PVD), along with this, we can change its properties easily by annealing and spurting to enhance region of absorption therefore it is a premium system to test new ideas and approaches, in addition, it exists so much known about this system. In the following section we will discuss the most important features and characteristics of water onto rutile (110).

## **II.6. Rutile TiO<sub>2</sub> (110) surface**

Among the three different crystallographic surfaces, rutile has attracted increasing interest from researchers compared with brookite and anatase [43]. In rutile the octahedron shows a slight orthorhombic distortion and has three different index faces (110), (001) and (100) as presented in the **Figure II.5**. Rutile (110) is a face resulting from the slab cut of the optimised bulk structure along the (110) plane and terminated on an atomic layer to ensure the electrostatic stability of the slab. It was chosen because it is the most stable under atmospheric pressure and room temperature conditions and has excellent optical, mechanical and chemical properties [44, 45]. In addition, the surface energy of rutile (110) is 1.78 J/m<sup>2</sup>[46]. The stoichiometric surface of rutile TiO<sub>2</sub> (110) (1x1) contains an alternative rows of oxygen (O<sub>3c</sub>) and five coordinate titanium (Ti<sub>5c</sub>) with one dangling bond along the [001] direction, whereas the oxygen bridging (O<sub>2c</sub>) located above the six fold coordinate titanium (Ti<sub>6c</sub>), due to their under saturation, bridging oxygen atoms can be easily released from TiO<sub>2</sub> surface giving rise to oxygen vacancies (O<sub>v</sub>) which act as the reactive site on TiO<sub>2</sub> (110) [47, 48]. The O<sub>v</sub>'s can be created with various experimental techniques including UV irradiation, electron bombardment and thermal annealing, detected by scanning tunnelling microscopy (STM) images that evidence O<sub>v</sub>'s as bright spots, which can be statistically counted, as represented in **Figure II.6** [49]. In addition, TiO<sub>2</sub> surface constitutes a major part of the bulk TiO<sub>2</sub> and is considered to be an essential model metal oxide system for the study of water chemistry; the rutile (110) surface was reconstructed for charge auto-compensation; the (110) oxygen terminated surface is non-polar and hence a dipole free surface was ensured [50].



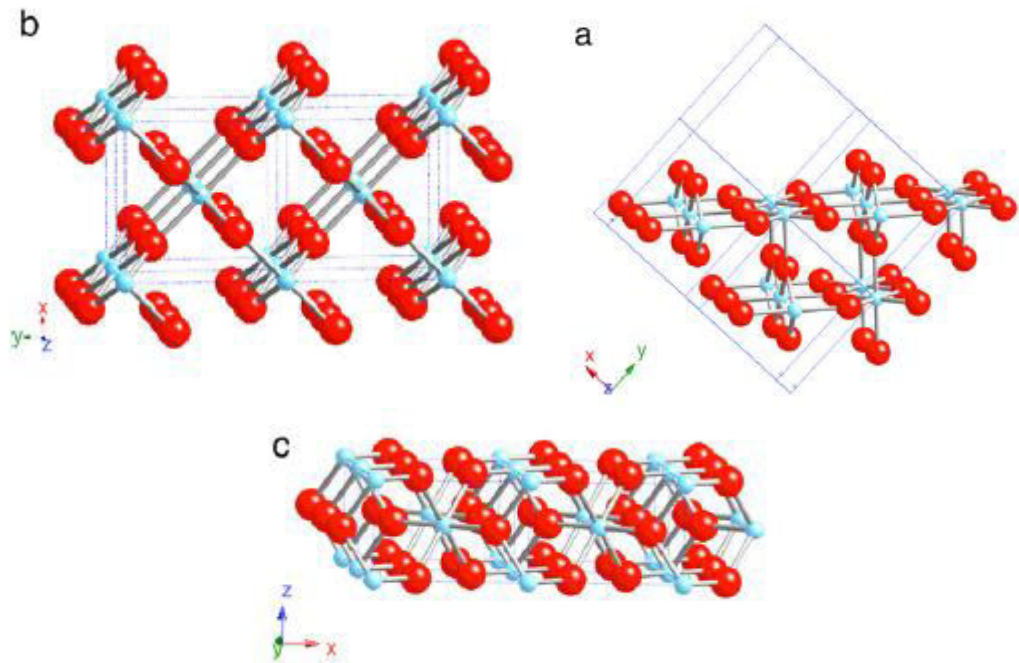


**Figure II.5:** The faces of rutile: (a) (110); (b) (100); (c) (001), taken from [51].

Each O released from the surface leaves behind two valence electrons occupying the Ti 3d orbitals and creating an energy state at 0.8 eV below the Fermi level. Along of this, these defects electrons play an essential role at the surface chemistry of  $\text{TiO}_2$ , which reduces the  $\text{Ti}^{4+}$  to  $\text{Ti}^{3+}$  [52]; besides, this finding is improved with many methods such as ultraviolet photoelectron spectroscopy [53].

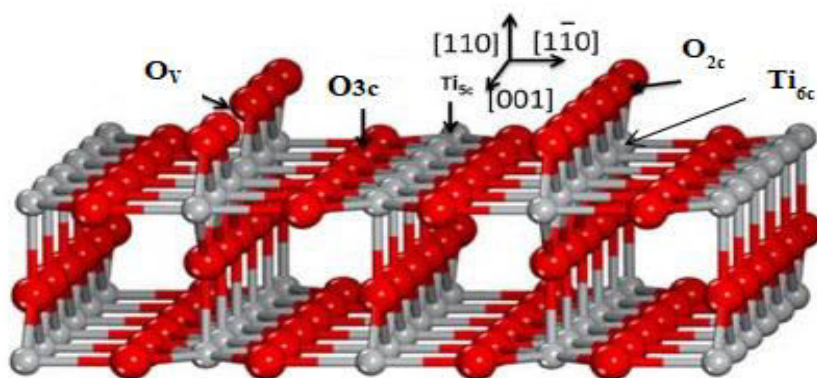


**Figure II.6:** The structure of rutile (110) (1x1), red (grey) balls are oxygen (titanium) atoms, taken from [54].

## II.7. Water properties

Water is an inorganic item and the ultimate renewable resource because it is constantly replenished in a cycle of evaporation and precipitation. The water molecules compound is discovered by the experience of Cavendish and Lavoisier in 1780 [55], which is constructed from one atom of oxygen is linked with two hydrogen atoms with bond distance around  $d_{\text{OH}} = 0.964 \text{ \AA}$  [56] by covalent bond and the corner angle  $\text{H}\hat{\text{O}}\text{H}$  is  $104^\circ$  as in **Figure II.7**, in addition, the difference between the charges create a strong polarity of water.  $\text{H}_2\text{O}$  is considered by wide researchers as complicated substance in view of its physical and chemical properties, which exists in three different cases gas, ice and liquid, it's has high dielectric constant,  $\text{H}_2\text{O}$  has well known temperature of fusion ( $0^\circ \text{C}$ ) and boiling ( $100^\circ \text{C}$ ) and the high capacity for heat storage is necessary in nature as well as in humans daily life and the water has a low density and others properties like viscosity, thermal conductivity and surface tension is well defined in [57, 58]. Therefore, water plays an active role especially at the interfaces, but if the readers wish to obtain more information about its description is referenced in [59].

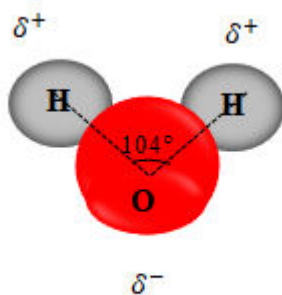


**Figure II.7:** The water molecule structure, red (grey) balls are oxygen and hydrogen atoms.

## II.8. Water adsorption onto rutile $\text{TiO}_2$ (110) surface

The interactions of  $\text{H}_2\text{O} - \text{TiO}_2$  interfaces has been an extensive subject in the last decades owing to their photocatalytic activity [60], especially in splitting of water resulting in green hydrogen, which is used as an alternative fuel to reduce greenhouse and pollutants [61, 62]. One of the most important influencing factors on adsorption itself is the pH of the surface. This latter effects the adsorption of water on the rutile (110) surface, thus at  $\text{pH} > (\text{pH}_{\text{pzc}} = 6.6)$  this surface has a neutral charge. But at  $\text{pH} > \text{pH}_{\text{pzc}}$  the surface is negatively charged whereas at  $\text{pH} < \text{pH}_{\text{pzc}}$  the surface is positively charged [63] as presented in **Figure II.8**. In this way, an alternative resolution of the adsorption of water on rutile (110) surface was developed in 1998 using first

principal molecular dynamic simulation to calculate the hydrogen vibrations for water (H-O-H) and hydroxyl (O-H) bonding bond; the purpose of this simulation is to determine whether water is adsorbed molecularly or dissociative on the surfaces [64]. Since then, the microscopic behaviour of H<sub>2</sub>O molecules on the rutile (110) surface is a matter of debate, to understand well these interactions between H<sub>2</sub>O molecules and the rutile (110) surface; we indicate that the most important vibrations that occur at the interfaces, as drawn in the following **Figure II.9**.

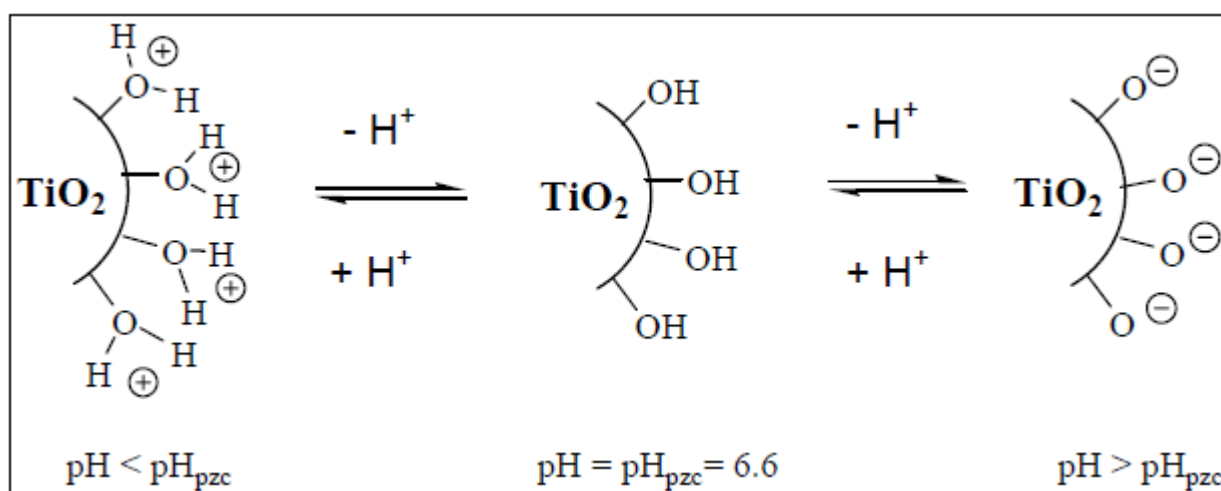


**Figure II.8:** The modification charge of rutile (110) surface depended on the pH factor [63].

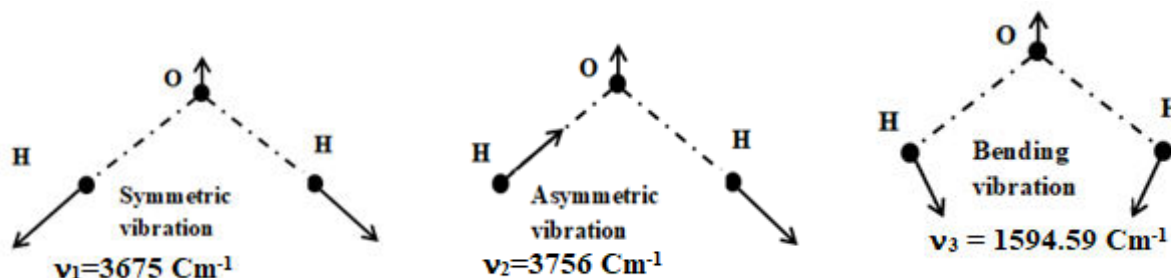


**Figure II.9:** The vibrational modes of isolated water molecule, dashed lines are the bonds of O-H and the arrows represent the relative and displacement direction of the nuclei [65].

We distinct two phases within the adsorption of water molecules on the rutile (110) surface: monolayer and multilayer. In multilayer H<sub>2</sub>O molecules diffuse rapidly and bind weakly on the surface. However, only the monolayer is strongly affected by the electric field of the surface because the dipole moment of water decays away from the surface [66], resulting in a hydrogen bond considered as an essential part of the interaction H<sub>2</sub>O-rutile (110) surface. Therefore, the relation between hydrogen bond strength and its vibration frequencies with stretching modes of water was mentioned in **Figure II.9**, these vibrational properties of H<sub>2</sub>O molecules have been used to identify and characterize the modes of water adsorption on surface [67]. H<sub>2</sub>O molecules adsorbed

on surface often accompanied by one or more preferential orientations mode of the molecule, usually its can be the oxygen-end down and one or both O-H away from the surface [68]. Indeed the most reliable term in the presence of the molecular adsorption is the vibrational bending (H-O-H) between [1590-1640]  $\text{cm}^{-1}$  corresponds to molecular form whereas symmetry and asymmetry stressing vibrations correspond to the hydroxyl groups (O-H) bending on surface in region 3200 - 3700  $\text{cm}^{-1}$  [68, 69].  $\text{H}_2\text{O}$  molecules stacked with cautions Ti with a covalent bond, whereas linked with second layer through hydrogen bond, several reviewers indicate that this interaction heavily depends to the orientation of water molecules on monolayer or with other way, the water dipole moment vectors in this surface rutile (110) between the first and second monolayer and the solidity of the first monolayer [70], thus,  $\text{H}_2\text{O}$  diffuses slowly and bonded strongly on surface, which competes with rutile (110) active sites. Overall, monolayer has the best limited applicability to understand the  $\text{H}_2\text{O-TiO}_2$  interface in aqueous and wet environments. Many theoretical and experimental measurements such as Monte Carlo, DFT, STM and FTIR-ATR have been carried out to study this type of interactions [71]; it is worth noting that in one hand, oxygen of water is linked with a chemical bond on under-coordinate  $\text{Ti}_{5c}$  atoms and as an H-bonding species on under-coordinated  $\text{O}_{2c}$  atoms. On the other hand, water molecules dissociate on the surface by two deferent types: thermal dissociation or light absorption and particle bombardment for creating two hydroxyl groups (As shown in **Figure II.10**).

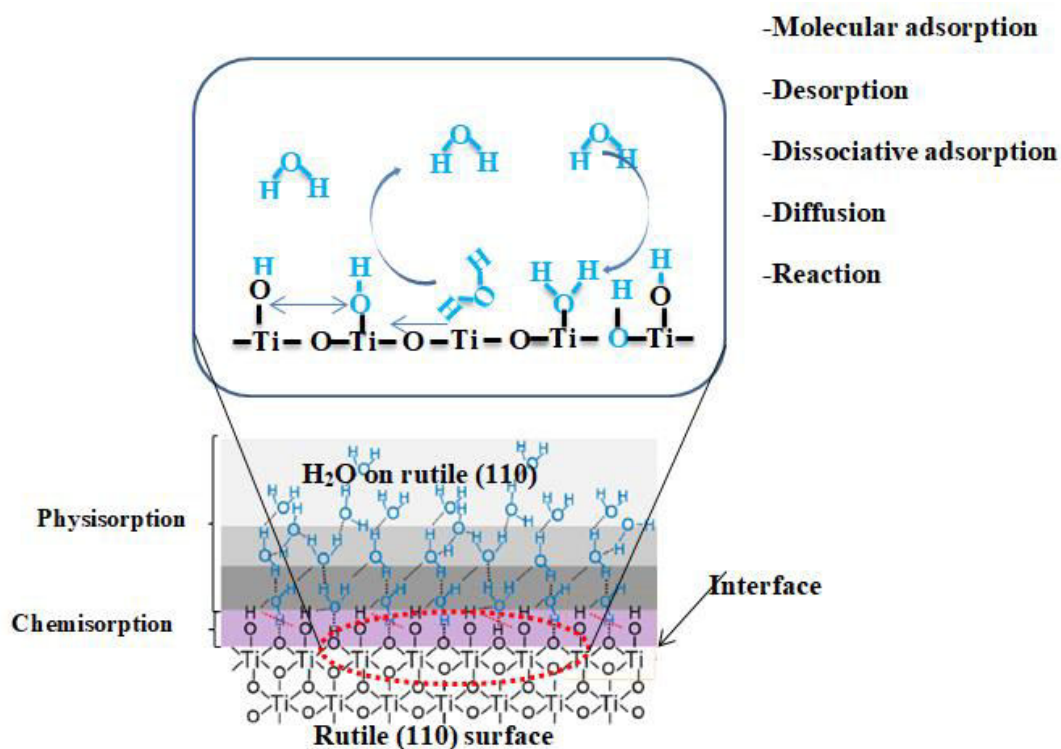


**Figure II.10:** Schematic illustrating the interactions of  $\text{H}_2\text{O}$  molecules on rutile (110) surface.

Taken and modified from [72].

H<sub>2</sub>O dissociates at Ti<sub>5c</sub> sites on a perfect surface; indeed, the surface structure known to significantly effects on the surface chemistry which giving rise favour the dissociation of water on defects, it's considered as direct active sites leads to the formation of OH hydroxyls group species [73], usually the dissociation on oxide surfaces is reversible and irreversible at metals and semiconductors but these results are controversy between them. Recently, Henderson et al., has shown and demonstrated that water dissociation on the rutile (110) face is much less facile than (100) face, to this way, Hugensmidt et al. reported that 25 % of H<sub>2</sub>O in the monolayer is dissociates. However, this phenomenon is not well understood and it's still under debate till now, because despite their correct explanation, these interactions are not well simulated by typical computational methods, such as density-functional theory which cannot accurately treat long-range interactions in weakly bound systems [74] and one of limitation of in situ FTIR-ATR spectroscopy cannot provide full three-dimensional information about water, in addition, didn't show the absolute the sites occupied but sufficient to improve the presence on molecules according its vibrational as indicating in **Figure II.11**. However, they could not unambiguously determine the atomic coordinates of this hydration layer, so the definitive way of the water behaviour on surface was not determined and understood till now.

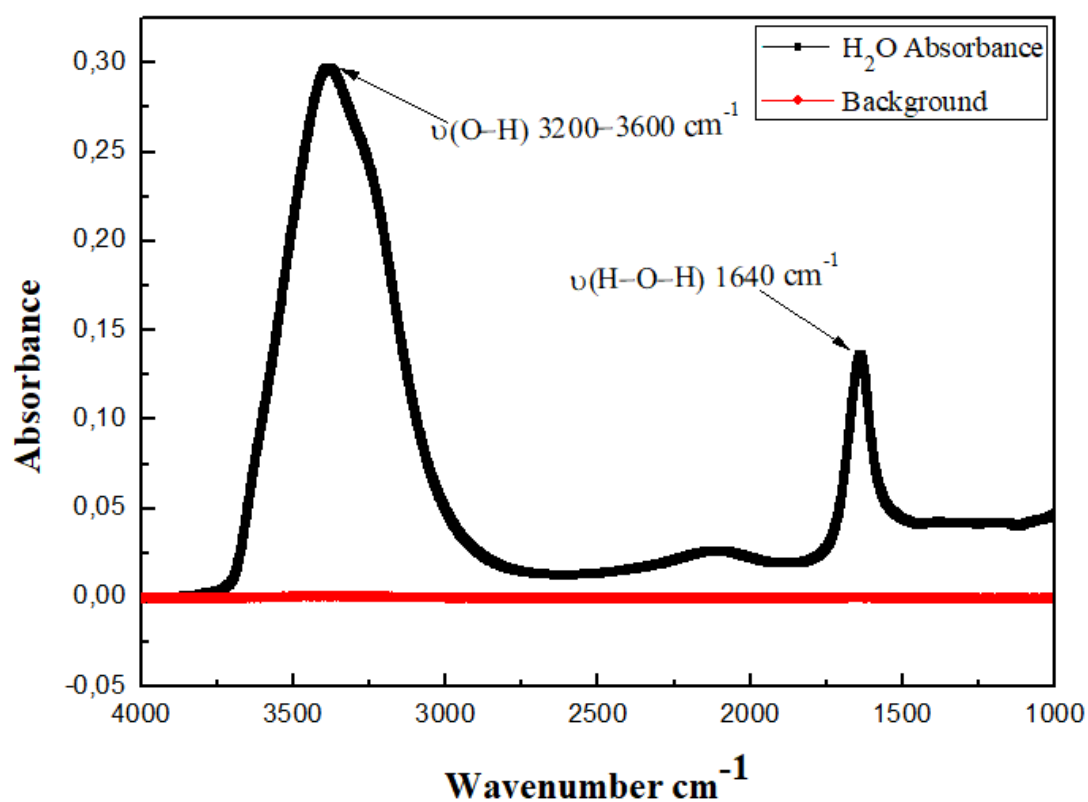


**Figure II.11:** FTIR-ATR spectrum of water adsorption on TiO<sub>2</sub> surface (dark line), pink line correspond to background. The spectra are kindly provided by Ahmed Bouhekka [75].

Therefore, in this study we address a number of issues not covered in the previous investigations. By using a theoretical system supported by Langmuir model, with taking an account all available sites on rutile (110) stable surface cases and water behaviour with them.

## **II.9. Conclusion**

In this chapter, we present the surface phenomena especially the adsorption process and its importance in the modern technology as prevent in photocatalysis with the most important factors influencing it and the corresponding equations used to quantify the adsorption isotherms, along of this way, we show also both of water and rutile (110) composition and their interactions and dynamics at the interface. In view of the inconclusive debate between the finding results in recent studies, we propose in next chapter a theoretical model based on the previous literatures taking into account all the possible mechanisms of H<sub>2</sub>O - rutile (110) interactions over the surface.

## References

- [1] **K.Y. Hameed and B.H. Foo**, An overview of landfill leachate treatment via activated carbon adsorption process, 54–60, s.l. Hazard Mater. (2009), Vol. 171.
- [2] **H.J. Kreuzer, S.H. Payne, A. Drozdowski and D. Menzel**, Theory of dissociative and nondissociative adsorption and desorption, 6982–6999, s.l. Chem. Phys. (1999), Vol. 110.
- [3] **F. Rouquerol, J. Rouquerol, K.S.W. Sing, P. Llewellyn and G. Maurin**, Adsorption by powders and porous solids: principle, methodology and applications, s.l. Academic Press, (2012).
- [4] **F.M. Propst and T.C. Piper**, Detection of the vibrational states of gases adsorbed on tungsten by low-energy electron scattering, 53-56, s.l. Vac. Sci. Technol, (1967), Vol. 4.
- [5] **H. Guo and B. Jiang**, Dynamics in reactions on metal surfaces: a theoretical perspective, 180901-180917, s.l. Chem. Phys. (2019), Vol. 150.
- [6] **A.C. Luntz**, In surface and interface sciences: solid-gas interface II, s.l. Wiley-VCH Verlag, (2015).
- [7] **X. Guo and J. Wang**, Adsorption kinetic models: physical meanings, applications, and solving methods, 122156-122226, s.l. Hazard Mater. (2020), Vol. 390.
- [8] **Z. Pinter**, Caractérisation des couches épaisses de semiconducteur  $\text{WO}_3$  et  $\text{WO}_3/\text{TiO}_2$  pour la réalisation de capteur à  $\text{NO}_2$ , PhD thesis, L'Institut National des Sciences, Appliquées de Lyon, France, (2002).
- [9] **P.W. Atkins**, Physical chemistry, s.l. Oxford University Press, Oxford, (1998).
- [10] **J.E. Lennard-Jones**, Processes of adsorption and diffusion on solid surfaces, 333-359, s.l. Trans. Faraday Soc. (1932), Vol. 28.
- [11] **J.D. Van der Waals**, Over de continuïteit van den gas- en vloeistofoestand, thesis, Leiden, Nederland, (1873).
- [12] **M. Kassir, T.R. Carmes, T. Hamieh, A. Razafitianamaharavo, O. Barres, J. Toufaily and F. Villieras**, Surface modification of  $\text{TiO}_2$  nanoparticules with AHAPS aminosaline: distinction between physisorption and chemisorption, 1197-1209, s.l. Adsorpt. (2013), Vol. 19.
- [13] **R. Miranda, S. Daiser, K. Wandelt and G. Ertl**, Thermodynamics of xenon adsorption on  $\text{Pd}(s)[8(100) \times (110)]$ : from steps to multilayers, 61-91, s.l. Surf. Sci. (1983), Vol. 131.
- [14] **K. Kern, R. David, P. Zeppenfeld and G. Comsa**, Registry effects in the thermodynamic quantities of Xe adsorption on  $\text{Pt}(111)$ , 353-370, s.l. Surf. Sci. (1988), Vol. 195.
- [15] **J.M. Thomas and W.J. Thomas**, Principles and practice of heterogeneous catalysis, weinheim: wiley, (1996).
- [16] **M.M. Khan and M. Jawaid**, Polymer-based nanocomposites for energy and environmental applications, composites science and engineering, s.l. Elsevier, (2018).



- [17] **P.W. Atkins**, Physical chemistry, 25-30, s.l. Oxford university press, Oxford, (1994).
- [18] **J.E. Jones**, Adsorption on the determination of molecular fields, from the equation of state of a gas (Chapter II), 463-477, s.l. Proc. Soc. Lond. A, (1924), Vol. 106.
- [19] **H.K. Onnes**, Expression of the equation of state of gases by means of series, 125-147, Amsterdam: Proc. Sect. Sci. (1901), Vol. 4.
- [20] **J.E. Lennard-Jones**, Processes of adsorption and diffusion on solid surfaces 'Cohesion', 333-359, s.l. Proc. Phys. Soc. (1931), Vol. 43.
- [21] **L.J. Lapidus**, Lennard -jones potential, s.l. Creative Commons Attribution- Non Commercial-Share Alike 4.0, (2023).
- [22] **D. Guignard**, L'essentiel de la cinétique et de la thermodynamique chimique, 85-96, Eyrolles, Paris, (1992).
- [23] **E.G. Dégréement**, Polyamines adsorbées sur silice caractérisation physico-chimique: application au traitement des eaux (étude préliminaire), PhD thesis, Lille, France, (1996).
- [24] **M.A. Barakat**, New trends in removing heavy metals from industrial wastewater, 361-377, s.l. Arabian J. of Chem. (2011), Vol. 4.
- [25] **A. Dąbrowski**, Adsorption from theory to practice, 135-224, s.l. Adv. in Colloid and Interface Sci, (2001), Vol. 93.
- [26] **K. Singh and M.A. Renu**, Heavy metal removal from wastewater using various adsorbents: a review, 387-419, s.l. Water Reuse and Desalination, (2016), Vol. 7.
- [27] **F. Bux and D. Gusain**, Batch adsorption process of metals and anions for remediation of contaminated water, s.l. Taylor & Francis Group, (2021).
- [28] **A.W. Adamson and A.P. Gast**, Physical chemistry of surfaces (6th ed), Wiley, New York, (1997).
- [29] **N. Bougdah**, Etude de l'adsorption de micropolluants organiques sur la bentonite, PhD thesis, Université de Skikda, Algeria, (2007).
- [30] **H.J. Butt, K. Graf and M. Kappl**, Physics and chemistry of interfaces, Weinheim: WILEY-VCH Verlag GmbH & Co. (2003).
- [31] **J.E. Shields, S. Lowell and M.A. Thomas**, Characterization of porous solids and powders: surface area pore size and density, 43-45, Kluwer Academic Publisher, Boston, MA, USA, (2004).
- [32] **C.H. Giles, T.H. Macewan and D.J. Smith**, Studies in adsorption, Part XI, a system of classification of solution adsorption isotherms, and its use in diagnosis of adsorption mechanisms and in measurement of specific surface areas of solids, 3973-3993, s.l. Chem. Soc. (1960), Vol.11.
- [33] **C. Letoquart, F. Rouquerol and J. Rouquerol**, Les chaleurs d'adsorption: expression des chaleurs d'adsorption physique, en termes d'énergie interne, à partir des données expérimentales, 559- 573, s.l. Chim. Phys. (1973), Vol. 70.



- [34] **H. Freundlich**, An adsorption in solutions, 89-146, s.l. Phys. Chem. (1906), Vol. 8.
- [35] **I. Langmuir**, Modelisation of adsorption, 1361-1403, s.l. Phys. Rev. (1915), Vol. 6.
- [36] **K.S.W. Sing, H.D. Everett, R.A.W. Haul, L. Moscou, R.A. Pierotti, J. Rouquerol and T. Siemieniewska**, Reporting physisorption for gas/solid systems with special reference to the determination of surface area and porosity, 603-619, s.l. Pure Appl. Chem. (1985), Vol. 57.
- [37] **A. Huitson and C.H. Giles**, A general treatment and classification of the solute adsorption isotherms, 755-777, s.l. Colloid Interface Sci. (1974), Vol. 47.
- [38] **J. Lyklema**, Fundamentals of interface and colloid science I: fundamentals, academic Press, San Diego, (1991).
- [39] **S. Brunauer**, The adsorption of gases and vapors, s.l. Princeton University Press, (1945).
- [40] **J.C.P. Broekhoff**, Mesopore determination from nitrogen sorption isotherm: fundamentals, scope, limitation, 633-684, s.l. Stud. Surf. Sci. Catal. (1979), Vol. 3.
- [41] **A. Naldoni, M. Altomare, G. Zoppellaro, N. Liu, S. Kment, R. Zboril and P. Schmuk**, Photocatalysis with reduced TiO<sub>2</sub>: from black TiO<sub>2</sub> to cocatalyst-free hydrogen production, 345-364, s.l. ACS Catal. (2019), Vol. 9.
- [42] **R. Lindsay, A. Wander, A. Ernst, B. Montanari, G. Thornton and N.M. Harrison**, Revisiting the surface structure of TiO<sub>2</sub> (110): a quantitative low-energy electron diffraction study, 246102-246106, s.l. Phys. Rev. Lett. (2005), Vol.3.
- [43] **K. Cao**, Surface science study of water and hydrogen adsorbed on rutile TiO<sub>2</sub> (110)-(1×1), Master thesis, Liuzhou, China, (2014).
- [44] **K. Asama and M. Shirasaki**, Compact optical isolator for fibers using birefringent wedges, 4296-4299, s.l. Appl. Optics. (1982), Vol. 21.
- [45] **M. Lazzeri, A. Vittadini and A. Selloni**, Structure and energetics of stoichiometric TiO<sub>2</sub> anatase surfaces, 155409-155418, s.l. Phys. Rev. B: Condens. Matter Phys. (2001), Vol. 63.
- [46] **P.M. Oliver, G.W. Watson, E.T. Kelsey and S.C. Parker**, Atomistic simulation of the surface structure of the TiO<sub>2</sub> polymorphs rutile and anatase, 563-568, s.l. Mater. Chem. (1997), Vol. 7.
- [47] **G. Pacchioni**, Oxygen vacancy: the invisible agent on oxide surfaces, 1041-1047, s.l. Chem. Phys. Chem, (2003), Vol. 4.
- [48] **U. Diebold**, Structure and properties of TiO<sub>2</sub> surfaces: a brief review, 681-687, s.l. Appl. Phys. A, (2003), Vol. 76.
- [49] **M. Ramamoorthy, D. Vanderbilt and R.D. King-Smith**, First principles calculations of the energetics of stoichiometric TiO<sub>2</sub> surfaces, 16721-16727, s.l. Phys. Rev. B, (1994), Vol. 49.
- [50] **H. Petek**, The interaction between adsorbed OH and O<sub>2</sub> on TiO<sub>2</sub> surface, 155-176, Progress in Surf. Sci. (2009), Vol. 84.

- [51] **M. Landmann, E. Rauls and W.G. Schmidt**, The electronic structure and optical response of rutile, anatase and brookite TiO<sub>2</sub>, 195503-195510, s.l. Phys. Condens. Matter. (2012), Vol. 24.
- [52] **R.L. Kurtz, R. Stock -bauer, T.E. Madey, E. Roman and J.L. De segovia**, Synchrotron radiation studies of H<sub>2</sub>O adsorption on TiO<sub>2</sub> (110), 178-200, s.l. Surf. Sci. (1989), Vol. 218.
- [53] **S. Leytner and J.T. Hupp**, Evaluation of the energetics of electron trap states at the nanocrystalline, 231-236, s.l. Chem. Phys. Lett. (2000), Vol. 330.
- [54] **X. Mao, Z. Wang, X. Lang, Q. Hao, B. Wen, D. Dai, Ch. Zhou, L.-M. Liu and X. Yang**, Effect of surface structure on the photoreactivity of TiO<sub>2</sub>, 6121-6127, s.l. Phys. Chem. C, (2015), Vol. 119.
- [55] **D. Eisenberg and W. Kauzmann**, The structure and the properties of water, Oxford, New York, (1969).
- [56] **W.S. Benedict, N. Gailar and E.K. Plyler**, Rotation-vibration spectra of deuterated water vapor, 1139–1165, s.l. Chem. Phys. (1956), Vol. 24.
- [57] **L. Theodore, R. Dupont and K. Ganesan**, Unit operations in environmental engineering, s.l. MA: Scrivener-Wiley, (2017).
- [58] **L. Theodore**, Chemical engineering: the essential reference, s.l. McGraw-Hill, new York, (2016).
- [59] **D. Eisemberg and W. Kauzmann**, The structure and propeerties of water, s.l. Oxford university press, (1969).
- [60] **T. Ohto, A. Mishra and S. Yoshimune**, Influence of surface polarity on water dynamics at the water/rutile TiO<sub>2</sub> (110) interface, 244102-244109, s.l. Phys. condens. Matter, (2014), Vol. 26.
- [61] **H. Weldekidan, V. Strezov and G. Town**, Review of solar energy for biofuel extraction, 184-192, s.l. Renew. Sustain. Energy Rev. (2018), Vol. 88.
- [62] **A.R.K. Gollakota, N. Kishore and S. Gu**, A review on hydrothermal liquefaction of biomass, 1378-1392, s.l. Renew. Sustain. Energy Rev. (2018), Vol. 81.
- [63] **V.M. Gunko, V.I. Zarko, R. Leboda and E. Chiboweski**, Aqueous suspension of fumed oxides: particule size distribution and zeta potential, 1-112, s.l. Adv. colloids interface sci. (2001), Vol. 91.
- [64] **M. Patel**, A quantum mechanical study of the interaction of water with rutile TiO<sub>2</sub> in photoelectrochemical water splitting, PhD thesis, Imperial College, London, (2014).
- [65] **F.A. Cotton**, Chemical application of group theory, wiley- interscience, New york, (1971).
- [66] **G.E. Ewing, M. Foster, W. Cantrell and V. Sadtchenko**, Thin film water on insulator surfaces: in water in confining geometries, 179, Springer, Berlin, (2003).

- [67] **A. Mills and M. Crow**, In situ, continuous monitoring of the photoinduced superhydrophilic effect: influence of UV-type and ambient atmospheric and droplet composition, 6009-6016, s.l. Physl. Chem. C, (2007), Vol. 111.
- [68] **P.A. Thiel and T.E. Madey**, The interaction of water with surfaces: fundamental aspects, 211-385, s.l. Surf. Sci. Rep. (1987), Vol. 7.
- [69] **G. Pirug and H.P. Benzel**, Short range interaction of K and CO coadsorbed on Pt (111), 371-390, s.l. Surf. Sci. (1988), Vol. 199.
- [70] **M. Chen, T.P. Straatsma and D.A. Dixon**, Molecular and dissociative adsorption of water on (TiO<sub>2</sub>)<sub>n</sub> clusters, n=1 to 4, The University of Alabama, Tuscaloosa, Alabama, (2016).
- [71] **L.Q. Wang, D.R. Baer, M.H. Engelhard and A.N. Shultz**, The adsorption of liquid and vapor water on TiO<sub>2</sub> (110) surfaces: the role of defects, 237-250, s.l. Surf. Sci. (1995), Vol. 344.
- [72] **C.Y. Wu, K.J. Tu, J.P. Deng, Y.S. Lo and C.H. Wu**, Markedly enhanced surface hydroxyl groups of TiO<sub>2</sub> nanoparticles with superior water dispersibility for photocatalysis, 566-581, s.l. Mater. (2017), Vol. 10.
- [73] **J. Balajka, U. Aschauer, S. F.L. Mertens, A. Selloni, M. Schmid and U. Diebold**, Surface structure of TiO<sub>2</sub> rutile (011) exposed to liquid water, 26424–26431, s.l. Phys. Chem. C, (2017), Vol. 121.
- [74] **J.K. Johnson and M.W. Cole**, Hydrogen adsorption in single-walled carbon nanotubes, 369-401, s.l. Adsorption by carbons, (2008).
- [75] **A. Bouhekka**, Adsorption of BSA protein on silicon, germanium and titanium dioxide investigated by in Situ ATR-IR spectroscopy, PhD thesis, Es-Senia University of Oran, Algeria, (2013).

# **Chapter III**

## **Mathematical modeling to investigate the dynamics of water adsorption on rutile TiO<sub>2</sub> (110) surface**

According to the theoretical background of adsorption concerning water and rutile (110) surface interactions reported in the previous chapter; The most important motivation is to understand the behaviour of water at surface with others methods, therefore, a theoretical model, based on the Langmuir equation, taking into account all the ways and mechanisms of water adsorption at the surface yielding to a system of nonlinear differential equations, its analytical solution is difficult even impossible in some cases. At the end, we describe the most important numerical methods used to solve this modeling to estimate the key factors that influence its behaviour.

### III.1. Introduction

Sorption phenomena and their mathematical description have a great importance to achieve effective operation of the chemical industry; therefore, numerous adsorption processes have been studied during the past years. The diffusion control, mass transfer, chemical reactions, and particle diffusion are different kinds of mechanisms related to adsorption processes [1]. Various theoretical methods including Langmuir, Freundlich and Langmuir-Hinshelwood... models were used for testing the dynamics of these types of interactions under different conditions. We will discuss an adaption of the Langmuir adsorption theory relevant for catalytic research [2], and focus on the behaviour of H<sub>2</sub>O molecules on rutile (110) surface taking into account all cases of adsorption using Langmuir equation to describe our model.

### III.2. Langmuir model theory

Generally the attractive strength between the surface and the first layer of adsorbed substance is much greater than the strength between the first and second layer. However, the ability to characterize the behaviour of wet or aqueous species on the surface is very important, particularly, we speak on the H<sub>2</sub>O- rutile (110) interface interactions using Langmuir equation. This latter was developed by Irving Langmuir in 1916 [3], it is the simplest and the most widely used expression for chemisorption (or even physisorption), generally for a monolayer adsorption from either gas-solid or liquid-solid interfaces [4], this expression is derived through rate expressions of both adsorption and desorption process. Langmuir assumptions used for deriving reversible reactions is as follows:



A, \* and A\* are the solutions close the surface, empty (active) surface sites and the molecules adsorbed on the surface, respectively.

From the basic reaction, using the mathematical formulation of the Langmuir equation one can describe the adsorption and desorption rates.

The variation of the adsorbed molecules on surface as a function of time is given by:

Adsorption rate:

$$\frac{d\theta^*}{dt} = c_A \cdot K_a \cdot \theta^* \quad (\text{III. 2})$$

Where:

$c_A$  and  $K_a$  are the concentration of adsorbate molecules and the rate constant of adsorption.

The number of molecules desorbed from the surface is independent to the number of sites occupied per unit of surface but it's related to the coverage of molecules adsorbed on the surface as indicated in Eq. (III. 3).

Desorption rate:

$$\frac{d\theta_A}{dt} = K_d \cdot \theta_A \quad (\text{III. 3})$$

Where:

$\theta^*$ ,  $\theta_A$  and  $K_d$  are the coverage of unoccupied surface, the coverage of adsorbent molecules, the rate constant of desorption, respectively.

Where, the fractional coverage of the surface is defined by the occupied number of sites and the total ones available of considered species at the surface as shown by Eq. (III. 4), where the total coverage ( $\theta$ ) on all surface is ranging from (0 to 1)[5].

$$\theta = \frac{N_s}{N} \quad (\text{III. 4})$$

Where:

$N_s$  is the number of occupied sites while  $N$  is the total number of available adsorption sites.

The association of the half reaction equation, we get elegant equation (III.5) describing the coverage of occupied sites (produced) on the whole surface [6, 7]:

$$\theta_A = \frac{K \cdot C_A}{1 + K \cdot C_A} \quad (\text{III. 5})$$

Where:

$K = \frac{K_a}{K_d}$ , is the equilibrium constant.

Inherent within this model, the following assumptions used specifically for the adsorption of single adsorbate on equivalent sites onto the surface are [8, 9]:

1. The adsorbate molecule takes place at well-defined localized states.
2. All the adsorption sites are identical (energetically)
3. Each site accommodates by maximum one adsorbate molecule.
4. There are no interactions (i.e., between neighbouring sites, occupied or otherwise).

### III.2.1. Limitation of Langmuir model

Langmuir adsorption model fails to study many cases at the interface, and this overbalance to the limitation of the model in which fail to calculate the rough of adsorbent, also the model ignores the interaction between adsorbate and adsorbent but in reality there are direct or indirect interactions between them especially at high concentration [9].

### III.3. Dynamic of water on rutile TiO<sub>2</sub> (110) surface

Over last decades, especially from the discovery of splitting of water by Fujishima in 1972 [10], a lot of research has been focused on the study of H<sub>2</sub>O molecules interactions with rutile (110) surface using different theoretical and experimental methods to understand the behaviour of this complex phenomenon.

#### III.3.1. Water adsorption on stoichiometric rutile TiO<sub>2</sub> (110) surface

Concerning the H<sub>2</sub>O interactions with stoichiometric rutile TiO<sub>2</sub> (110) surface, in one hand, at low temperature (160 K) and low coverage the water molecules adsorb in molecular form on defect-free sites (Ti<sub>5c</sub>) with its O ending at the top of a surface Ti<sub>5c</sub> atom in forward direction. as reported in many literatures [11-14], with adsorption energy around (0.5 to 0.7 eV) [15-17], which creates a covalent bond length ranges between (2.16 to 2.29) Å [18] as illustrated bellow in the **Figure III.1**.

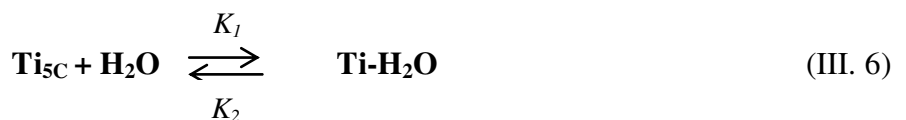
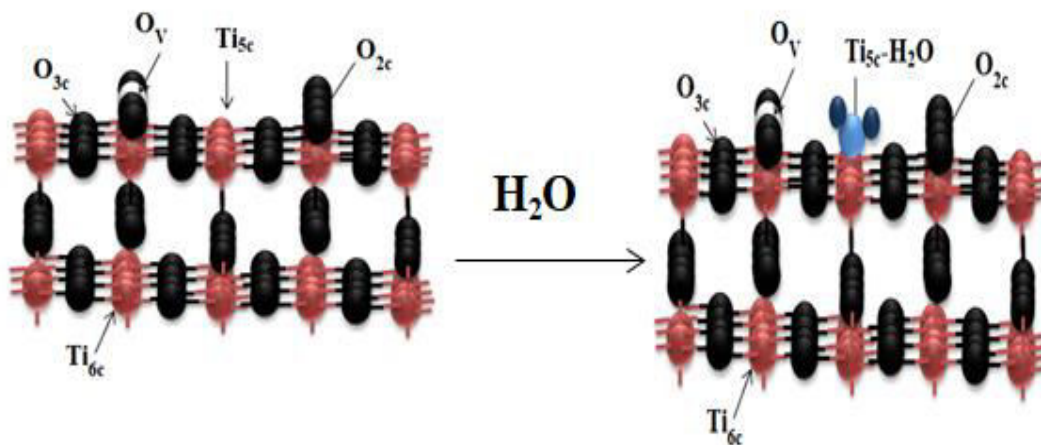


**Figure III.1:** The adsorption of molecular water on defect-free (Ti<sub>5c</sub>) sites, dark (light) blue balls hydrogen (oxygen of water) atoms,  $K_1$ ,  $K_2$  are the rates constant of adsorption and desorption respectively.

The experimental studies indicate that water molecules release from the surface only in molecular form, when annealing the surface somewhat below room temperature with desorption energy ranges between 0.7 eV to 0.8 eV [19]. In other hand, despite the overwhelming wealth of literature, the dissociation of water on defect-free titanium (Ti<sub>5c</sub>) sites has been disputed for decades. In recent studies, with variety of modern techniques including scanning tunnelling microscopy (STM) and infrared reflection absorption improved that The H<sub>2</sub>O has the possibility to dissociate on (Ti<sub>5c</sub>) sites, and create two hydroxyl groups OH<sub>t</sub> and OH<sub>b</sub> on Ti<sub>5c</sub> and O<sub>b</sub> sites, respectively, with dissociation energy 0.36 eV and 0.41 eV under low temperature [20].

The association of the hydroxyls occur at temperature (>110 K) [21] Eq. (III. 7), which indicates that molecular adsorption is preferred over the surface-bound hydroxyls by 0.035 eV relative to dissociative adsorption [22] as shown in **Figure III.2**.

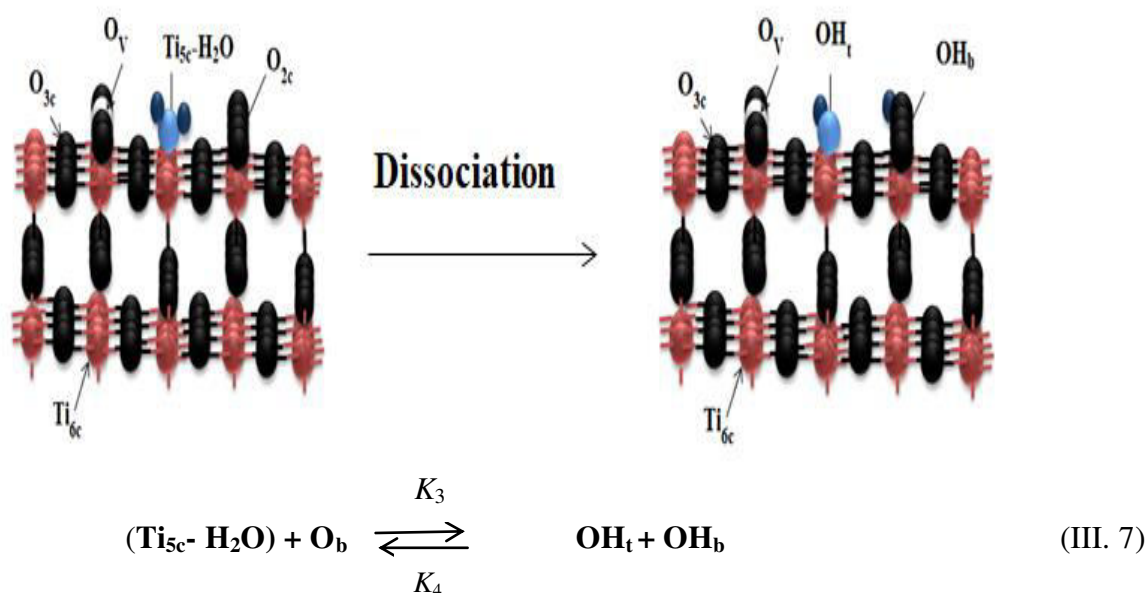


**Figure III.2:** The dissociative adsorption of water on defect-free (Ti<sub>5c</sub>) sites, where  $K_3$  and  $K_4$  are the rates constant of dissociation and recombination reaction, respectively.

### III.3.2. Water adsorption on defective rutile TiO<sub>2</sub> (110) surface

The oxygen vacancies are considered as direct active sites on rutile TiO<sub>2</sub> (110) surface for many adsorbate [21, 23, 24], the reduction reaction can occur as follow  $2\text{O}_b^{2-} \rightarrow \text{O}_2 + 2\text{V}_0 + 4\text{e}^-$  yielding scavenger of charge filled Ti 3d orbitals [25, 26]. When the water molecules close the surface, they diffuse along it until they find bridging oxygen vacancies on which the adsorption takes place, afterward the H proton hopping to near bridging oxygen and create the second OH<sub>b</sub> and left behind OH<sub>v</sub> with activation barrier >1eV [27, 28] as indicated in (III. 8) under room temperature, this reaction is described as shown in the **Figure III.3**. Annealing the surface at temperature above



450 K leads to the recombination of two OH groups which forming H<sub>2</sub>O molecules and O<sub>V</sub>'s [20, 29].

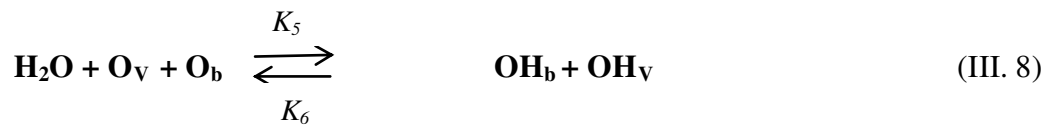
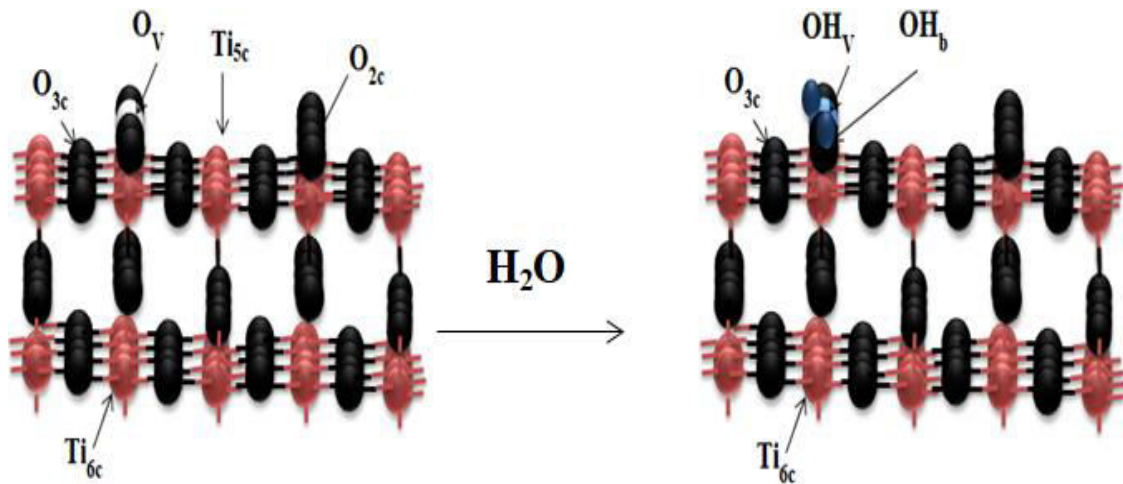
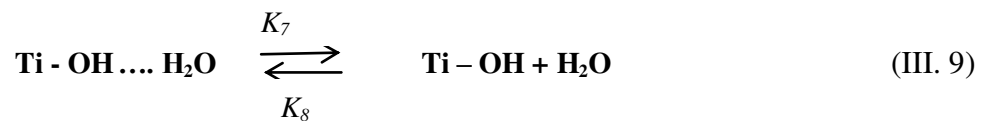


**Figure III.3:** The dissociative adsorption of water on Ti<sub>5C</sub> sites, where  $K_3$  and  $K_4$  are the rates constant of dissociation and recombination reaction, respectively.

In other case, the H<sub>2</sub>O can also diffuse on the surface but in case the molecule close the surface and across with Ti-OH yielding to weak hydrogen bond which breaks it and diffuses on surface as illustrated by the following reaction.



The variation of the adsorption rate by time is denoted by  $d\theta/dt$  which shows the amount of adsorbate that can be adsorbed from bulk liquid onto the adsorbent within a unit time. This can be presented as given by the following Eq. (III. 10):

$$\frac{d\theta}{dt} = \phi P_{ads} - K \theta \quad (\text{III. 10})$$

Where:

$\Phi, \theta, P_{ads}$  and  $K$  are the flux, the surface sites coverage, the probability of the molecule to find adsorption site and desorption rate constant, respectively. The probability of adsorption  $p_{ads}$  is given by the following Eq. (III. 11) [30]

$$p_{ads} = k \left( \frac{n_a(1-\theta_a)}{n_s} \right) \quad \text{(III. 11)}$$

Where:

$K, n_a, n_s, \theta_a$  the adsorption rate constant ( $s^{-1}$ ), the concentration of adsorption sites, the concentration of all atoms at the surface and the coverage of the adsorption sites respectively.

The rate constant of each stage  $K_i$  can be expressed with an Arrhenius equation (III. 12) [31]

$$K_i = K_0 \exp\left(\frac{-E_a}{RT}\right) \quad \text{(III. 12)}$$

Where:

$K_0, E_a, R$  and  $T$  are the attempt frequency ( $s^{-1}$ ), the activation energy (Kj/mole, 1 eV = 96.482 Kj), universal gas constant (8.314 j/mole. K) and the temperature (K).

$K_0$  can be calculated from the kinetic theory of gases by using the following relationship (III. 13) [32]

$$K_0 = S_i (2 \pi m_i K_\beta T_{gas})^{-1/2} (N)^{-1} \quad \text{(III. 13)}$$

Where:

$S_i, m_i [kg], K_\beta [J/ K]$  and  $T_{gas} [K]$  are the sticking coefficient, the molecular mass, Boltzmann constant and the gas phase temperature.

From the Langmuir adsorption process, we can determine if the adsorption is favourable or not using dimensionless separatin factor,  $R_L$  (also called equilibrium parameter) given by the following equation (III. 14) [33, 34]

$$R_L = \frac{1}{(1 + K_L C_0)} \quad \text{(III. 14)}$$

Where:

$K_L$  and  $C_0$  are denote the Langmuir constant and initial concetration of solution.

if:

$R_L > 1$ , the isotherm is unfavourable

$0 < R_L < 1$ , the isotherm is favourable

$R_L = 1$ , the isotherm is linear

$R_L = 0$ , the isotherm is irreversible

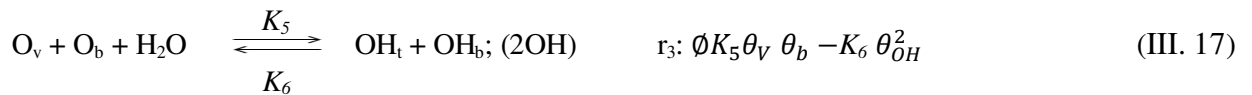
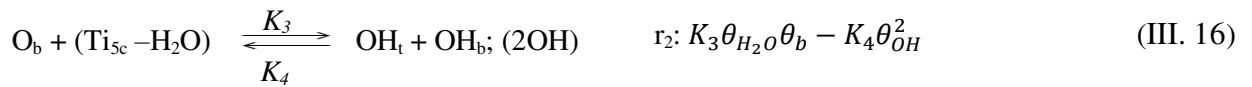
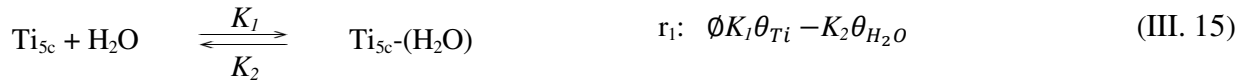
According to the Eq. (III. 12), we calculate the rate constant  $K_i$  which corresponds to each reaction as classified in following **Table III.1**.

Step,(i)	$K_0$ [s <sup>-1</sup> ]	$E_a$ [eV]	$T$ [K]	$K_i$ [s <sup>-1</sup> ]	References
1. H <sub>2</sub> O adsorption	10 <sup>13</sup>	0.5-0.7	150-160	0.0018	[15, 22]
2. H <sub>2</sub> O desorption	10 <sup>12</sup>	0.73-0.8	200-275	4.10 <sup>-7</sup>	[21]
3. H <sub>2</sub> O dissociation on defect free	10 <sup>12</sup>	0.36,0.44,0.97	80-140	0.0015	[11, 35]
4. OH association	10 <sup>12</sup>	0.355	110-130	5.43.10 <sup>-5</sup>	[36-38]
5. H <sub>2</sub> O dissociation on O <sub>v</sub>	10 <sup>13</sup>	0.93-1.5	300,187	0.0024	[35, 39, 40]
6. OH recombination	10 <sup>8</sup>	0.12-0.18	450-500	10 <sup>-4</sup>	[41, 42]

**Table III.1:** Kinetic parameters used in the mathematical models of H<sub>2</sub>O reactions on rutile TiO<sub>2</sub> (110) surface

### III.4. Proposed theoretical model

A mathematical description of the equations (III. 6) - (III. 9) for the adsorption of H<sub>2</sub>O molecules at different cases onto rutile (110) surface can be derived using an adaptation of the Langmuir adsorption model above [43]. Therefore, we obtain:



The relation (III. 9) is ignored from the system, because it does not affect the interactions at the surface. The physisorption of water molecules on the OH stucked at Ti will lead quickly desorption thus the final statistics sites remain the same. The rate coverage of each species that can be found at the surface is defined as indicated in **Table III. 2** bellow.

Surface site	Surface coverage
Titanium five coordinate (Ti <sub>5c</sub> )	$\theta_{Ti_{5c}}$
H <sub>2</sub> O linked on Ti <sub>5c</sub> (H <sub>2</sub> O- Ti <sub>5c</sub> )	$\theta_{H_2O}$
Oxygen bridging (O <sub>2c</sub> )	$\theta_b$ or $\theta_{O_b}$
Hydroxyl group (OH)	$\theta_{OH}$
Oxygen vacancy (O <sub>v</sub> )	$\theta_v$ or $\theta_{O_v}$

**Table III.2:** Nomenclature of the surface coverage

In this proposed model, all the impurities that can be found at the surface like CO, CO<sub>2</sub>, N, C and O<sub>2</sub> are totally ignored to avoid the complexity of the phenomenon and make the solution of the system of equations possible. These exterior elements (impurities) can directly be adsorbed on O<sub>v</sub> sites, besides it's a reason of the surface oxidation surface [44], O<sub>2</sub> can be easily dissociated on the surface yielding to access of electrons which changes the reaction pathway [45] and acts as electron trapped on CB of TiO<sub>2</sub> leading to increase the electric resistance on the surface [46], besides to the roughness of the surface and the pressure. We considered also that water molecules approaching at Ti-OH sites can only be physisorbed and then they can diffuse randomly to one of the adjacent sites without changing the coverage of the surface at its final result.

Generally, the coverage of Ti atoms and the bridging oxygen atoms is the same at the perfect rutile (110) surface  $n_{Ti} = n_{O_b} = 5, 2 \times 10^{14} \text{ cm}^{-2}$  and assumed the amount of H<sub>2</sub>O flux arrived on surface is  $\emptyset = 7, 2 \times 10^{14} \text{ H}_2\text{O molecules cm}^{-2}$  which is an important initial condition [30]. The basic system conditions, the sum of all the different rates coverage at the rutile (110) surface and the variation are equal:

$$\begin{aligned} \sum \theta_i &= 1 \\ \sum \frac{d\theta_i}{dt} &= 0 \end{aligned} \quad \text{(III. 18)}$$

The adsorption rate of each component on the surface (reactants or products) is expressed by the variation of coverage at unit time ( $\frac{d\theta_i}{dt}$ ), a combination between the equations (III. 14) - (III. 16) and the relation (III. 10) leads to an elegant of the following equations set that describes the physics of water at our considered surface.

$$\frac{d\theta_v}{dt} = -r_3 = -\emptyset K_5 \theta_v \theta_b + K_6 \theta_{OH}^2 \quad \text{(III. 19)}$$

$$\frac{d\theta_b}{dt} = -r_3 - r_2 = -\emptyset K_5 \theta_v \theta_b + K_4 \theta_{OH}^2 - K_3 \theta_{H_2O} \theta_b + K_6 \theta_{OH}^2 \quad \text{(III. 20)}$$

$$\frac{d\theta_{OH}}{dt} = r_3 + r_2 = +\phi K_5 \theta_V \theta_b - K_4 \theta_{OH}^2 + K_3 \theta_{H_2O} \theta_b - K_6 \theta_{OH}^2 \quad (III. 21)$$

$$\frac{d\theta_{Ti}}{dt} = -r_1 = -\phi K_1 \theta_{Ti} + K_2 \theta_{H_2O} \quad (III. 22)$$

$$\frac{d\theta_{H_2O}}{dt} = r_1 - r_2 = \phi K_1 \theta_{Ti} - K_2 \theta_{H_2O} - K_3 \theta_{H_2O} \theta_b + K_4 \theta_{OH}^2 \quad (III. 23)$$

This final system of nonlinear coupled differential equations is used extensively to describe how the compounds change on surface over time, at the atomic, level to analysing the chemical reactions [47]. The traditional methods (pencil and paper) is excellent means but they have limited practical value, according that this system is not easy to be solved analytically due to its complexity, for this reason they must be dealt with by computational methods (numerical methods and software tools) that deliver approximation solution [48] including Euler' method, Taylor method, linear multistep methods, Runge–Kutta order 2 and 4 and Runge-Kutta-Fehlberg 4-5. Within this section we have included a wealth of most popular theoretical methods that motivate and illustrate the ideas considered to solve these types of equations.

### III.5. Numerical methods

In physics, there are many well-known and useful numerical methods like which play a crucial role in solving some complex systems of equations where the accuracy of the determined values strongly depends on the technique itself and other parameters:

#### III.5.1. Euler's method

This method is considered as one of appreciate means to solve linear, scalar equation as well as system of ordinary differential equations (ODE) [49]. When a given derivative function of  $x(t)$  equation with initial condition  $x(t_0)$  at  $t_0$  donated as:

$$x'(t_0) = f(t, x(t)) \quad (III. 24)$$

From (III. 24) the definition of derivative, we get:

$$\frac{x(t+h)-x(t)}{h} \approx x'(t) \quad (III. 25)$$

Since  $h$  (step size) takes a small value, we reformulate (III. 25) we obtain [50]

$$f(x_0 + h) = f(x_0) + h f'(x_0) \quad (III. 26)$$

To improve the accuracy of the approximation by adding a second order term of the form  $R_1(t)$  is called the local truncation errors (LTR) according (Taylor series) so we get:

$$f(x_0 + h) = f(x_0) + h f'(x_0) + R_1(t) \quad (\text{III. 27})$$

Where:

$$R_1(t) = \frac{h^2}{2} f''(x_0)$$

According Euler's approximation, the  $R_1(t)$  can be ignored by taking the step size ( $h$ ) sufficiently small, The general solution from  $t_n$  to  $t_{n+1}$  is [51]:

$$x_{n+1} = x_n + h f'(t_n, x_n), \quad n = 1, 2, 3 \dots \quad (\text{III. 28})$$

To get the approximation solution, we should initially use a small step size noted ( $h$ ) is equal to the interval  $[a, b]$  over  $M$  (subinterval). To seek approximation solution at particular time  $t$ , in which  $t = t_0, (t_0 + h), (t_0 + 2h) \dots (t_0 + nh)$  we can put  $t_{n+1} = t_n + h$ , and approximations to the sequence of numbers  $x(t_0), x(t_0 + h), x(t_0 + 2h) \dots x(t_0 + nh)$  [52].

$$h = \frac{b-a}{M} \quad (\text{III. 29})$$

To get more accurate results, they induce some modification on Euler's equation noted Euler's modified or Heuns' method as:

$$x_{n+1}^{(i+1)} = x_n + \frac{h}{2} (f'(x_n) + f'_{n+1}^{(i)}) \quad (\text{III. 30})$$

### III.5.2. Runge-Kutta-Fehlberg (RKF 45)

Runge-Kutta-Fehlberg denoted (RKF4-5) is one of the most important methods used in solving differential equations. It's one -step methods composed with multiple stages, the starting state of system is usually known for initial time value, which a complement of Runge-Kutta order 4. The mains difference between them is the order of errors value [53, 54]

Each step requires the use of the following six values:

$$k_1 = h_f(t_k, y_k)$$

$$k_2 = h_f(t_k + (1/4) h, y_k + (1/4) k_1)$$

$$k_3 = h_f(t_k + (3/8) h, y_k + (3/32) k_1 + (9/32) k_2)$$

$$k_4 = h_f(t_k + (12/13) h, y_k + (1932/2197) k_1 - (7200/2197) k_2 + (7296/2197) k_3)$$

$$k_5 = h_f(t_k + h, y_k + (439/216) k_1 - 8 k_2 + (3680/513) k_3 - (845/4104) k_4)$$

$$k_6 = h_f(t_k + (1/2) h, y_k - (8/27) k_1 + 2 k_2 - (3544/2565) k_3 + (1859/4104) k_4 - (11/40) k_5) \quad (\text{III. 32})$$

The approximation to the solution by using a Runge-Kutta method of order 4 is:

$$y_{k+1} = y_k + (25/216) k_1 + (1408/2565) k_3 + (2197/4101) k_4 - 1/5 k_5 \quad (\text{III. 33})$$

Where the best solution for 5<sup>th</sup> order is given by:

$$y_{k+1} = y_k + (16/135) k_1 + (6656/12825) k_3 + (28,561/56,430) k_4 - (9/50) k_5 + (2/55) k_6 \quad (\text{III. 34})$$

### III.6. Conclusion

In this chapter, we discussed the mathematical description of Langmuir model used to derive our proposed one used to study the dynamics of water molecules on rutile (110) surface. At the end of this chapter, we also gave an idea about the most useful numerical methods that can be used in solving complex systems of nonlinear equations.

In the next chapter, we will present the results of the behaviour of water molecules onto rutile (110) surface under different conditions (the coverage of oxygen vacancies, temperature and  $H_2O$  flux) and in different cases such as steady state to see effect on the adsorption molecular and dissociative adsorption. The variation regime under stopping the arriving flux of water will be also taken into account. The interactions between the  $H_2O$  molecules and the rutile (110) surface need to be well understood because of the important applications of this kind of adsorption in a lot of disciplines. A simple comparison between the adsorption of simple water molecules and biomolecules like protein will be mention at the end of the chapter.

## References

- [1] **M.A. Shaheed and F.H. Hussein**, Adsorption of reactive black 5 on synthesized titanium dioxide nanoparticles: equilibrium isotherm and kinetic studies, 198561-198571, s.l. Nanomaterials, (2014), Vol. 2014.
- [2] **D.D. Do**, Adsorption analysis: equilibria and kinetics, London : Imperial College Press, (1998).
- [3] **I. Langmuir**, The construction and fundamental properties of solids and liquids part I, Solids, 2221-2295, s.l. Am. Chem. Soc. (1916), Vol. 38.
- [4] **I. Langmuir**, The dissociation of hydrogen into atoms Part III. The hydrogen of the reaction, 1145-1156, s.l. Amer. Chem.Soc. (1916), Vol. 38.
- [5] **P. Connor and A.J. Mcquillan**, Phosphate adsorption onto TiO<sub>2</sub> from aqueous solution: an in situ internal reflection infrared spectroscopic study, 2916-2921, s.l. Langmuir , (1999), Vol. 15.
- [6] **D. Haydon**, A study of the relation between electrokinetic potential and surface charge density, 319-328, s.l. Proceeding of the royal society of london, series a mathematical and physical science, (1960), Vol. 258.
- [7] **K.A. Connors**, Chemical kinetics: the study of reaction rates in solution, VCH Publishers, United States, America (1990).
- [8] **R.I. Masel**, Principles of adsorption and reaction on solid surfaces, New York: John Wiley and Sons, ( 1996).
- [9] **D.A.H. Hanaor, M. Ghadiri, W. Chrzanowski and Y. Gan**, Scalable surface area characterization by electrokinetic analysis of complex anion adsorption, 1543-15152, s.l. Langmuir, (2014), Vol. 30.
- [10] **A. Fujishima and K. Honda**, Electrochemical photolysis of water at a semiconductor electrode, 37-38, s.l. Nat. (1972), Vol. 238.
- [11] **D. Brinkley, M. Dietrich, T. Engel, P. Farrall, G. Gantner, A. Schafer and A. Szuchmacher**, A modulated molecular beam study of the extent of H<sub>2</sub>O dissociation on TiO<sub>2</sub> (110), 292-306, s.l. Surf. Sci. (1998), Vol. 395.
- [12] **S. Krischok, O. Hofft, J. Gunster, J. Stultz, D. W. Goodman and V. Kempter**, H<sub>2</sub>O interaction with bare and Li-precovered TiO<sub>2</sub>: studies with electron spectroscopies (MIES and UPS(HeI and II)), 8- 18, s.l. Surf. Sci. (2001), Vol. 495.
- [13] **S. Suzuki, K.I. Fukui, H. Onishi, T. Sasaki and Y. Iwasawa**, Observation of individual adsorbed pyridine, ammonia, and water on TiO<sub>2</sub> (110) by means of scanning tunneling microscopy, 753-756, s.l. Stud. Surf. Sci. Catal. (2001), Vol. 132.
- [14] **F. Labat, P. Baranek, C. Domain, C. Minot and C. Adamo**, Density functional theory analysis of the structural and electronic properties of TiO<sub>2</sub> rutile and anatase polytypes: performances of different exchange-correlation functionals, 154703-154716, s.l. Chem. Phys. (2007), Vol. 126.



- [15] **M. Elahifard, H. Heydari, R. Behjatmanesh Ardakani, P. Bijan and S. Ahmadvand**, A computational study on the effect of Ni impurity and O-vacancy on the adsorption and dissociation of water molecules on the surface of anatase (101), 109176-109184, s.l. Phys. Chem. Sol. (2020), Vol. 136.
- [16] **A. Fahmi and C.A. Minot**, Theoretical investigation of water adsorption on titanium dioxide surfaces, 343-359, s.l. Surf. Sci. (1994), Vol. 304.
- [17] **S. Wendt, R. Schaub, J. Matthiesen, E.K. Vestergaard, E. Wahlstrom, M.D. Rasmussen, P. Thostrup, L.M. Molina, E. Lagsgaard, I. Stensgaard, B. Hammer and F. Besenbacher**, Oxygen vacancies on TiO<sub>2</sub> and their interaction with H<sub>2</sub>O and O<sub>2</sub>: a combined high-resolution STM and DFT study, 226-245, s.l. Surf. Sci. (2005), Vol. 598.
- [18] **J. Zhang, R. Zhang, B. Wang and L. Ling**, Insight into the adsorption and dissociation of water over different CuO (111) surfaces: the effect of surface structures, 758-768, s.l. Appl. Surf. Sci. (2016), Vol. 364.
- [19] **R. Mu, Z. Zhao, Z. Dohnalek and J. Gong**, Structural motifs of water on metal oxide surfaces, 1785-1806, s.l. Chem. Soc. Rev. (2017), Vol. 46.
- [20] **Z. Zhang, O. Bondarchuk, B.D. Kay, J.M. White and Z. Dohnalek**, Imaging water dissociation on TiO<sub>2</sub> (110): evidence for inequivalent geminate OH groups, 21840-21845, s.l. Phys. Chem. B, (2006), Vol. 110.
- [21] **Z.T. Wang, Y.G. Wang, R. Mu, Y. Yoon, A. Dahal, G.K. Schenter, V.A. Glezakou, R. Rousseau, L. Lyubinetzky and Z. Dohnalek**, Probing equilibrium of molecular and deprotonated water on TiO<sub>2</sub> (110), 1801-1805, s.l. Proc. Nat. Acad. Sci. (2017), Vol. 114.
- [22] **U. Diebold**, Perspective: a controversial benchmark system of water-oxide interfaces: H<sub>2</sub>O / TiO<sub>2</sub> (110), 040901-040904, s.l. Chem. Phys. (2017), Vol. 147.
- [23] **O. Dulub, M. Batzill, S. Solovev, E. Loginova, A. Alchagirov, T.E. Madey and U. Diebold**, Electron-induced oxygen desorption from the TiO<sub>2</sub>(011)-2×1 surface leads to self-organized vacancies, 1052-1056, s.l. Sci. (2007), Vol. 317.
- [24] **C. Pang, O. Bikondoa, D. Humphrey, A. Papageorgiou, G. Cabailh, R. Ithnin, Q. Chen, C. Muryn, H. Onishi and G. Thornton**, Tailored TiO<sub>2</sub> (110) surfaces and their reactivity, 5397-5405, s.l. Nanotechnology, (2006), Vol. 17.
- [25] **C.M. Yim, C.L. Pang and G. Thornton**, Oxygen vacancy origin of the surface band-gap state of TiO<sub>2</sub>(110), 036806-036809, s.l. Phys. Rev. Lett. (2010), Vol. 104.
- [26] **Z.M. Zhang, S.P. Jeng and V.E. Henrich**, Cation-ligand hybridization for stoichiometric and reduced TiO<sub>2</sub> (110) surfaces determined by resonant photoemission, 12004-12011, s.l. Phys. Rev. B, (1991), Vol. 43.

- [27] **S. Wendt, J. Matthiesen, R. Schaub, E.K. Vestergaard, E. Laegsgaard, F. Besenbacher and B. Hammer**, Formation and splitting of paired hydroxyl groups on reduced TiO<sub>2</sub>(110), 066107-066110, s.l. Phys. Rev. Lett. (2006), Vol. 96.
- [28] **H. Heydari, M.R. Elahifard and R. Behjatmanesh-Ardakania**, Role of oxygen vacancy in the adsorption and dissociation of the water molecules on the surfaces of pure and Ni doped rutile (110): a periodic full-potential DFT study, 218-224, s.l. Surf. Sci. (2019), Vol. 679.
- [29] **M.A. Anderson**, An HREELS and TPD study of water on TiO<sub>2</sub> (110): the extent of molecular versus dissociative adsorption, 151-166, s.l. Surf. Sci. (1996), Vol. 355.
- [30] **N Bundaleski, A.G. Silva, U. Schröder, A.M.C. Moutinho and O.M.N.D. Teodoro**, Adsorption dynamics of water on the surface of TiO<sub>2</sub> (110), 012008-012019, s.l. Phys.: Conf. Series. IOP Publishing, (2010), Vol. 257.
- [31] **D.A. Wood**, Sustainable geoscience for natural gas subsurface systems, 159-195, Lincoln, United Kingdom, DWA energy limited, (2022), Vol. 691.
- [32] **A. G. Makeeva and M. M. Slinko**, Mathematical modeling of CO oxidation on Pd(100) at near-atmospheric pressures: effect of mass-transfer limitations, 121488-121496, s.l. Surf. Sci. (2020), Vol. 691.
- [33] **J.V. Barth, H. Brune, B. Fischer, J. Weckesser and K. Kern**, Dynamics of surface migration in the weak corrugation regime, 1732-1735, s.l. Phys. Rev. Lett. (2000), Vol. 84.
- [34] **B. Meroufel, O. Benali, M. Benyahya and M.A. Zenasni**, Adsorptive removal of anionic dye from aqueous solutions by algerian kaolin: characteristics, isotherm, kinetic and thermodynamic studies, 482-491, s.l. Mater. Environ. Sci. (2013), Vol. 4.
- [35] **K.R. Eagleton, L.C. Acrivers and T. Vermeulen**, Pore and solid diffusion kinetics in fixed adsorption constant pattern conditions, 212-223, s.l. Ind. Eng. Chem. Res. (1966), Vol. 5.
- [36] **K. Sebbari, C. Domain, J. Roques, H. Perron, E. Simoni and H. Catalette**, Investigation of hydrogen bonds and temperature effects on the water monolayer adsorption on rutile TiO<sub>2</sub> (110) by first-principles molecular dynamics simulations, 1275-1280, s.l. Surf. Sci. (2011), Vol. 605.
- [37] **M.B. Hugenschmidt, L. Gamble and C.T. Campbell**, The interaction of H<sub>2</sub>O with a TiO<sub>2</sub> Surface, 329-340, s.l. Surf. Sci. (1994), Vol. 302.
- [38] **M.F. Calegari Andrade, H.Y. Ko, L. Zhang, R. Car and A. Selloni**, Free energy of proton transfer at the water-TiO<sub>2</sub> interface from Ab initio deep potential molecular dynamics, 2335-2341, s.l. Chem. Sci. (2020), Vol. 9.
- [39] **G. Fazio, D. Selli, L. Ferraro, G. Seifert and C. Di Valentin**, Curved TiO<sub>2</sub> nanoparticles in water: short (chemical) and long (physical) range interfacial effects, 29943-29953, s.l. ACS Appl. Mater. Interfaces, (2018), Vol. 35.

- [40] **R. Schaub, N. Lopez, E. Laegsgaard, J.K. Norskov and F. Besenbacher**, Oxygen vacancies as active sites for water dissociation on rutile TiO<sub>2</sub> (110), 266104-266107, s.l. Phys. Rev. Lett. (2001), Vol. 87.
- [41] **Z. Futera and N.J. English**, Oscillating electric-field effects on adsorbed-water at rutile- and anatase-TiO<sub>2</sub> surfaces, 204706-204714, s.l. Chem. Phys. (2016), Vol. 145.
- [42] **A.V. Bandura, D.G. Sykes, V. Shapovalov, T.N. Troung, J.D. Kubicki and R.A. Evarestov**, Adsorption of water on the TiO<sub>2</sub> rutile (110) surface: a comparison of periodic and embedded cluster calculations, 7844-7853, s.l. Phys. Chem. B, (2004), Vol. 108.
- [43] **F. K. Djebbar and H.K. Tahri**, The interactions of water molecules with TiO<sub>2</sub> porous thin films, master thesis, Chlef, Algeria, (2018).
- [44] **W. Gopell, G. Rocker and R. Feierabend**, Intrinsic defects of TiO<sub>2</sub>(110): interaction with chemisorbed O<sub>2</sub>, H<sub>2</sub>, CO, and CO<sub>2</sub>, 3427-3438, s.l. Phys. Rev. B, (1983), Vol. 29.
- [45] **Z. Dohnalek, I. Lyubinetsky and R. Rousseau**, Thermally- driven processes on rutile TiO<sub>2</sub>(110)-(1x1): a direct view at the atomic scale, 161-205, s.l. Progress in surf. sci. (2010), Vol. 85.
- [46] **W. Zeng, T. Liu, Z. Wang, S. Tsukimoto, M. Saito and Y. Ikuhara**, Oxygen adsorption on anatase TiO<sub>2</sub> (101) and (001) surfaces from first principle, 171-175, s.l. Materials Transactions, (2010), Vol. 51.
- [47] **U. Alon**, An introduction to systems biology, Chapman & Hall/CRC, London, (2006).
- [48] **D.F. Griffiths and D.J. Higham**, Numerical methods for ordinary differential equations, Springer ungraduate mathematics series, New York, (2010).
- [49] **C.T. Kelley**, Iterative methods for linear and nonlinear equations, Frontiers in Applied Mathematics, Philadelphia, USA, (1995), Vol. 16.
- [50] **A. Gil, J. Segure and M.N. Temme**, Numerical methods for special functions, s.l. Soc. Indust. Appl. Math, (2007).
- [51] **M. Braun**, Differential equations and their applications, Springer-Verlag, Berlin, (1983).
- [52] **E. Hairer, S.P. Nørsett and G. Wanner**, Solving ordinary differential equations I: nonstiff problems, Springer-Verlag, Berlin, (1993).
- [53] **J.H. Mathews and K.D. Fink**, Numerical methods using matlab, Congress of cataloging, United State, America, (2004).
- [54] **D.F. Griffiths, P.K. Sweby and H.C. Yee**, On spurious asymptotic numerical solutions of explicit Runge–Kutta methods, 319-338, s.l. Num. Anal. (1992), Vol. 12.

# Chapter IV

## Results and discussion

Understanding the kinetics behaviour of water on rutile  $\text{TiO}_2$  (110) surface is very important. Therefore, we are going to discuss the environmental factors that affect this dynamics, we will present the most important results taking into account temperature, oxygen vacancies and the amount of  $\text{H}_2\text{O}$  flux arrived on surface under different cases. At the end of this chapter, we show the behaviour of proteins adsorption, complex phenomenon, in the presence of water.

#### IV.1. Introduction

This chapter contains an extensive study on how the water molecules take place at a perfect and defective rutile (110) surface of monolayer (ML) coverage. The purpose is to develop a better understanding of the behaviour of H<sub>2</sub>O on the surface, firstly in section (IV. 2) we show how adsorbed H<sub>2</sub>O molecules behave with time when supposing that after some water molecules arrived at the surface and then the flux is stopped, and in the next section (IV. 3) the effect of temperature on the dissociation and the association of H<sub>2</sub>O molecules and OH, in section (IV. 4) we investigate the influence of H<sub>2</sub>O flux and the coverage of oxygen vacancies on the dynamics of water at rutile TiO<sub>2</sub> (110) surface in the steady state case. In the last section, a simple illustration for comparison between the adsorption of water and proteins, complex structure, will be indicated.

#### IV.2. Water molecules behaviour on rutile (110) surface: Stopping the flux before equilibrium ( $\phi = 0$ )

A theoretical method was carried out to determine whether the H<sub>2</sub>O flux has an influence on the behaviour of water on rutile (110) face and how the H<sub>2</sub>O attached on surface behave. Before presenting these results, we describe theoretically the sample of TiO<sub>2</sub> over germanium that could be prepared and used experimentally. A thin film of the rutile (110) can be fabricated on germanium substrate with dimensions (5 cm length, 2 cm width, 0.1 cm height), where many techniques can be used to prepare these kinds of films including spin coating [1]. In the first part, to fulfill the behaviour of H<sub>2</sub>O adsorbed on the surface when the H<sub>2</sub>O flux is stopped, we let an amount of H<sub>2</sub>O molecules equal to ( $\phi = 7.2 \times 10^{13} \text{ cm}^{-2}$ ) at a time ( $t_0$ ) equivalent to (0.07ML) close to the rutile (110) surface, generally, after monuments the system dynamics reach to the equilibrium ( $t = t_e$ ). We assume before the system close to this point, we considered  $\phi = 0$  at ( $t_0 < t < t_e$ ). Overall, in a perfect structure, the number of Ti<sub>5c</sub> atoms and the number of bridging oxygen on surface are the same and equal ( $n_{Ti} = n_{ob} = 5.2 \times 10^{14} \text{ cm}^{-2}$ ), and in the near perfect surface the concentration of oxygen vacancies range from (5- 10) % which is created from the bridging oxygen [2]. By injecting this simplification assumption into the theoretical model (III. 18) presented in the previous chapter; the equations that control the evolution of compounds at the surface as function of time can be summarized in the following set:

Assume:  $\phi=0$

$$\frac{d\theta_v}{dt} = K_6 \theta_{OH}^2 \quad (\text{IV. 1})$$

$$\frac{d\theta_b}{dt} = K_4 \theta_{OH}^2 - K_3 \theta_{H_2O} \theta_b + K_6 \theta_{OH}^2 \quad (\text{IV. 2})$$

$$\frac{d\theta_{OH}}{dt} = -K_4 \theta_{OH}^2 + K_3 \theta_{H_2O} \theta_b - K_6 \theta_{OH}^2 \quad (\text{IV. 3})$$

$$\frac{d\theta_{Ti}}{dt} = K_2 \theta_{H_2O} \quad (\text{IV. 4})$$

$$\frac{d\theta_{H_2O}}{dt} = -K_2 \theta_{H_2O} - K_3 \theta_{H_2O} \theta_b + K_4 \theta_{OH}^2 \quad (\text{IV. 5})$$

The Runge- Kutta - Fehlberg 45 numerical method, as described at the end of the previous chapter, was used to solve this system of nonlinear differential equations. In this simulation we considered only a monolayer (ML) coverage, because in the first layer it makes strong bonds with surface unlike in the presence of additional layers they create a physical bonds, therefore, since we are interested to study these processes at high temperature because it is released from the surface at modest temperature [4]. The initial conditions, the coverage of each compound at  $t = t_0$  ( $t_0$  is the time where the water flux is stopped), where,  $\theta_{Ti} = 0.2$ ,  $\theta_b = 0.15$ ,  $\theta_v = 0.05$ ,  $\theta_{OH} = 0.35$ ,  $\theta_{H_2O} = 0.2$ , we take ( $t_0 = t$  the beginning time of the new system without flux). In this work, we examine the behaviour of water kinetics at temperature around 300 K, because the dissociation energy of water on  $Ti_{5C}$  sites is 0.35 eV which is much smaller than the dissociation energy of  $H_2O$  on  $O_v$  sites, so when we calculate the rate constant at high temperature; it will be so high and the calculations are impossible.

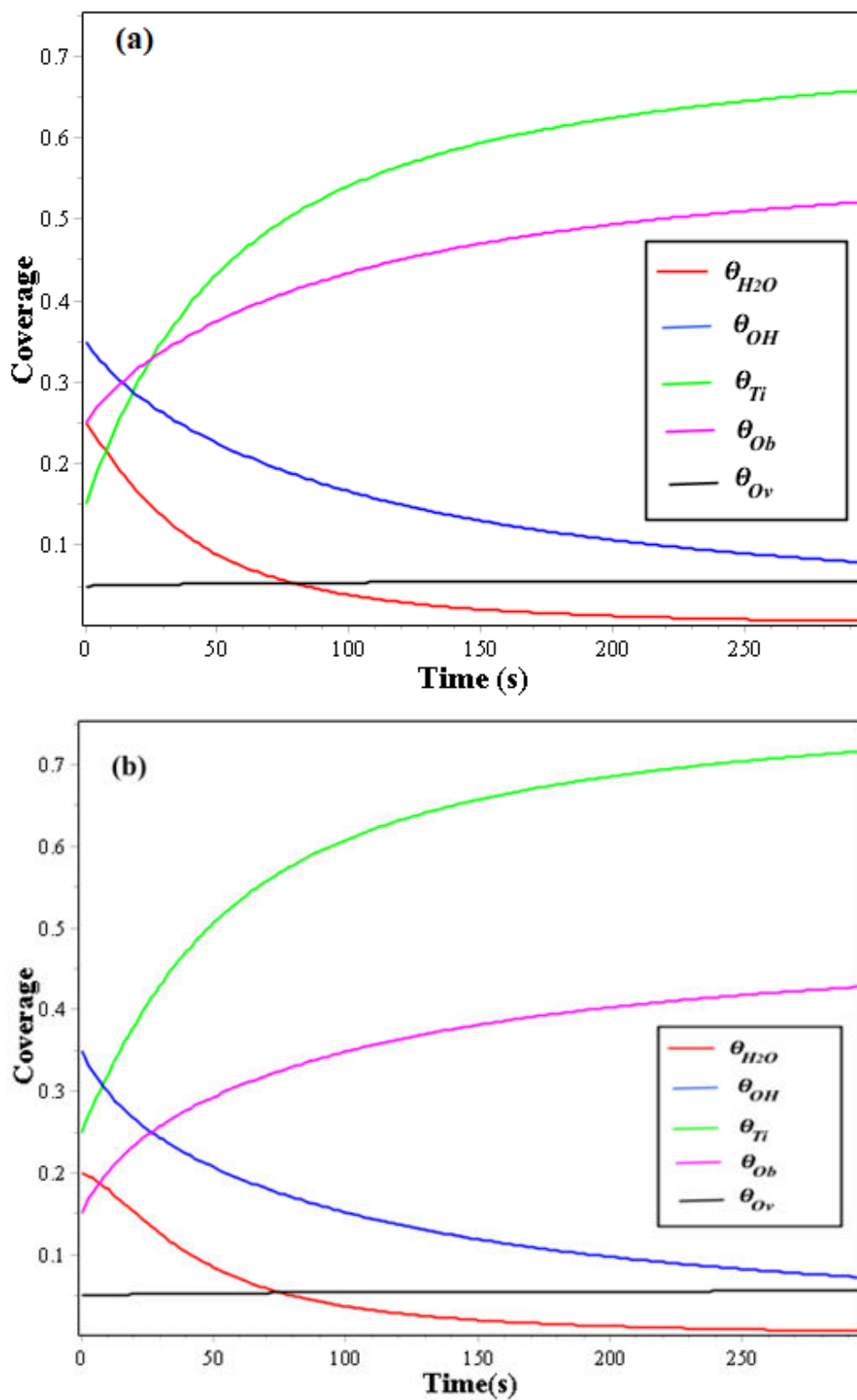


**Figure IV.1:** The coverage of Ti, OH, Ob, Ov, H<sub>2</sub>O as a function of time, at different values of H<sub>2</sub>O, a)  $\theta_{H_2O} = 0.25$ , b)  $\theta_{H_2O} = 0.2$ . The time starts from the moment where the H<sub>2</sub>O flux is stopped.

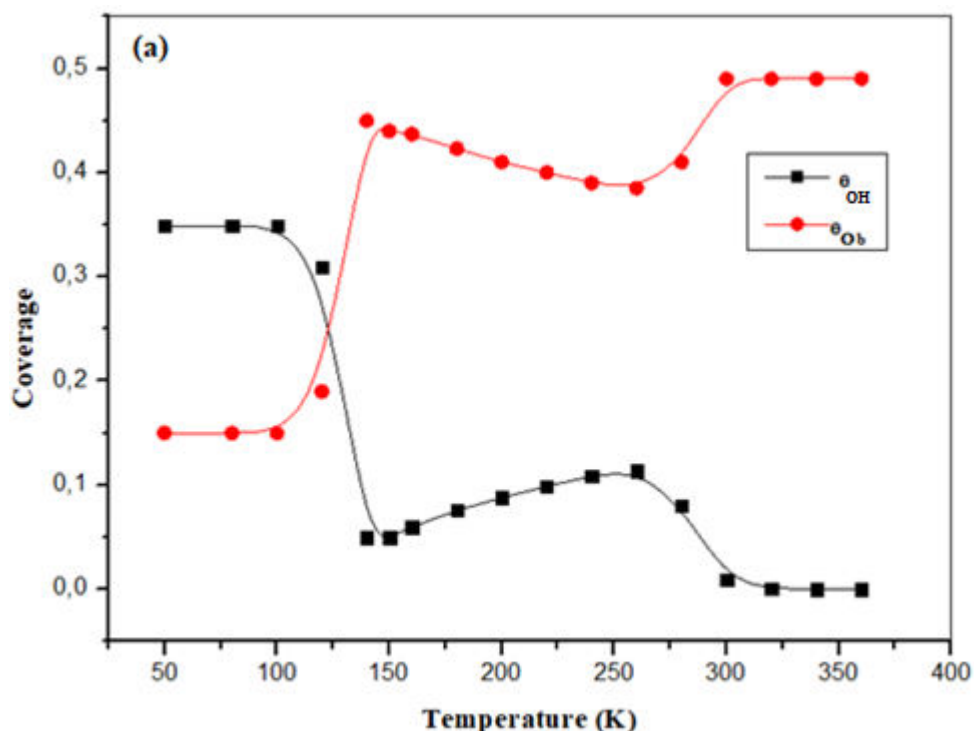
The previous procedures were repeated two times to investigate the effect of the initial concentration on the behaviour of H<sub>2</sub>O molecules at the surface. The results shown in **Figure IV.1** (a)-(b) clearly illustrate the variation of the surface coverage (Ti<sub>5c</sub>, O<sub>v</sub>, OH, O<sub>b</sub> and H<sub>2</sub>O) in time ranging from 0 to 300 s, it obviously shows that the curve of OH decreases with time corresponding to the association of OH pairs, where correspond to the proton H ripe from the neighbouring bridging oxygen O<sub>2c</sub> and convert back to molecular H<sub>2</sub>O (4) which is also released from Ti<sub>5c</sub> sites [5, 6], whereas, The surprising is the oxygen vacancies that has no strong influence on the dissociation of H<sub>2</sub>O on surface as the equation (IV. 1) and **Figure IV. 1**, overbalance to the increases of the coverage of O<sub>b</sub> this means that the coverage of O<sub>v</sub> healing and covered only by the H<sub>2</sub>O flux arrived on surface [7], meanwhile, the coverage of oxygen vacancies increases but gradually with slow manner, and this reflects to the rate constant of desorption which is very slow because association of the OH groups should have high temperature [8]. On other hand, the coverage of H<sub>2</sub>O decreases with the coverage of Ti increases because the water molecules desorbed from the surface only in molecular form [9], and also due to the dissociation of H<sub>2</sub>O molecules on free- defect sites Ti<sub>5c</sub>. For comparison, the amount of association is strongly depending on the coverage of H<sub>2</sub>O attached at the surface where the association of OH decreases with the coverage of H<sub>2</sub>O adsorbed on surface and take long time to reach the equilibrium around 270 s at high concentration ( $\theta_{H_2O} = 0.25$ ) compared with concentration at ( $\theta_{H_2O} = 0.2$ ) reaches the equilibrium around 300 s, see **Figure IV.1**. (a)-(b). These results indicate that water dissociates on free-defect surface and they are in good agreement with literature [10].

### **IV.3. Temperature effect**

Temperature has significant effects on various chemical and environmental processes and for this reason; we want to highlight its importance in understanding and managing this system. Therefore, we study the influence of temperature on the behaviour of water molecules on the surface and enhance OH production; we calculate the rate constant of reaction for each value of temperature from (80 K to 360 K) when solving the system. From following **Figure IV.2** (a)-(b), we can identify fourth region. In **Figure IV.2** (a), below 100 K no reactions (dissociation, association even diffusion) exists because the mobility of molecules is very slow, thus the competitive ability of water molecules reacts with surface is small and does not change at this region, by increasing slightly the temperature of surface from (100 K to 150 K) as shown in the following **Figure IV.2** (a)-(b), the coverage of H<sub>2</sub>O and O<sub>b</sub> increase with a sharp drop in the coverage of OH groups due to the OH pairs associated and converted back



to H<sub>2</sub>O molecules but remained onto under coordinate Ti<sub>5c</sub> sites [11] as indicated in **Figure IV.2 (b)** at the same region because also under < 150 K the H<sub>2</sub>O molecules cannot diffuse onto Ti<sub>5c</sub> and this features hindered the adsorption of defects sites as well as on defect-free sites meanwhile promote the recombination of OH hydroxyls. These results are in good agreement with the adsorption of water at the surface [12]. In the third region, from [150 K to 250 K] illustrate that the dissociation of H<sub>2</sub>O molecules on defective sites are the predominant because the dissociation on O<sub>v</sub>'s occurs at temperature > 160 K [13], this is due to the mobility of H<sub>2</sub>O molecules on surface where the dissociation of H<sub>2</sub>O increases from [0.05 to 0.1] by increasing the temperature [14], such these OH that play important role in the photocatalytic reactions treatment of water of rutile TiO<sub>2</sub> (110) surface under sun light shining [15, 16] as well as effects on the electronic properties of surface and this reflects to the sharp decreases in the coverage of H<sub>2</sub>O molecules on surface in two ways, first from the dissociation as mention before and the second, the H<sub>2</sub>O molecules released from the surface [17].



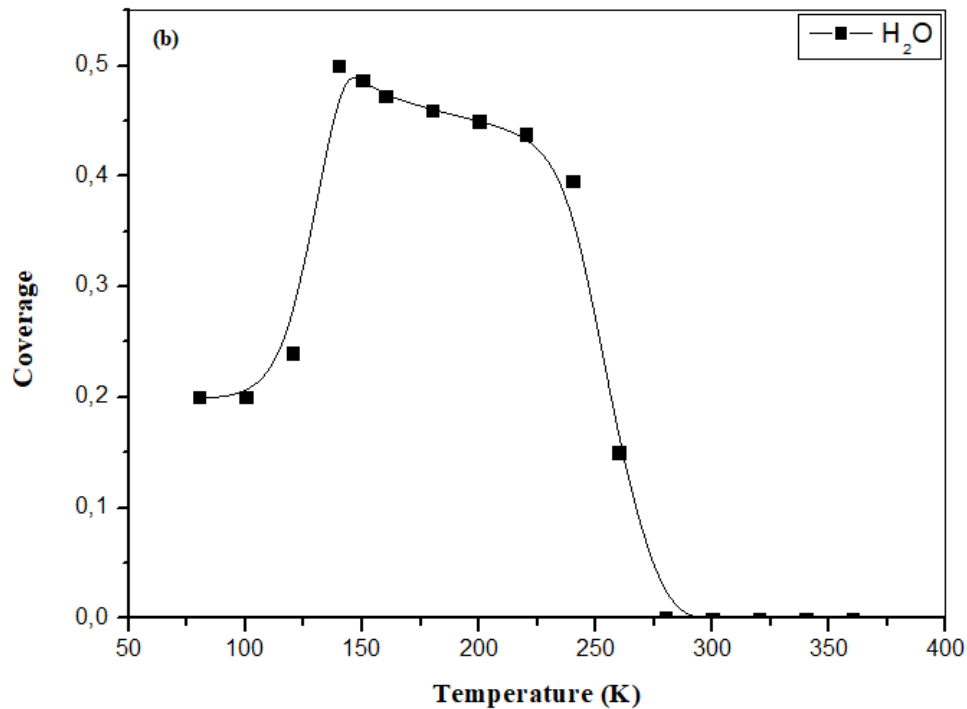


**Figure IV.2:** Represent the variation of the surface rate coverage as a function of temperature (K), a) for OH and  $O_b$  and b) for  $H_2O$ .

In the fourth region from 250 K and more, we show the predominant reaction in these temperatures is the association of OH groups from the defect sites and desorption of water molecules from the surface and remained constant up to 320 K ([4] and references therein). These results strongly agree with experimental results reported in [18] that the desorption move to high temperature at low coverage due to increasing the binding energy with coverage. To complete the discussion the coverage of vacancies depends only with the association of OH groups in addition to that this reaction occurs at high temperature.

#### IV.4. Effect of oxygen vacancies and $H_2O$ flux: Steady state case

We suppose the variation of the system on the surface remains constant or stable over time of the reaction, setting these rates to zero in the steady state gives the system of equations (IV. 6) - (IV. 9) as indicated below. The stability of the set of equations is very important because any bifurcation parameter can dramatically change it and to avoid such behaviour we took the rates constants  $K_i$  with similar thermal stability.

$$-\phi K_5 \theta_V \theta_b + K_6 \theta_{OH}^2 = 0 \quad (IV. 6)$$

$$-\phi K_5 \theta_V \theta_b + K_4 \theta_{OH}^2 - K_3 \theta_{H_2O} \theta_b + K_6 \theta_{OH}^2 = 0 \quad (IV. 7)$$

$$-\phi K_1 \theta_{Ti} + K_2 \theta_{H_2O} = 0 \quad (IV. 8)$$

$$\phi K_5 \theta_V \theta_b - K_4 \theta_{OH}^2 + K_3 \theta_{H_2O} \theta_b - K_6 \theta_{OH}^2 = 0 \quad (IV. 9)$$

$$\phi K_1 \theta_{Ti} - K_2 \theta_{H_2O} - K_3 \theta_{H_2O} \theta_b + K_4 \theta_{OH}^2 = 0 \quad (IV. 10)$$

We use a Mathematica software tool to solve this system of equations above, and the corresponding solution of surface rate coverage for each species is given by the following set of equations:

$$\theta_{OH} = 0.16 \left( -750 \phi \theta_{O_V} + 2.24 \sqrt{1875 \phi \theta_{O_V} - 2237 \phi \theta_{O_V}^2 + 96210. \phi^2 \theta_{O_V}^2} \right) \quad (IV. 11)$$

$$\theta_{Ti} = 0.2 \theta_{O_V} \quad (IV. 12)$$

$$\theta_{H_2O} = 8.7 \phi \theta_{O_V} \quad (IV. 13)$$

$$\theta_{O_b} = \frac{5.10^{-4} (10^3 \phi \theta_{O_V} - 2.10^3 \phi \theta_{O_V}^2 + 2.10^5 \phi^2 \theta_{O_V}^2 - 670.8 \phi \theta_{O_V} \sqrt{\phi \theta_{O_V} (1.8.10^3 - 2.2.10^3 \theta_{O_V} + 9.6.10^4 \phi \theta_{O_V})})}{\phi \theta_{O_V}} \quad (IV. 14)$$

These solutions of surface compounds rates coverage depend on the H<sub>2</sub>O flux and oxygen vacancies (O<sub>V</sub>). As indicated in **Figure IV. 3** (a), OH hydroxyls increases and reaches a maximum at 0.7 for O<sub>V</sub> = 0.04 then it decreases sharply to the minimum for a higher value of O<sub>V</sub>'s, this finding is strongly in accordance with the work reported in [19]. The same behaviour for OH hydroxyls is illustrated in **Figure IV. 3** (b) when this H<sub>2</sub>O flux varied from 0 to 1 ML. This graph illustrates that the coverage of OH (hydroxyls) increases at low H<sub>2</sub>O flux values and reaches a maximum around 0.7 (for a flux value around 0.4) afterward it decreases which means that OH hydroxyls production is slightly reduced.

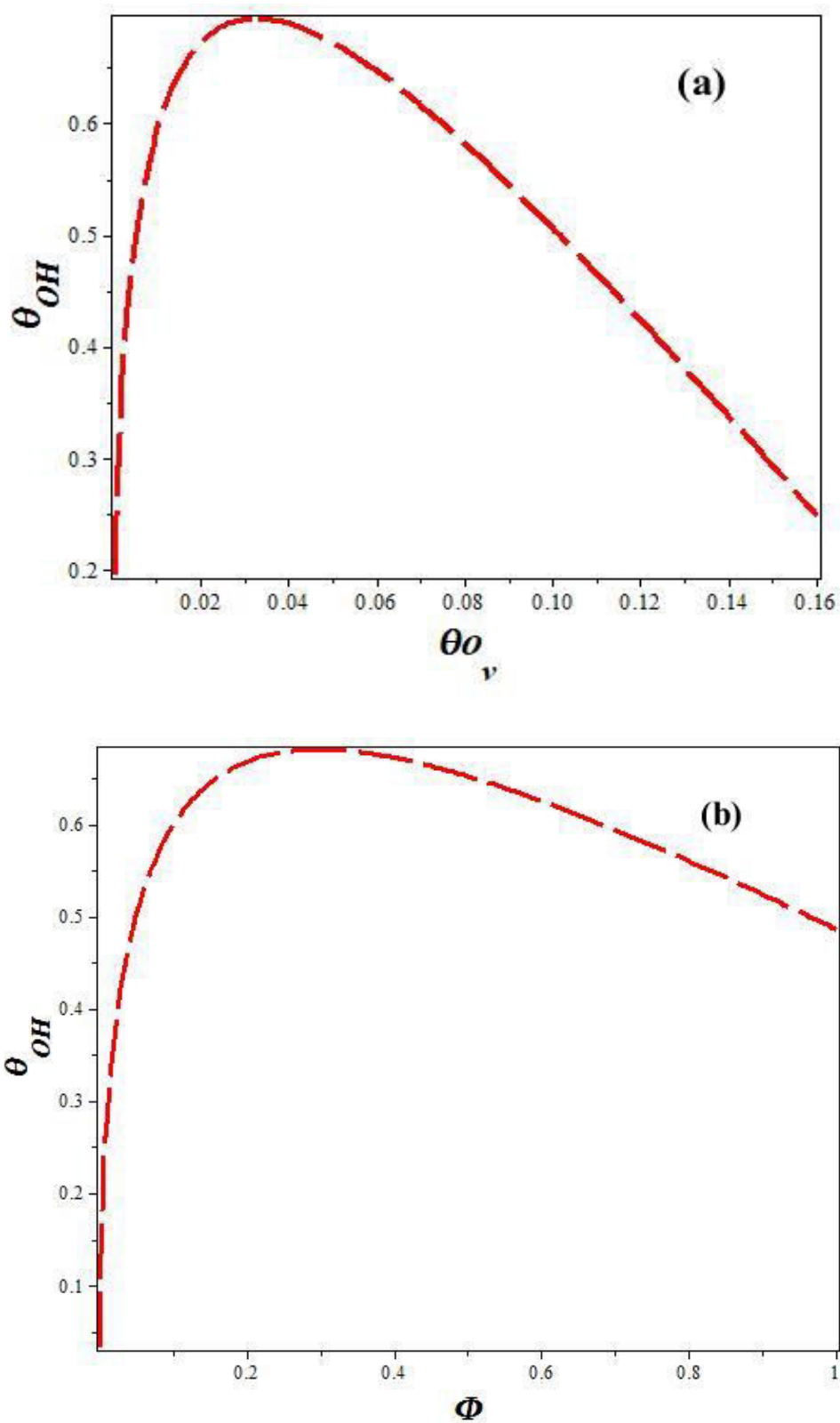


**Figure IV.3:** The effect of: a) oxygen vacancies, b) H<sub>2</sub>O flux on the behaviour of water on rutile (110) surface.

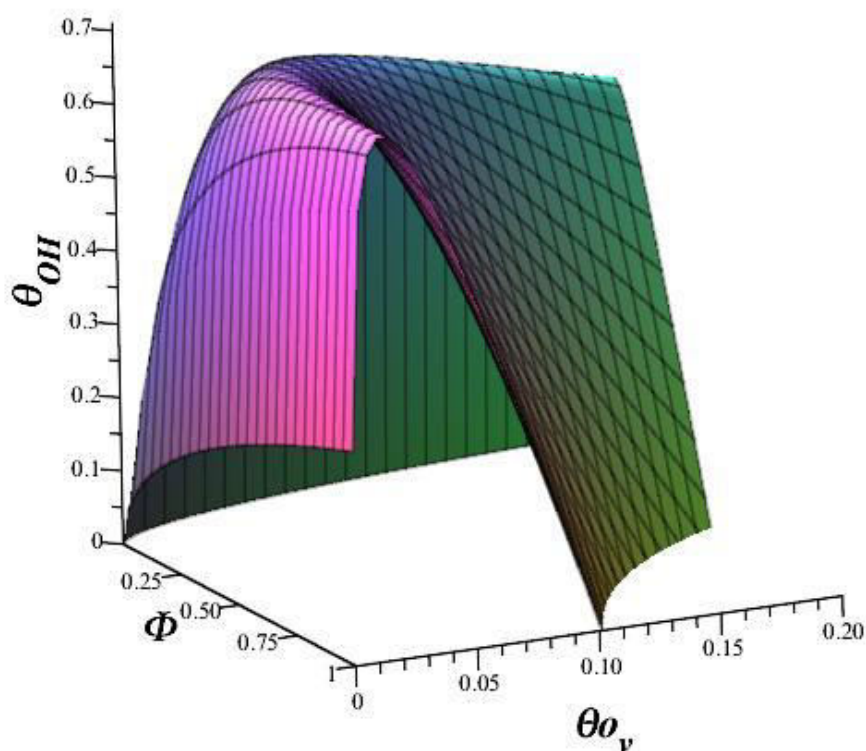
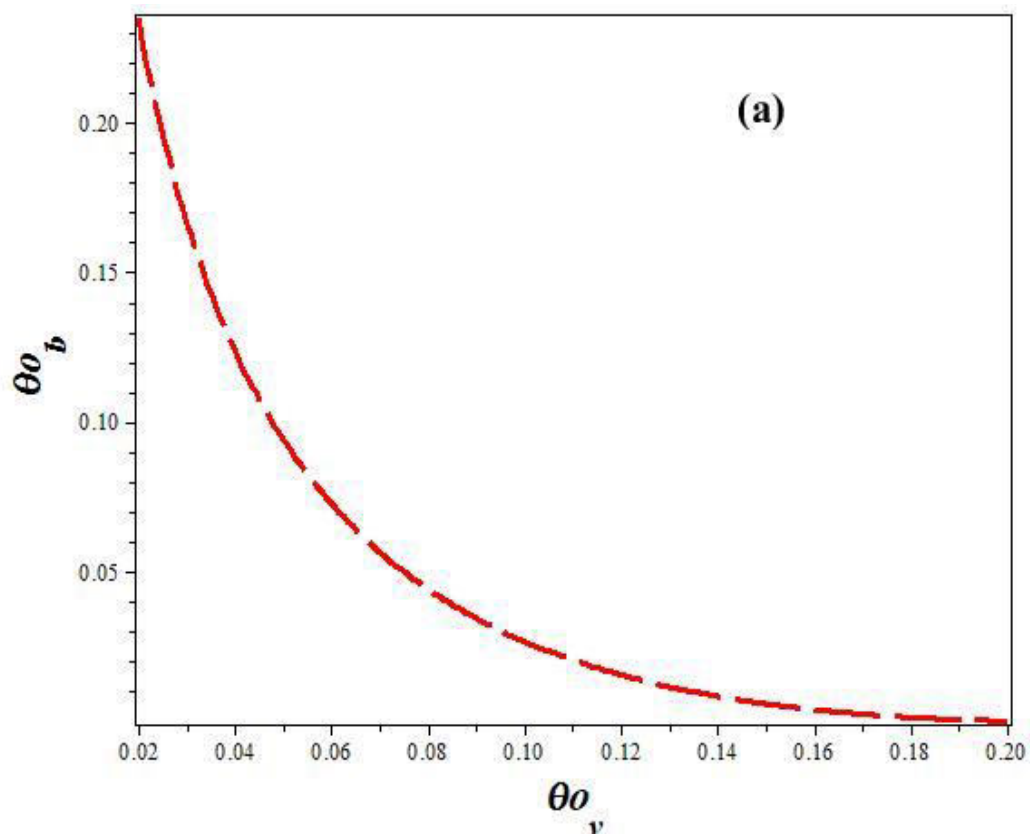


**Figure IV.4:** Kinetic curves for the OH hydroxyls at rutile TiO<sub>2</sub> (110) surface for various H<sub>2</sub>O flux and concentration of O<sub>v</sub> on the surface.

To illustrate these variations of OH on the surface versus H<sub>2</sub>O flux and O<sub>v</sub>, a three dimension (3D) curve is shown in **Figure IV.4**, the coverage of hydroxyls grows with increasing the O<sub>v</sub> because the excess electrons due to OH adsorption [20] and reaches to a maximum around 0.7 ML at O<sub>v</sub> equal 0.04 ML. At high coverage of O<sub>v</sub> up to 10 % the production of OH decays and gets a small value almost zero. In other hand, the coverage of OH depends on the arriving H<sub>2</sub>O molecules; when the H<sub>2</sub>O flux arrived at surface increases, the production of OH increases and reaches a maximum at 0.7 ML for H<sub>2</sub>O flux around 0.4 ML, despite, for H<sub>2</sub>O flux takes value more than 0.4 ML and filling all the surface leading to no production of OH hydroxyls more on the surface which is occupied only with H<sub>2</sub>O molecules with creating a chain of H<sub>2</sub>O and multilayer of water.

Using the equation (IV. 14), the variation curve of the coverage of O<sub>b</sub> for different concentrations of O<sub>v</sub> and H<sub>2</sub>O flux is shown in **Figure IV. 5**.

**Figure IV.5** (a) illustrates the variation of  $\theta_{Ob}$  as a function of  $\theta_{Ov}$  for the H<sub>2</sub>O flux taken 0.4 ML.



The graph clearly shows that  $\theta_{O_b}$  decreases when the concentration of  $O_v$  grows (increases) because the oxygen vacancies are created from the bridging oxygen, meanwhile the coverage of  $O_b$  decays exponential-like with increasing the  $H_2O$  flux at the concentration of  $\theta_{O_v}$  on surface constant and equals 0.05 ML as shown in **Figure IV.5 (b)**.

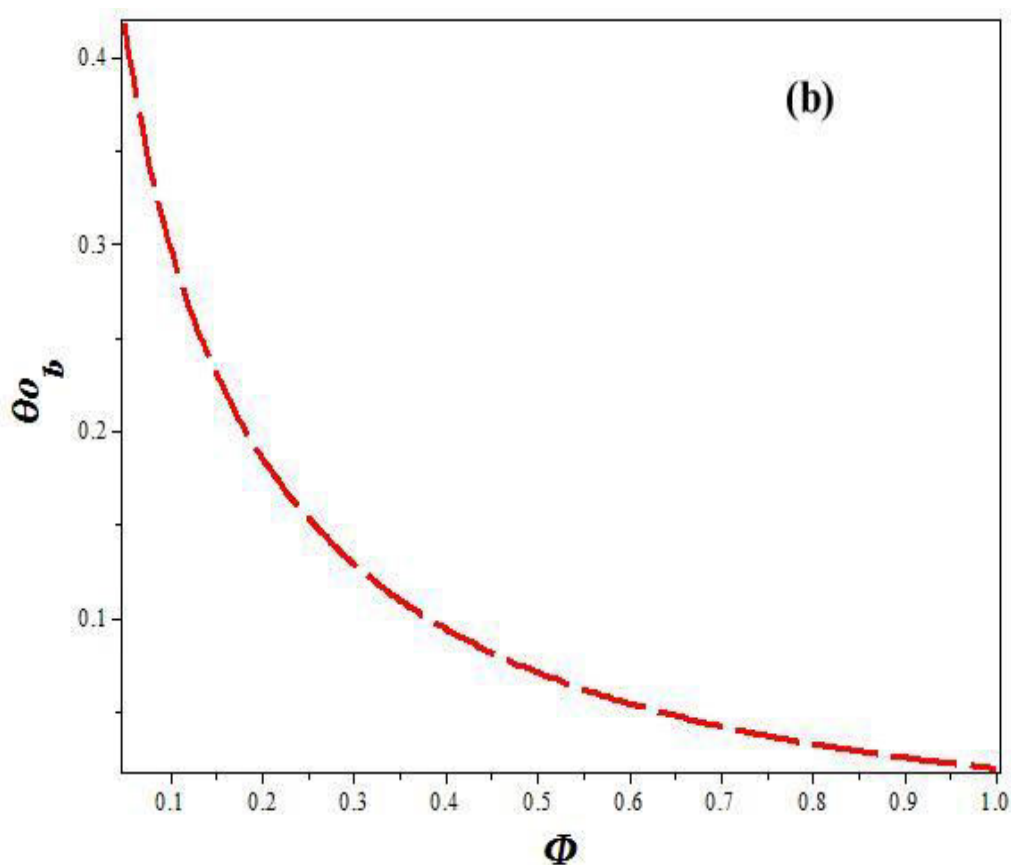


**Figure IV.5:** The effects of: a) oxygen vacancies and b) H<sub>2</sub>O flux of the variation of oxygen bridging ( $O_b$ ).

**Figure IV.6** is plotted using equation (IV. 14), it is interesting to note some common relations; the coverage of  $O_b$  decreases exponential-like with increasing the coverage of  $O_v$  and tends to a small value for large value of  $O_v$ , also at high value for the H<sub>2</sub>O flux, the coverage of  $O_b$  decreases. This figure demonstrates that the  $O_b$  is a key factor in the dissociation and the adsorption of H<sub>2</sub>O molecules.

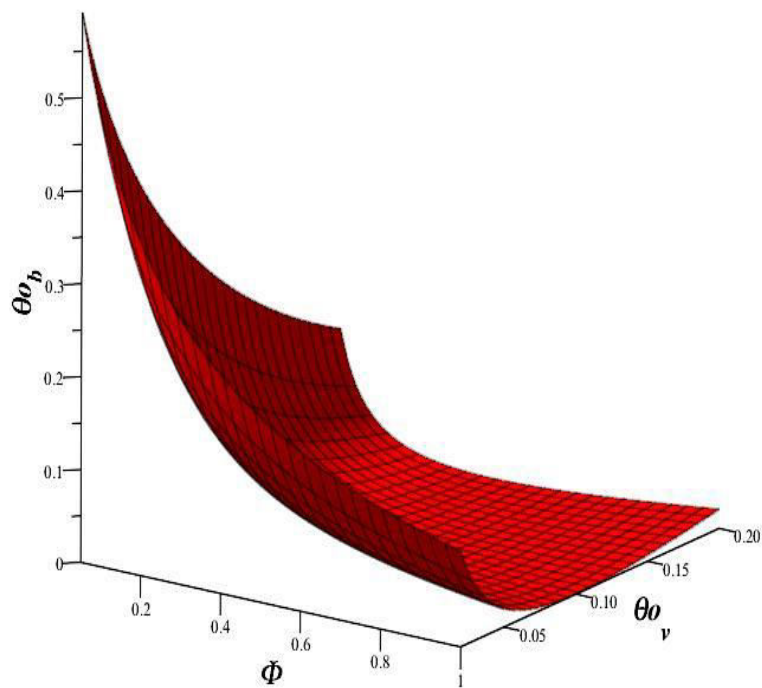


**Figure IV.6:** The coverage of  $O_b$  as a function of  $H_2O$  flux and  $O_v$  defects on rutile  $TiO_2$  (110) surface.

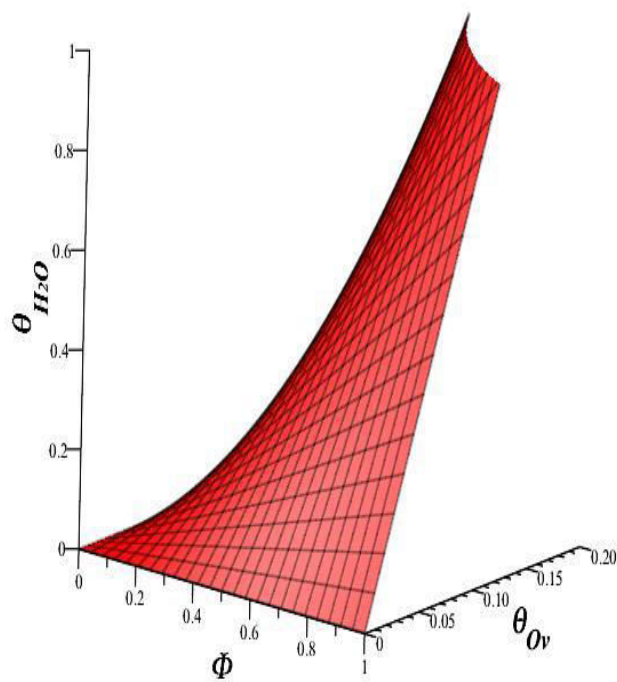


**Figure IV.7:** The coverage of  $H_2O$  on surface versus  $H_2O$  flux and the coverage of oxygen vacancies  $O_v$ .



The equation (IV. 13), variation of H<sub>2</sub>O uptake on surface versus the and the H<sub>2</sub>O flux, indicating, the coverage of H<sub>2</sub>O takes small values almost plateau when the H<sub>2</sub>O flux and the concentration of O<sub>v</sub> on surface is very small, afterward, the coverage of H<sub>2</sub>O increases steadily with H<sub>2</sub>O flux and the concentration of O<sub>v</sub>, as illustrated in **Figure IV.7**.

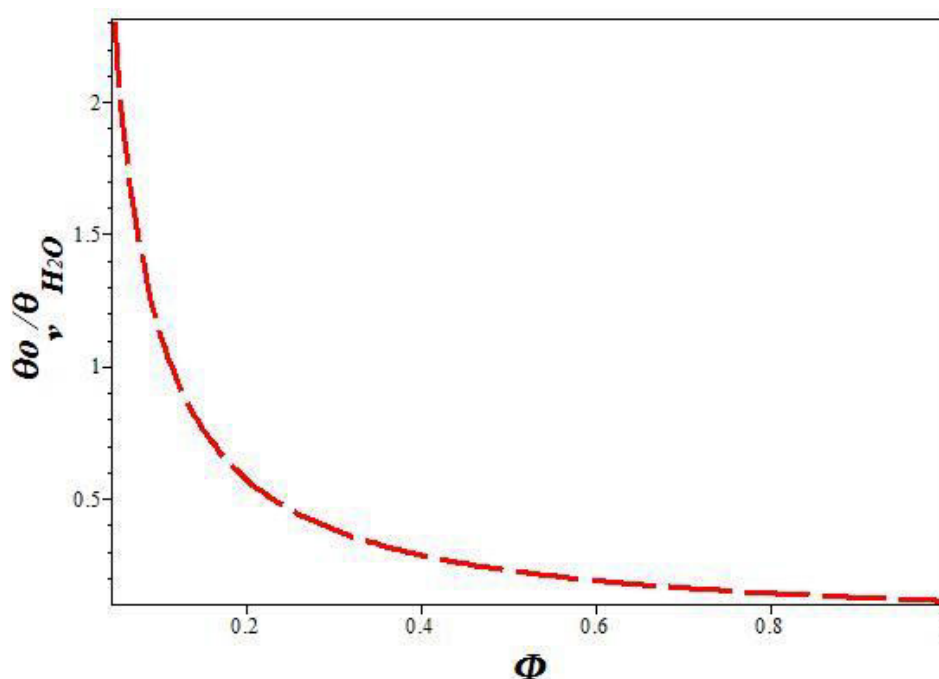


**Figure IV.8:** The ratio of ( $\theta_{O_v} / \theta_{H_2O}$ ) on rutile TiO<sub>2</sub> (110) surface versus H<sub>2</sub>O flux.

**Figure IV. 8** illustrates the ratio of ( $\theta_{O_v} / \theta_{H_2O}$ ), from equation. (IV. 13), versus the H<sub>2</sub>O flux; indicating that the fraction of ( $\theta_{O_v} / \theta_{H_2O}$ ) decreases with increasing the H<sub>2</sub>O flux. This can be explained that increasing the coverage of H<sub>2</sub>O at the surface is caused by the filling of oxygen vacancies sites.

From these results, we can clearly indicate that the interactions of H<sub>2</sub>O with rutile TiO<sub>2</sub> (110) surface were heavily affected by the O<sub>v</sub> and H<sub>2</sub>O flux. As expected, since the H<sub>2</sub>O flux arrived on rutile TiO<sub>2</sub> (110) surface, they can firstly adsorb up to Ti<sub>5c</sub> sites because the adsorption energy increased when the coverage decreases (which is positively charged) in this case the binding of H<sub>2</sub>O increased on surface [21, 22]. Therefore, we carried out to study the effect of H<sub>2</sub>O flux and the coverage of O<sub>v</sub> on the behaviour of H<sub>2</sub>O molecules on rutile TiO<sub>2</sub> (110) surface. We conclude that at low values of H<sub>2</sub>O flux, the mobility of H<sub>2</sub>O molecules to be high which is helpful for the H<sub>2</sub>O molecules adsorbed and diffuse on the surface in direction (001) which is adsorbed in oxygen vacancies and promote the H proton hopping at the bridging oxygen and create OH pairs, deal to heal the vacancies and secondly adsorbed on

defect-free sites as well as to form two OH, because dissociation at bridging oxygen vacancies is more favourable than H<sub>2</sub>O adsorption on the defect-free Ti<sub>5c</sub> sites in term of dissociation energy [23], resulting the OH increases till reach the maximum at 0.7ML for 0.4 of H<sub>2</sub>O flux. This is in good accordance with the prediction by Lindan and Zhang [24]. At a high H<sub>2</sub>O flux, water may adsorbed molecularly by make chains of water molecules linked together a hydrogen bonds, with a small fraction of dissociative on O<sub>v</sub> because at least one or two H<sub>2</sub>O molecules uptake on Ti<sub>5c</sub> sites and form multilayers of H<sub>2</sub>O molecules also at large amount of H<sub>2</sub>O molecules exist on surface hinders the diffusion of H<sub>2</sub>O molecules and remains in molecular forms, therefore, H<sub>2</sub>O molecular adsorption is more favourable at high coverage as see in Figure IV.7 [25].

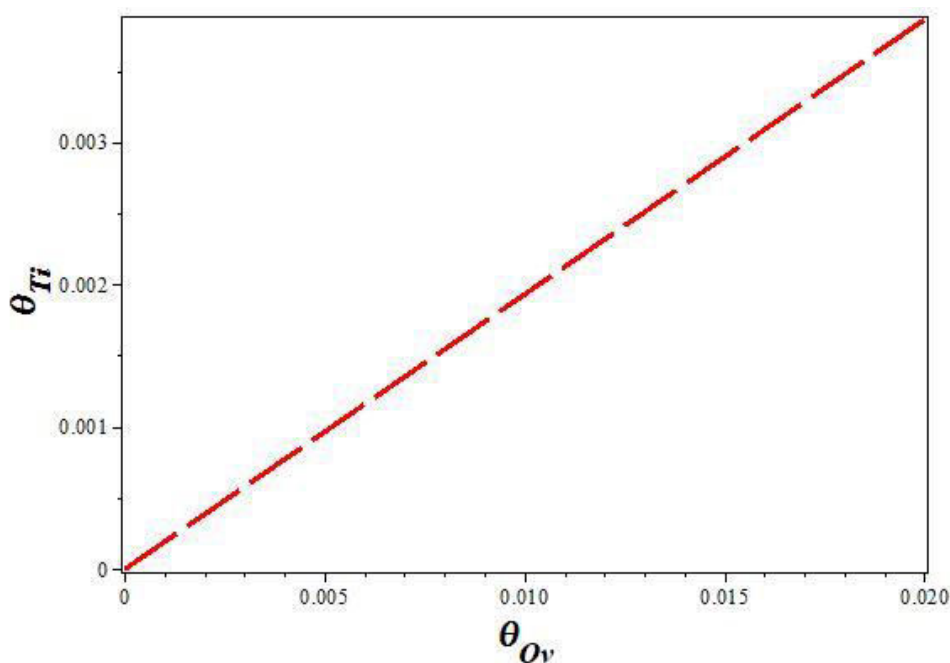


**Figure IV.9:** The coverage of Ti<sub>5c</sub> on rutile TiO<sub>2</sub> (110) surface as a function of the concentration of oxygen vacancies (O<sub>v</sub>).

As observed, O<sub>v</sub> is a key factor in water dissociation process, where the coverage of O<sub>v</sub> affects on the adsorption and dissociation of water, however, the amount of OH formed on rutile TiO<sub>2</sub> (110) surface increases at low coverage on O<sub>v</sub> this process occurs extremely fast because the H<sub>2</sub>O favours the dissociation at oxygen vacancies [22] reach to the maximum around 0.7 ML because the repulsive interaction between the functional groups, afterward, when the coverage of O<sub>v</sub> increases beyond to 0.05 ML, the OH groups coverage decreases, because at high concentration of O<sub>v</sub> it affects on the structure properties, which leads to (2x1) reconstruction surface [2], additionally, we know that the O<sub>v</sub>'s created from the bridging

oxygen, this implies that the coverage of  $O_v$  increases due to decrease the bridging oxygen as illustrated in **Figure IV.6**. In noting, when ( $N_{Ob} < N_{Ov}$ ) deficient the dissociation in  $O_v$  and the defect-free sites, this is in a good agreement with previous works reported in [26]. The production of hydroxyls leads to growth the electron scavengers which promote the charge separation in photocatalysis process as well as the oxidation of organic substances and several applications (self-cleaning, pharmaceutical and green  $H_2$  production...) [27-29]. OH hydroxyls create by dissociation of water is more stable than the OH produced by UV light irradiation [30]. The dissociation of  $H_2O$  molecules in either terminal hydroxyl or OH in vacancy need a neighbouring oxygen atoms for the H proton creates the second OH on  $O_b$ , besides, the coverage of bridging oxygen decreases with  $H_2O$  increases as **Figure IV.3** (a) improved that clearly. This inhibit the production of OH, meanwhile the molecular adsorption will be the predominant as **Figure IV.7** illustrates that; where the vacancies increasing the asymmetry for titanium atoms near vacancies that leads to enhance the water adsorption further the  $H_2O$  adsorbed molecular at high and low coverage [31, 32]. **Figure IV.9** shows a plot of the linearized form of the reaction in equation (IV. 11) it is clearly shown that the coverage of  $Ti_{5c}$  is independent to the flux; it depends only on the concentration of the surface  $O_v$ . Many authors overbalanced the increase to transfer the  $Ti_{6c}$  coordinate underneath the  $O_v$  to  $Ti_{5c}$  [21, 33]. In other hand,  $H_2O$  adsorbed molecular on  $Ti_{5c}$  meanwhile diffuses toward the vacancy site where the dissociation takes place, thus,  $H_2O$  let behind a  $Ti_{5c}$  site. These results accordance with the Linden and co-workers predict that mixed molecular/dissociate is the most stable configuration on rutile  $TiO_2$  (110) surface [34, 36], it is worth noting that the behaviour of the water (molecular or dissociative) moderate by environmental factors which lead to change dramatically its dynamics under the structure and termination of the surface changes.

### **VI.5. Water- proteins interactions on $TiO_2$ surface**

The water molecules have curious behaviour during the interactions with proteins that are going to be adsorbed. Water still considered as the best solvent to keep proteins in their native structure properties unlike deuterium  $D_2O$  that changes somehow their properties [37]. The  $H_2O$  molecules have invaluable role for dynamics and stability of proteins on surface; in the following section we give simple idea that clearly demonstrates the difference between the adsorption of simple and complex bio-molecules like BSA proteins. From the experimental work reported by A. Bouhekkka [38] using FTIR-ATR spectroscopy, where the system (Ge,  $TiO_2$  + water) was taken, the  $H_2O$  on surface is very important in the background which is our

study interest to highlight on it, to this way we show that when the proteins solved in water arrive on the surface, they start to be adsorbed and at the same time some water molecules should be released from the surface as indicated by the negative peaks in the region 3000-3600  $\text{cm}^{-1}$  [37] as illustrated in the following **Figure IV.10**.

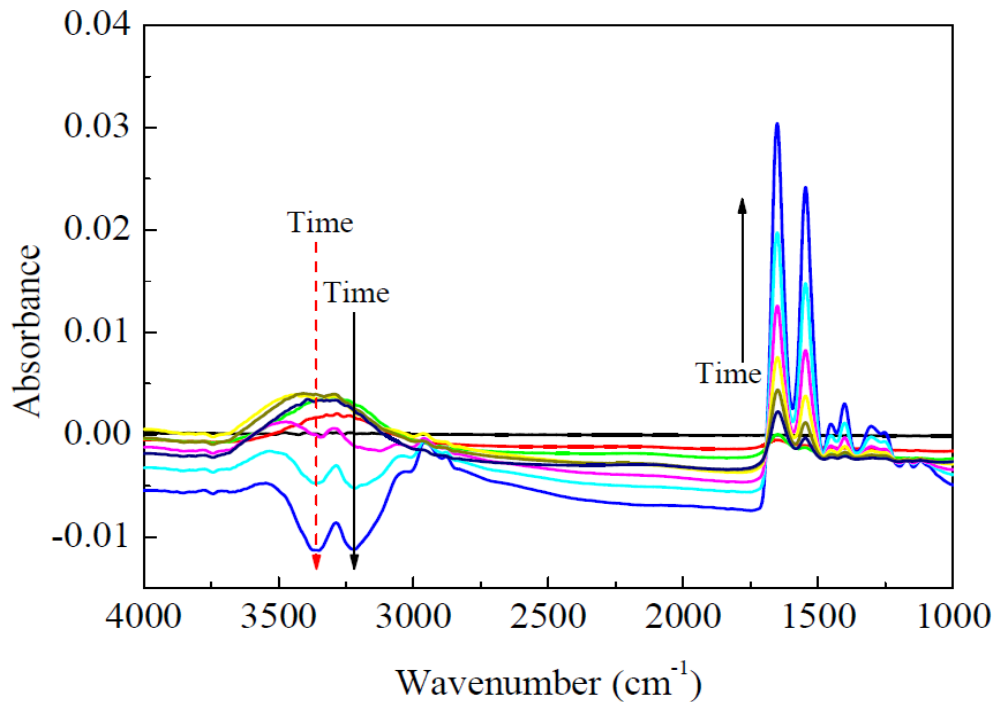


**Figure IV.10:** Adsorption spectra of BSA on  $\text{TiO}_2$  close to equilibrium situation. Spectra were recorded during flowing BSA solution drop by drop and rinsing with water in between two successive drops. The graph is kindly given by A. Bouhekka [38].

This figure clearly shows that the sensitive spectral region of proteins adsorption on surface is the amide I band range between (1600 to 1700  $\text{cm}^{-1}$ ) overlapping to the H-O-H bending as illustrated in chapter II, it strongly agrees with the findings in [40]. Surprising, the adsorption of proteins lead to expelled the water molecules from the surface as the two negative peak located near 3200  $\text{cm}^{-1}$  and 3500  $\text{cm}^{-1}$  associated with strong bonds of water (ice-like) [41] and liquid water molecules [42], respectively, meanwhile it could appear and increase a positive peak located around 3700  $\text{cm}^{-1}$  which may correspond to free OH appears on surface (in the cell) during warming or visible light shining, that means the adsorption of proteins changes the morphology of the surface as well as the water structure resulting change the proteins structure. The protein can be adsorbed in both native ( $\theta_N$ ) and unfolded state ( $\theta_U$ ). The full surface coverage  $\theta$  is naturally determined by the sum of  $\theta_N$  and  $\theta_U$  [43], as:

$$\theta = \theta_N + \theta_U \quad (\text{IV. 15})$$

The kinetic equations for the time evolution for both  $\theta_N$  and  $\theta_U$  forms, without desorption, are as follows:

$$\frac{d\theta_N}{dt} = K_N C_0 (1 - \theta_N - \theta_U) - K_U \theta_N (1 - \theta_N - \theta_U) \quad (\text{IV. 16})$$

$$\frac{d\theta_U}{dt} = K_U \theta_N (1 - \theta_N - \theta_U) \quad (\text{IV. 17})$$

Where:

$K_N, K_U, C_0$  and  $t$  are the adsorption, spreading rates constant, the concentration of proteins on surface and the time.

Considering equations (IV. 15), (IV. 16) and (IV. 17), the expression for the variation of  $\theta$  can be obtained and given by:

$$\frac{d\theta}{dt} = \frac{d\theta_U}{dt} + \frac{d\theta_N}{dt} = K_N C_0 (1 - \theta_N - \theta_U) \quad (\text{IV. 18})$$

Which is solved by the well-known kinetic equation is able to describe the adsorption of proteins particles on surface is Langmuir equation, as demonstrated in [43].

$$\theta(t) = 1 - e^{-(K_N C_0 t)} \quad (\text{IV. 19})$$

This behaviour overbalances to the hydrophobic core buried inside on the native structure, so when it's close the surface its initial structure collapse and followed by expelled the water from the surface which achieves the adsorption, resulting in a dry and packed protein, which the water considered as a lubricant for packing the hydrophobic core after the transition state [44, 45]. The water cannot be released completely from the surface but it creates hydrogen bonds with the protein backbone. Therefore, many research groups carried out to clearly explain this complex phenomenon.

## IV.6. Conclusion

The issue of the interaction water-rutile  $\text{TiO}_2$  (110) interface is often intriguing and amazing complicated. The present results show that this interaction water- rutile  $\text{TiO}_2$  (110) interface has distinct effects on the behaviour of  $\text{H}_2\text{O}$  molecules controlled with relative parameters. These results allow us choosing good conditions for clearly indicate the water behaviour at the surface besides the production of OH,  $\text{H}_2\text{O}$  molecules closed on surface firstly adsorbed in molecular form after then it dissociate at oxygen vacancies and defect-free species because  $\text{O}_v$  is more favourable than  $\text{Ti}_{5C}$  sites, at low coverage oxygen vacancies on surface because a high amount of  $\text{O}_v$  destroy the structure of surface and hindered the

dissociation, and the H<sub>2</sub>O flux play a key factor in the dynamics of water which adsorption increases with increasing H<sub>2</sub>O flux. These radicals are likely to play the major role for producing green H<sub>2</sub> as well as the purification of wastewater.

As indicated at the end of this chapter, adsorption of proteins at a considered surface as that of TiO<sub>2</sub> will lead to release water molecules from the surface. The kinetic of adsorption is different because water is a simple molecule however bio-molecules, like BSA protein, have complex structures where the parameters that control the adsorption still not well understood.

## References

- [1] **S. Gelover, P. Mondragón and A. Jiménez**, Titanium dioxide sol–gel deposited over glass and its application as a photocatalyst for water decontamination, 241–246, s.l. Photochem. and Photobiol. A: Chem. (2004), Vol. 165.
- [2] **N. Bundaleski, A.G. Silva, U. Schröder, A.M.C. Moutinho and O. Teodoro**, Adsorption dynamics of water on the surface of TiO<sub>2</sub> (110), 012008-012018, Phys.: Conf. Series. IOP Publishing, (2010), Vol. 257.
- [3] **K. Muralidharan, P. Deymier, M. Stimpfel, N.H.D. Leeuw and M.J. Drake**, Origin of water in the inner solar system: a kinetic monte carlostudy of water adsorption on forsterite, 400-407, s.l. Icarus, (2008), Vol. 198.
- [4] **P.J.D. Lindan, N.M. Harrison, J.M. Holender and M.J. Gillan**, First principals molecular dynamics simulation of water dissociation on TiO<sub>2</sub> (110), 246-252, Chem. Phys. Lett. (1996), Vol. 261.
- [5] **S. Wendt, J. Matthiesen, R. Schaub, E.K. Vestergaard, E. Lægsgaard, F. Besenbacher and B. Hammer**, Formation and splitting of paired hydroxyl groups on reduced TiO<sub>2</sub>(110), 066107-066110, s.l. Phys. Rev. Lett. (2006), Vol. 96.
- [6] **Z. Dohnalek, I. Lyubinetsky and R. Rousseau**, Thermally-driven processes on rutile TiO<sub>2</sub> (110)-(1 x 1): a direct view at the atomic scale, 161–205, s.l. Prog. Surf. Sci. (2010), Vol. 85.
- [7] **M.B. Hugenschmidt, L. Gambel and C.T. Campbell**, The interaction of H<sub>2</sub>O with a TiO<sub>2</sub> surface, 329-340, s.l. Surf. Sci., (1994), Vol. 302.
- [8] **M.A. Henderson**, Structural sensitivity in the dissociation of water on TiO<sub>2</sub> single-crystal surfaces, 5093-5098, s.l. Langmuir, (1996), Vol. 12.
- [9] **J. Lausmaa, P. Lofgren and B. Kasemo**, Adsorption and coadsorption of water and glycine on TiO<sub>2</sub>, s.l. John Wiley & Sons, Inc. (1999).
- [10] **U. Diebold**, Perspective: a controversial benchmark system for water-oxide interfaces: H<sub>2</sub>O / TiO<sub>2</sub>(110), 040901-040904, s.l. Chem. Phys. (2017), Vol. 147.
- [11] **W.Z. Tao, W.Y. Gang, R. Mu, Y. Yoon, A. Dahal, G.K. Schenter, V.A. Glezakou, R. Rousseau, I. Lyubinetsky and Z. Dohnálek**, Probing equilibrium of molecular and deprotonated water on TiO<sub>2</sub> (110), 1801-1805, Proc. Natl. Acad. Sci. (2017), Vol. 114.
- [12] **J. Matthiesen, J. Hansen, S. Wendt, E. Lira, R. Schaub, S. Leagsgaard, F. Besenbacher and B. Hammer**, Formation and diffusion of water dimers on rutile TiO<sub>2</sub>, 226101-226104, s.l. Phys. Rev. Lett. (2009), Vol. 102.

- [13] **I.M. Brookes, C.A. Muryn and G. Thornton**, Imaging water dissociation on TiO<sub>2</sub> (110), 266103-266106, s.l. Phys. Rev. Lett. (2001), Vol. 87.
- [14] **R. Shaub, P. Thotrup, N. Lopez, E. Lagsgaard, J.K. Norskov and F. Besenbacher**, Oxygen vacancies as active sites for water dissociation on rutile TiO<sub>2</sub> (110), 266104-266107, s.l. Phys. Rev. Lett. (2001), Vol. 87.
- [15] **A. Nakajima, S. Koizumi, T. Watanabe and K. Hashimoto**, Photoinduced amphiphilic surface on polycrystalline anatase TiO<sub>2</sub> thin films, 7048-7050, s.l. Langmuir, (2000), Vol. 16.
- [16] **T. Minabe, A. Nakajima, A. Fujishima, T. Watanabe and K. Hashimoto**, Effects of thermal and evacuating treatments on photoinduced hydrophilic conversion at TiO<sub>2</sub> surface, 779-782, s.l. Electrochem. (2000), Vol. 68.
- [17] **P.J.D. Lindan**, Water chemistry at the SnO<sub>2</sub> (110) surface: the role of inter-molecular interactions and surface geometry, 325-329, s.l. Chem. Phys. Lett. (2000), Vol. 325.
- [18] **C. Zhang and P.J.D. Lindan**, Multilayer water adsorption on rutile TiO<sub>2</sub> (110): a first-principles study, 4620-4625, s.l. Chem. Phys. (2003), Vol. 118.
- [19] **X.L. Yin, M. Calatayud, H. Qiu, Y. Wang, A. Birkner, C. Minot and C. Woll**, Diffusion versus desorption: complex behavior of H atoms on an oxide surface, 253-256, s.l. Chem. Phys. Chem. (2008), Vol. 9.
- [20] **L.M. Liu, P. Crawford and P. Hu**, The interaction between adsorbed OH and O<sub>2</sub> on TiO<sub>2</sub> surfaces, 155-176, s.l. Prog. Surf. Sci, (2009), Vol. 84.
- [21] **M. Menetrey, A. Markovits and C. Minot**, Reactivity of a reduced metal oxide surface: hydrogen, water and carbon monoxide adsorption on oxygen defective rutile TiO<sub>2</sub> (110), 49-62, s.l. Surf. Sci. (2003), Vol. 524.
- [22] **A.V. Bandura, D.G. Sykes, V. Shapovalov, T.N. Troung, J.D. Kubicki, and R.A. Evarestov**, Adsorption of water on the TiO<sub>2</sub> rutile (110) surface: a comparison of periodic and embedded cluster calculations, 7844-7853, s.l. Phys. Chem. B, (2004), Vol. 108.
- [23] **L.Q. Wang, K.F. Ferris, P.X. Skiba, A.N. Shultz, D.R. Baer and M.H. Engelhard**, Interactions of liquid and vapor water with stoichiometric and defective TiO<sub>2</sub> (100) surfaces, 60-68, s.l. Surf. Sci. (1999), Vol. 440.
- [24] **P.J.D. Lindan and C. Zhang**, Comment on “molecular chemisorption as the theoretically preferred pathway for water adsorption on ideal rutile TiO<sub>2</sub> (110), 029601, s.l. Phys. Rev. Lett. (2005), Vol. 95.
- [25] **R. Mu, Z.j. Zhao, Z. Dohnálek and J. Gong**, Structural motifs of water on metal oxide surfaces, 1785-1806, s.l. Chem. Soc. Rev. (2017), Vol. 46.



- [26] **Z. Dohnálek, I. Lyubinetsky and R. Rousseau**, Thermally-driven processes on rutile  $\text{TiO}_2$  (1 1 0)-(1x 1): a direct view at the atomic scale, 161-205, s.l. *Prog. Surf. Sci.* (2010), Vol. 85.
- [27] **X. Pan, M.Q. Yang, X. fu, N. Zhang and Y.J. Xu**, Defective  $\text{TiO}_2$  with oxygen vacancies: synthesis, properties and photocatalytic applications, 3601-3614, s.l. *Nanoscale*, (2013), Vol. 5.
- [28] **A. Tilocca, C.D. Valentin and A. Selloni**,  $\text{O}_2$  interaction and reactivity on a model hydroxylated rutile (110) surface, 20963-20967, s.l. *Phys. Chem. B*, (2005), Vol. 109.
- [29] **S.J. Boyd, D. O'carroll, Y. Krishnan, R. Long and N.J. English**, Self-diffusion of individual adsorbed water molecules at rutile (110) and anatase (101)  $\text{TiO}_2$  interfaces from molecular dynamics, 398-414, s.l. *Cryst.* (2022), Vol. 12.
- [30] **K. Hashimoto, H. Irie and A. Fujishima**,  $\text{TiO}_2$  photocatalysis: a historical overview and future, 8269-8285, s.l. *Appl. Phys.*, (2005), Vol. 44.
- [31] **S. Malali and M. Foroutan**, Dissociative behavior of water molecules on defect free and defective rutile  $\text{TiO}_2$  (101) surfaces, 295-302, s.l. *Appl. Surf. Sci.* (2018), Vol. 457.
- [32] **L. Huang, K. Gubbins, L. Li and X. Lu**, Water on titanium dioxide surface: a revisit by reactive molecular dynamics simulations, 14832-14840, s.l. *Langmuir*, (2014), Vol. 30.
- [33] **K.P. Gopinath, N.V. Madhav, A. Krishnan, R. Malolan and G. Rangarajan**, Present application of titanium dioxide for the photocatalytic removal of pollutants from water: a review, 110906-110932, s.l. *Environ. Manag.* (2020), Vol. 270.
- [34] **L.J.D. Lindan, N.M. Harrison and M.J. Gillan**, Mixed dissociative and molecular adsorption of water on the rutile (110) surface, 762-765, s.l. *Phys. Rev. Lett.* (1998), Vol. 80.
- [35] **C.J. Zhang and P.J.D. Lindan**, A density functional theory study of the coadsorption of water and oxygen on  $\text{TiO}_2$  (110), 3811-3815, s.l. *Chem. Phys.* (2004), Vol. 121.
- [36] **H. Zhou, H. Zhang and S. Yuan**, Comparison of  $\text{H}_2\text{O}$  adsorption and dissociation behaviors on rutile (110) and anatase (101) surfaces based on reaxFF molecular dynamics simulation, 6823-6837, s.l. *Molecules* (2023), Vol. 28.
- [37] **Y. Levy and J. Onuchic**, Water and proteins: a love-hate relationship, 3325-3326, s.l. *Proc. Natl. Acad. Sci. USA*, (2004), Vol. 101.
- [38] **A. Bouhekka**, Adsorption of BSA protein on silicon, germanium and titanium dioxide investigated by in Situ ATR-IR spectroscopy, PhD thesis, Es-Senia University of Oran, Algeria, (2013).

- [39] **M. Takeuchi, G. Martra, S. Coluccia and M. Anpo**, Mechanism of photoinduced superhydrophilicity on the TiO<sub>2</sub> photocatalyst surface, 15422-15428, s.l. Phys. Chem. B. (2005), Vol. 109.
- [40] **J. Kong and S. Yu**, Fourier transform infrared spectroscopic analysis of protein secondary structures, 549-559, s.l. ACTA Biochim. Biophys.Sinica, (2007), Vol. 39.
- [41] **M.R. Yalamanchili, A.A. Atia and J.D. Miller**, Analysis of interfacial water at a hydrophilic silicon surface by in-situ FTIR/internal reflection spectroscopy, 4176-4184, s.l. Langmuir, (1996), Vol. 12.
- [42] **P.A. Giguere**, Bifurcated hydrogen bonds in water, 354-359, s.l. Raman Spectrosc. (1984), Vol. 15.
- [43] **B.A. Kostyukevich and E.V. Snopok**, Kinetic studies of protein–surface interactions: a two-stage model of surface-induced protein transitions in adsorbed biofilms, 222–231, s.l. Anal. Biochem. (2006), Vol. 348.
- [44] **M.S. Cheung, A.E. Garcia and J.N. Onuchic**, Protein folding mediated by solvation: water expulsion and formation of the hydrophobic core after the structural collapse, 685-690, s.l. PNAS, (2002), Vol. 99.
- [45] **A.E. Garcia and J.N. Onuchic**, Folding a protein in a computer: an atomic description of the folding /unfolding of protein A, 13898-13903, s.l. Proc. Natl. Acad. Sci. (2003), Vol. 100.

## **General conclusion and recommendations**

Liquid – solid interfaces are very interesting subjects in the physical-chemistry surface sciences, especially in recent decades with the increase of environmental crisis (waste water, pollution, CO<sub>2</sub> in industry ...), and because these interfaces are special case from the bulk of each residue (liquid and solid). Therefore, many chemical reactions that occur on the surface/at the interfaces that play a significant role in modern technology, photocatalysis, biosensor, biocompatibility and green H<sub>2</sub> production that may solve the energy crisis in the world. To this end, we focused in this research on studying the interactions of water molecules (H<sub>2</sub>O) on rutile (110) face taking into account all the available surfaces adsorption sites. There are several theoretical and experimental techniques that have been carried out to study and investigate these interfaces, including DFT, STM and FTIR-ATR under different conditions such as temperature, pH and concentration. Both methods (theory and experiment) have advantages and disadvantages because in most cases we cannot get all the information and knowledge needed. For this reason a complementary research using both would be the best to get accurate information about this complex phenomenon occurring at the 2D defect (surface). Among different adsorption theoretical models, the Langmuir one is able to describe the water molecule adsorption dynamics on rutile (110) surface taking into account only one monolayer of surface coverage, implying that chemisorption may be the predominant adsorption mechanism on its.

The H<sub>2</sub>O molecules have intriguing dynamics on surfaces, therefore, in this thesis, we studied the adsorption and the behaviour of water on the rutile TiO<sub>2</sub> (110) surface and explored the factors affecting on its dynamics using theoretical methods. We formulated the dynamics of water at the surface in a system of coupled differential equations that was solved in non-equilibrium and in the steady state cases.

In the findings of chapter IV, we investigated the behaviour of water attached on surface after cutting off (stopping) the H<sub>2</sub>O flux incoming to the surface (before reaching an equilibrium) under different temperature and various H<sub>2</sub>O coverages. The results indicated that the dissociation of water molecules passed through many stages depending on the temperature where its remains stable at low temperature, and when warming the surface it has a positive effect on the formation of OH in temperature varied from 150-250 K. More

addition to this, it leads to the association and desorption of water from the surface at temperature greater than 250 K.

The oxygen vacancies coverage and the amount of H<sub>2</sub>O flux arrived on the surface play a pivotal role in the dynamics of water on surface. We demonstrate the correlation between the extent of OH production and the surface properties, where the coverage of OH increases at low coverage of Ov's and H<sub>2</sub>O flux as discussed in second part of the last chapter, the mixed molecular and dissociative adsorption configurations presented for various conditions agree with previous theoretical and experiment studies.

Finally, we describe a simple comparison between the dynamics of water considered as simple molecule and complex species like bio-molecules, hence, In situ FTIR-ATR spectroscopy allowed monitoring the interaction between proteins adsorbed on TiO<sub>2</sub> surface and the formation of hydroxyls, as well as providing evidence for OH expulsion from the surface meanwhile the proteins particles take place. A detailed mechanistic understanding of the water adsorption on the rutile (110) process is still missing.

The findings described here allow designing a high-performance of OH on the surface by controlling the distribution of oxygen vacancies on surface, temperature, properties of surface ...

## Nomenclature

IEO	International Energy Outlook
TiO <sub>2</sub>	Titanium dioxide
Ge	Germanium
Si	Silicon
H <sub>2</sub> O	Water
E <sub>f</sub>	Fermi energy
E <sub>c</sub>	lowest unoccupied band (Conduction band )
E <sub>v</sub>	highest occupied band (Valence band)
E <sub>g</sub>	Band gap energy
K <sub>B</sub>	Boltzmann constant (J/ K)
N <sub>c</sub>	Effective density of state at conduction band
N <sub>v</sub>	Effective density of state at valence band
E <sub>A</sub>	Acceptors energy
E <sub>D</sub>	Donors energy
N <sub>A</sub>	Concentration of charge acceptors
N <sub>D</sub>	Concentration of charge donors
EC-IR	Electrochemical Infrared Spectroscopy
IRAS	Infrared Reflection Absorption Spectroscopy
SEIRA	Surface Enhanced Infrared Absorption
ATR	Attenuated Total Reflection
DSSC	Dye Sensitized Solar Cell
CE	Counter Electrode
IRE	Internal Reflection Element
DFT	Density Functional Theory
STM	Scanning tunnelling microscopy
FTIR-ATR	Fourier transform infrared attenuated total reflection spectroscopy
P	Pressure of gas (Pa)
V	Volume (m <sup>3</sup> )
ε	Depth of the potential well (dispersion energy)
σ	The finite distance at which the inter-particle potential is zero
IUPAC	International Union of Pure and Advanced Chemistry

pzc	Point Zero Charge
$S_i$	Sticking coefficient
$m_i$	Molecular mass (kg)
$Ti_{5c}$	Titanium fivefold coordinate
$Ti_{6c}$	Titanium sixfold coordinate
$O_{2c}$	Oxygen twofold coordinate (bridging)
$O_{3c}$	Oxygen threefold coordinate
$O_v$	Oxygen Vacancy
OH	Hydroxyl groups
$\Phi$	Water flux
$\theta$	Coverage
$\theta_{Ti}$	Coverage of fivefold coordinate of titanium
$\theta_b$	Coverage of oxygen bridging
$\theta_v$	Coverage of oxygen vacancies
$\theta_{H_2O}$	Coverage of water molecules adsorbed on surface
$\theta_{OH}$	Coverage of hydroxyls groups on surface
$K_i$	Rate constant ( $s^{-1}$ )
$K_0$	Attempt frequency ( $s^{-1}$ )
$E_a$	Activation energy (Kj/mole)
T	Temperature (K)
R	Universel gas constant (K j/mole. K)
ML	Mono layer
$n_a$	The concentration of the adsorption sites
$n_s$	The concentration of all the atomes in the surface
BSA	Serum Albumin Bovine

## **List of publications**

### **1- Publication internationale de rang « A »**

- **Fatima Bouzidi**, Moustafa Tadjine, Abderrezak Berbri, and Ahmed Bouhekka, “Water adsorption on rutile titanium dioxide (110): Theoretical study of the effect of surface oxygen vacancies and water flux in the steady state case”,  
*Rev. Mex. Fis.*, Vol. 69, N° 3 May-June, pp. 031004 1–9, May 2023.  
ISSN : 0035-001X, eISSN : 2683-2224, **facteur d’impact**: 1.702.  
DOI: <https://doi.org/10.31349/RevMexFis.69.031004>  
URL: <https://rmf.smf.mx/ojs/index.php/rmf/article/view/6562>

### **2- Article dans le proceeding de « The 2nd international Scientific and practical Conference » : SCIENTIFIC GOALS AND PURPOSES IN XXI CENTURY**

- **Fatima Bouzidi**, Moustafa Tadjine, Abderrezak Berbri, and Ahmed Bouhekka, ” THE IMPACT OF TEMPERATURE AND H<sub>2</sub>O FLUX ON THE ADSORPTION OF WATER ON RUTILE TiO<sub>2</sub> (110)”,  
Scientific Collection «InterConf» : SCIENTIFIC GOALS AND PURPOSES IN XXI CENTURY, N° 95, 652-661 (2022).  
ISSN : 2709-4685, ISBN : 978-1-0848-4533-6  
DOI : [10.51582/interconf.19-20.01.2022.073](https://doi.org/10.51582/interconf.19-20.01.2022.073)  
URL : <https://ojs.ukrlogos.in.ua/index.php/interconf/issue/view/19-20.01.2022/714>

## **List of conferences**

1. **Fatima Bouzidi**, Moustafa Tadjine, Abderrezak Berbri, and Ahmed Bouhekka, «Theoretical study of water at titanium dioxide: the extent of molecular versus dissociative adsorption», Séminaire international sur les sciences de la matière (Physique et Chimie), USTO- Oran, 17-18 Septembre 2021.

2. Moustafa Tadjine, **Fatima Bouzidi** and Ahmed Bouhekka, « Etude cinétique de l'adsorption des protéines à la surface du solide : Cas de la protéine étendue à pH < 2 », Séminaire International sur les sciences de la matière (Physique et Chimie), USTO-Oran, 17-18 Septembre 2021.
3. **Fatima Bouzidi**, Moustafa Tadjine, Abderrezak Berbri, and Ahmed Bouhekka, « Theoretical study of water at titanium dioxide surface in the presence of defects », Webinar on Materials Science & Nanotechnology, USA, September 17-18/ 2021.
4. **Fatima Bouzidi**, Moustafa Tadjine, Abderrezak Berbri, and Ahmed Bouhekka, « Mathematical model of the behavior of water on titanium dioxide (110) surface », DZHydraulic'21 International Conference, Hydraulic Engineering and Smart Application, Batna, Algeria, October 26-27/ 2021.
5. **Fatima Bouzidi**, Moustafa Tadjine, Abderrezak Berbri, and Ahmed Bouhekka, « A THEORETICAL INVESTIGATION OF THE BEHAVIOR OF WATER ON TITANIUM DIOXIDE SURFACE », 2<sup>nd</sup> International Webinar on BIOCATALYSIS & GREEN CHEMISTRY, USA, November 11-12/ 2021.
6. **Fatima Bouzidi**, Moustafa Tadjine, Abderrezak Berbri, and Ahmed Bouhekka, « The Impact of Temperature and H<sub>2</sub>O Flux on the Adsorption of Water on Rutile TiO<sub>2</sub> (110) », International Scientific and Practical Conference, Scientific Goals and Purposes in XXI Century”, Seattle, USA, January 19-20/ 2022.
7. **Fatima Bouzidi**, Abderrezak Berbri, Ahmed Bouhekka, and Moustafa Tadjine, “Theoretical calculation investigation of water Titanium dioxide surface: Temperature effect on H<sub>2</sub>O behavior”, Sixth student’s symposium on engineering application of mechanics, SSENAM 6, UHBC, Chlef, Nov 30- Dec 01/ 2022.



# Water adsorption on rutile titanium dioxide (110): Theoretical study of the effect of surface oxygen vacancies and water flux in the steady state case

F. Bouzidi<sup>a,d,\*</sup>, M. Tadjine<sup>a</sup>, A. Berbri<sup>a</sup> and A. Bouhekkab<sup>b,c</sup>

<sup>a</sup>*Department of Physics, Faculty of Exact Sciences and Informatics, Hassiba Benbouali University of Chlef, P. B. 78 C, National Road N° 19, Ouled Fares 02180, Chlef, Algeria.*

<sup>b</sup>*Department of Materials Sciences, Faculty of Sciences and Technology, Tissemsilt University, Algeria.*

<sup>c</sup>*Thin-Film Physics Laboratory and Materials for Electronics, Oran 1 Ahmed Ben Bella University, P.B. 1524, El M'naouar 31000, Oran, Algeria.*

<sup>d</sup>*Laboratory of Mechanics and Energy, Hassiba Benbouali University of Chlef, Hay Salem, National Road N° 19, 02000, Chlef, Algeria.*

\*e-mail: bouzidifatima94@gmail.com

Received 16 May 2022; accepted 4 November 2022

The aim purpose of the present work is highlighting the impact of surface oxygen vacancies and H<sub>2</sub>O flux on the behavior of water adsorption at the rutile titanium dioxide (110). Therefore, a theoretical model, based on molecular and dissociation mechanisms at different surface atomic sites, was formulated in a system of partial differential coupled equations. The proposed model used to study, in an atomic scale, this complex phenomenon of adsorption governed by several factors including surface vacancies defects and water flux. The findings of the solution of the system of equations in the steady state case, presented in this paper, strongly indicated that the rate coverage of surface oxygen vacancies has an important role in the dissociation of H<sub>2</sub>O as well as the flux which is a key factor in the behavior of water adsorption on the rutile TiO<sub>2</sub> (110) and the rate coverage of OH groups.

**Keywords:** Water adsorption; rutile titanium dioxide (110); oxygen vacancies; hydroxyls groups; H<sub>2</sub>O flux; steady state.

DOI: <https://doi.org/10.31349/RevMexFis.69.031004>

## 1. Introduction

Among a lot of important materials, titanium dioxide (TiO<sub>2</sub>) takes a particular attention in the recent years in several industrial applications especially in the elimination of organic contamination, sensor, splitting of water, self-cleaning and photocatalytic [1–5]. Furthermore, TiO<sub>2</sub> is abundance [3], inexpensive, nontoxic [4], inert and chemical stability [5, 6]. Rutile TiO<sub>2</sub> (110) surface is the lowest surface energy, thus is very important in studying, especially in catalysis [7]. Furthermore, TiO<sub>2</sub> has a high refractive index ranges between 2.4–2.6. Unfortunately, one of the drawbacks of TiO<sub>2</sub> is the wide band gap of 3–3.2 eV, reacts only in the (UV) light under (380 nm), that is available only around 5% in solar energy [8–11]. Many researchers treated this deficiency by generating electronic states inside the forbidden gap via inducing defects (oxygen vacancy, Ti interstitial, dislocation,...) and doping with impurities (metal transition, noble metal,...) in the structures of TiO<sub>2</sub>. This leads to extend its response in the visible light and near infrared (NIR) region [12–17]. One of the most important applications of TiO<sub>2</sub> surface is water splitting. The H<sub>2</sub>O can be adsorbed in two different mechanisms either molecular or dissociative onto rutile TiO<sub>2</sub> (110) surface [18, 19]. But this is an intriguing phenomenon, because the adsorption process is affected by many factors (phase components, temperature, vacancies, water coverage...) [20]. Several theoretical methods (Langmuir, Freundlich, Langmuir-

Hinshelwood...) are widely used to study the kinetics of adsorptions [21–25]. These phenomena have been studied by using various ab initio quantum mechanical approximations highlighting on the important factors that affect on the adsorption and the dissociation of H<sub>2</sub>O such as (DFT and DFT-PW and HF...) calculations and molecular dynamics ([21] and references therein) which have provide numerous groundbreaking insight into the water -TiO<sub>2</sub> interface. However, it is not possible to get adsorption information taking in consideration all the surface sites at the same time. Experimentally, the infrared spectroscopy, especially in Situ ATR-FTIR, is one of the most important and powerful technique used to investigate the water molecules adsorption at solid surfaces [26]. But in experimental, it is not clear and easy to get details at the atomic scale level of adsorption therefore; the theory becomes a useful tool. In light of the above information, we are interested in this context, to study the effect of oxygen vacancies concentration at rutile TiO<sub>2</sub> (110) surface and water flux on the behavior of H<sub>2</sub>O molecules adsorption using a system of nonlinear differential equations, carried out taking into account the different cases of adsorption and all surface available sites. This indicates a better understanding of structural and dynamical properties changes of the behavior of H<sub>2</sub>O on rutile TiO<sub>2</sub> (110) surface. Thereby, these factors greatly enhancing chemical/catalytic reactivity (among other properties) as well as the splitting of water and self-cleaning. At the end, a summary will be given together with

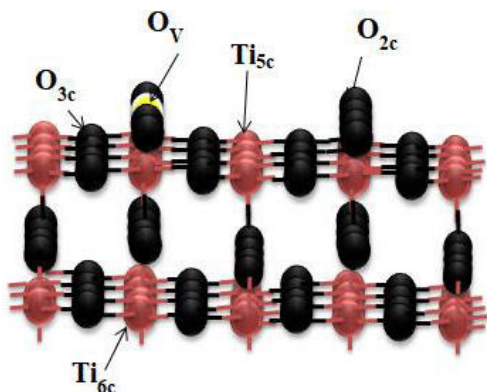


FIGURE 1. Structure of rutile  $\text{TiO}_2$  (110) surface in the z-direction, black balls represent O atoms of the bridge-bonded O species ( $\text{O}_{2c}$ ) and three coordinated ( $\text{O}_{3c}$ ), red balls are fivefold coordinated surface Ti ( $\text{Ti}_{5c}$ ) and six fold coordinated Ti atoms ( $\text{Ti}_{6c}$ ), white ball is single oxygen vacancies ( $\text{O}_V$ ).

a brief outlook towards challenges and prospects for future theoretical studies [27,28].

## 2. The surface structure of rutile $\text{TiO}_2$ (110)

Naturally,  $\text{TiO}_2$  exists in three different crystallography forms rutile, anatase and brookite. The structure of each form is described as a chain of octahedron (one atom of Ti surrounded by six oxygen atoms) as shown in Fig. 1. Among the three structures anatase (101) and rutile (110) are the most stable faces and more reactive especially in photocatalytic applications [7].

The different surface sites illustrated in this figure play a crucial role in the adsorption and the behavior of water molecules. It is still not clear to distinguish which kind of site is primordial in controlling the adsorption phenomenon. In the following part, we give the possible mechanisms of adsorption used to formulate the proposed theoretical model.

## 3. Kinetics model description of $\text{H}_2\text{O}$ - rutile $\text{TiO}_2$ (110) surface interactions

A kinetics model of  $\text{H}_2\text{O}$  on rutile  $\text{TiO}_2$  (110) surface, in bellow figures, was developed to describe the behavior of  $\text{H}_2\text{O}$  adsorption, assumed to adsorb in reversible states; different forms model, two types of features found on rutile  $\text{TiO}_2$  (1x1) (110) surface as indicated in Fig. 2 and reaction (1).  $\text{H}_2\text{O}$  molecules adsorb in molecular form on defect-free sites ( $\text{Ti}_{5c}$ ) at low temperature around 160 K [29] is due a Ti - $\text{H}_2\text{O}$  bond length (2.16 - 2.29) Å [30], with adsorption energy around (0.5 - 0.7 eV) [1, 28, 33–35]. When annealing the surface below room temperature, only the  $\text{H}_2\text{O}$  molecules are desorbed from surface with energy ranges between 0.7 eV to 0.8 eV depending on the water rate coverage [36]. In the other hand, The  $\text{H}_2\text{O}$  has the possibility to dissociate on ( $\text{Ti}_{5c}$ ) sites, however, the second proton  $\text{H}^+$  transfer to the neighbouring bridging oxygen ( $\text{O}_{2c}$ ) and forms two OH

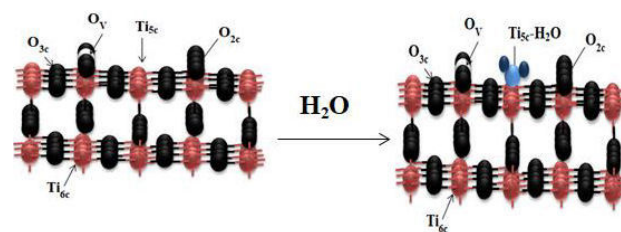


FIGURE 2. The adsorption of molecular water on free defect surface, dark (light) blue balls hydrogen (oxygen of water) atoms,  $K_1$ ,  $K_2$  are the rates constants of adsorption and desorption respectively.

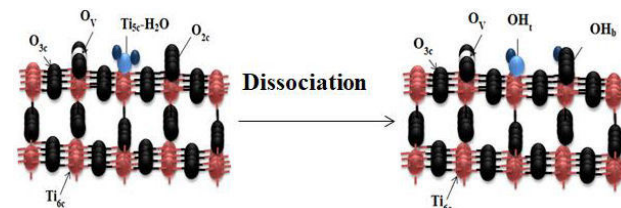
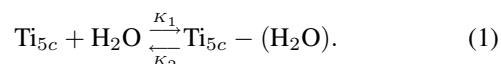
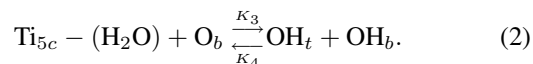


FIGURE 3. The dissociative adsorption of water on  $\text{Ti}_{5c}$  sites, where  $K_3$  and  $K_4$  are the rates constants of dissociation and recombination reaction, respectively.

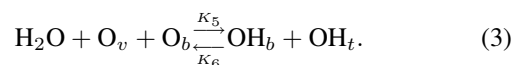
hydroxyl groups  $\text{OH}_t$  and  $\text{OH}_b$  respectively, which was discussed in details in Ref. [3] with dissociation energy toward 0.36 eV and 0.41 eV, when annealing the surface to room temperature under reaction (2) [31–33] as shown in Fig. 3. This competition between molecular and dissociated adsorption is mostly governed by the basic strength of the bridging O atom receiving the H.



A missing of an oxygen atom, by removing the oxygen bridging ( $\text{O}_{2c}$ ) from the surface using electron bombardment or other methods, leads to the creation of a surface oxygen vacancy ( $\text{O}_V$ ) (none thermally). This was discussed in more details in Ref. [2].



With its concentration around 15% ML (Mono Layer) (1 ML is defined with respect to the coverage of  $\text{Ti}_{5c}$  sites of  $5.2 \cdot 10^{14} \text{ cm}^{-2}$ ) from the surface of  $\text{TiO}_2$  (110) [34,35]. The water favoured dissociate in the oxygen defect at below temperature (130-200 K) and forms two OH hydroxyl groups in the  $\text{O}_V$  and the  $\text{H}^+$  proton of water transfer nearby bridging oxygen and creates the other hydroxyl for every vacancy as given in Fig. 4 [36–39], the recombination of the two OH occurs at temperature above 490 K [3, 18]. This reaction can be written as Eq. (3) indicates.



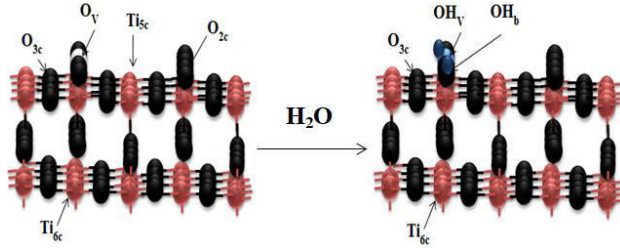


FIGURE 4. The dissociative adsorption of water on the surface oxygen vacancy, where the  $K_5$  and  $K_6$  are the dissociation and recombination rates constants, respectively

#### 4. Model and method

A mathematical description of these equations (1)-(3) for the adsorption of water in different cases onto rutile  $\text{TiO}_2$  (110) surface can be derived using an adaptation of the Langmuir adsorption model. This model is the most commonly applied of single component liquid-solid adsorption. Based on the kinetics principle, Langmuir isotherm model assuming that only monolayer adsorption exists; no impurities ( $\text{CO}_2$ ,  $\text{O}_2$ ...) are considered at the surface and to avoid interactions between water molecules the incident  $\text{H}_2\text{O}$  flux density can be supposed very weak and more addition the adsorbent surface is uniform with the same adsorption probability [22,24]. Therefore, the adsorption rate of each chemical reaction can be presented as following Eq. (4):

$$\frac{d\theta}{dt} = \Phi P_{\text{ads}} - K\theta, \quad (4)$$

where  $\Phi$ ,  $\theta$ ,  $P_{\text{ads}}$ ,  $K$  are the flux, the surface sites coverage, the probability of the molecule will find adsorption sites and the desorption rate constant, respectively. The probability of adsorption is given by the following Eq. (5).

$$P_{\text{ads}} = K \left( \frac{n_a(1 - \theta_a)}{n_s} \right), \quad (5)$$

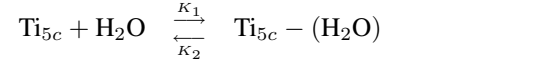
where  $K$ ,  $n_a$ ,  $n_s$ ,  $\theta_a$  the adsorption rate constant ( $\text{s}^{-1}$ ), the concentration of adsorption sites, the concentration of all atoms in the surface and the coverage of the adsorption sites

respectively. The rate constant  $K_i$  can be expressed with an Arrhenius Eq. (6),

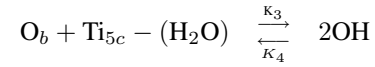
$$K_i = K_0 \exp\left(\frac{-E_a}{RT}\right), \quad (6)$$

where  $K_0$ ,  $E_a$ ,  $R$  and  $T$  are the attempt frequency ( $\text{s}^{-1}$ ), the activation energy (Kj/mole,  $1\text{eV} = 96.482\text{Kj}$ ), universal gas constant ( $8.314\text{J/mole.K}$ ) and the temperature K.

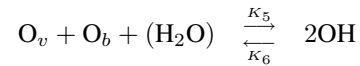
The different reactions (1) to (3) using Eq. (4) are organized below,



$$r_1 : \Phi K_1 \theta_{\text{Ti}} - K_2 \theta_{\text{H}_2\text{O}}, \quad (7)$$



$$r_2 : K_3 \theta_{\text{H}_2\text{O}} \theta_b - K_4 \theta_{\text{OH}}^2, \quad (8)$$



$$r_3 : \Phi K_5 \theta_v \theta_b - K_6 \theta_{\text{OH}}^2, \quad (9)$$

where  $\theta_{\text{Ti}}$ ,  $\theta_{\text{OH}}$ ,  $\theta_{\text{H}_2\text{O}}$ ,  $\theta_b$  and  $\theta_v$  are the coverage of titanium, hydroxyl groups, water, bridging oxygen and oxygen vacancies on the surface respectively. The adsorption rate is proportional to the  $\text{H}_2\text{O}$  flux arrived on surface and the coverage of active sites ( $\text{Ti}_{5c}$ ,  $\text{O}_v$  and  $\text{O}_{2c}$ ), desorption rate is proportional to the number of association and desorption adsorbed molecules, under such assumptions; in the adsorption process we have [39].

$$\frac{d\theta_v}{dt} = -r_3 = -\Phi K_5 \theta_v \theta_b + K_6 \theta_{\text{OH}}^2,$$

$$\begin{aligned} \frac{d\theta_b}{dt} &= -r_3 - r_2 = -\Phi K_5 \theta_v \theta_b + K_4 \theta_{\text{OH}}^2 \\ &\quad - K_3 \theta_{\text{H}_2\text{O}} \theta_b + K_6 \theta_{\text{OH}}^2, \end{aligned}$$

$$\begin{aligned} \frac{d\theta_{\text{OH}}}{dt} &= +r_3 + r_2 = \Phi K_5 \theta_v \theta_b - K_4 \theta_{\text{OH}}^2 \\ &\quad + K_3 \theta_{\text{H}_2\text{O}} \theta_b - K_6 \theta_{\text{OH}}^2, \end{aligned}$$

TABLE I. Kinetic parameters used in the mathematical models of  $\text{H}_2\text{O}$  reactions on rutile  $\text{TiO}_2$  (110), the rate constant ( $K_i$ ) extracted from the Arrhenius Eq. (6).

Step, (i)	$K_0[\text{s}^{-1}]$	$E_a$ [eV]	$T$ [K]	$K_0$ [ $\text{s}^{-1}$ ]	Reference
1. $\text{H}_2\text{O}$ adsorption	$10^{13}$	0.5 – 0.7	150 – 160	0.0018	[1,3]
2. $\text{H}_2\text{O}$ desorption	$10^{12}$	0.73 – 0.8	200 – 275	$4.10^{-7}$	
3. $\text{H}_2\text{O}$ dissociation on free defect	$10^{12}$	0.36, 0.44, 0.97	80 – 140	0.0015	[29,30]
4. OH Association	$10^{12}$	0.355	110 – 130	$5.43.10^{-5}$	
5. $\text{H}_2\text{O}$ dissociation on $\text{O}_v$	$10^{13}$	0.93 – 1.5	300, 187	0.0024	[41–47], [51,54]
6. OH recombination	$10^8$	0.12 – 0.18	450 – 500	$10^{-4}$	

$$\begin{aligned}\frac{d\theta_{Ti}}{dt} &= -r_1 = -\Phi K_1 \theta_{Ti} + K_2 \theta_{H_2O} \\ \frac{d\theta_{H_2O}}{dt} &= r_1 - r_2 = \Phi K_1 \theta_{Ti} - K_2 \theta_{H_2O} \\ &\quad - K_3 \theta_{H_2O} \theta_b + K_4 \theta_{OH}^2\end{aligned}\quad (10)$$

The sum of all the different coverage at the rutile (110) surface are  $\sum \theta_i = 1$  and the variation equal

$$\sum \frac{d\theta_i}{dt} = 0 \quad (11)$$

We suppose the variation of the coverage's remains the same in duration of the reaction, setting these rates to zero in the steady state gives the system (12) as indicated bellow. The stability of the set of equations is very important because any bifurcation parameter can dramatically change it and to avoid such behavior we took the rates constants  $K_i$  have similar thermal stability.

$$\begin{aligned}-\Phi K_5 \theta_v \theta_b + K_6 \theta_{OH}^2 &= 0 \\ -\Phi K_5 \theta_v \theta_b + K_4 \theta_{OH}^2 - K_3 \theta_{H_2O} \theta_b + K_6 \theta_{OH}^2 &= 0 \\ \Phi K_5 \theta_v \theta_b - K_4 \theta_{OH}^2 + K_3 \theta_{H_2O} \theta_b - K_6 \theta_{OH}^2 &= 0 \\ -\Phi K_1 \theta_{Ti} + K_2 \theta_{H_2O} &= 0 \\ \Phi K_1 \theta_{Ti} - K_2 \theta_{H_2O} - K_3 \theta_{H_2O} \theta_b + K_4 \theta_{OH}^2 &= 0\end{aligned}\quad (12)$$

## 5. Results and discussion

We use a numerical method to solve this system Eq. (12) and the corresponding solution of coverages is given by the following equations:

$$\begin{aligned}\theta_{OH} &= 0.16 \left( -750 \Phi \theta_v + 2.24 \right. \\ &\quad \left. \times \sqrt{1875 \Phi \theta_v - 2237 \Phi \theta_v^2 + 96210 \Phi^2 \theta_v^2} \right),\end{aligned}\quad (13)$$

$$\theta_{Ti} = 0.2 \theta_v, \quad (14)$$

$$\theta_{H_2O} = 8.7 \Phi \theta_v, \quad (15)$$

$$\theta_{O_v} = \frac{5.10^{-4} (10^3 \Phi \theta_{O_v} - 2.10^3 \Phi \theta_{O_v}^2 + 2.10^5 \Phi^2 \theta_{O_v}^2 - 670.8 \Phi \theta_{O_v} \sqrt{\Phi \theta_{O_v} (1.8 \cdot 10^3 - 2.2 \cdot 10^3 \theta_{O_v} + 9.6 \cdot 10^4 \Phi \theta_{O_v})})}{\Phi \theta_{O_v}}. \quad (16)$$

It is clear that the solutions of each surface site strongly depends on the flux of water and the surface oxygen vacancies ( $O_V$ ). As indicated in Fig. 5 (a), OH hydroxyls increases and reaches a maximum for  $O_V = 0.04$  then it decreases to the minimum for a higher value of  $O_V$ . The same behavior for OH hydroxyls is illustrated in Fig. 5 (b) when this flux changes from 0 to 1. This graph indicates that the coverage of OH hydroxyls increases at low flux values and reaches a maximum around 0.7 (for a flux value around 0.4) afterward it decreases which means that OH hydroxyls production is slightly reduced.

To illustrate these variations of OH hydroxyls on the surface versus  $H_2O$  flux and  $O_V$ , a three dimension (3D) is shown in Fig. 6. The coverage of OH hydroxyls grows with increasing the  $O_V$  and reaches to a maximum around 0.7 ML at  $O_V$  equal 0.05 ML. At high coverage of  $O_V$  up to 10 % the production of OH hydroxyls decays and gets a small value almost zero. In

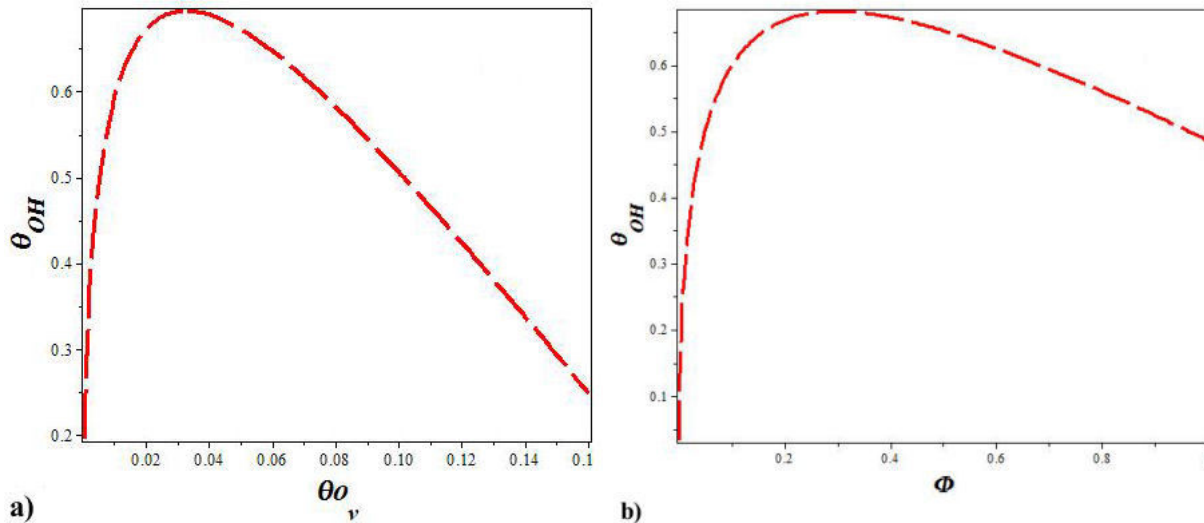


FIGURE 5. a) The effect of oxygen vacancies on the production OH hydroxyls at  $H_2O$  flux equal 0.4. b) The effect of  $H_2O$  flux on the production OH hydroxyls at  $O_v$  around 0.05 in the steady state solution.

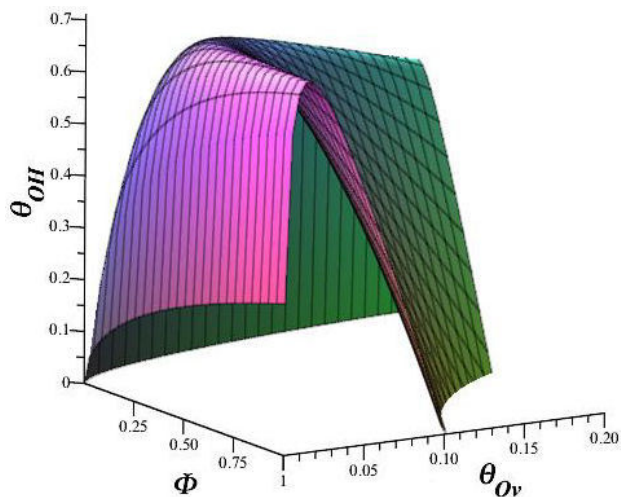
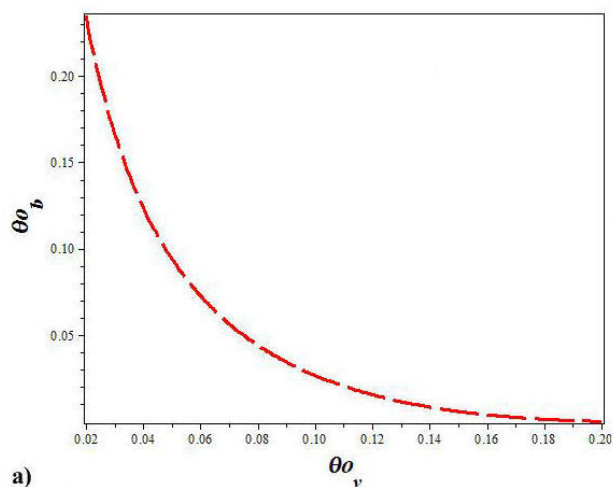
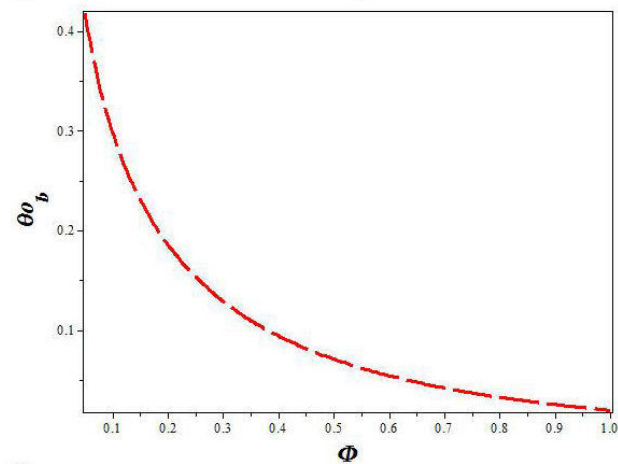


FIGURE 6. Kinetic curves for the OH hydroxyls at rutile TiO<sub>2</sub> (110) surface for various H<sub>2</sub>O flux and concentration of O<sub>v</sub> on the surface.



a)



b)

FIGURE 7. The coverage of bridging oxygen change versus: a) the coverage of O<sub>v</sub> with the H<sub>2</sub>O flux remains 0.4 ML, b) H<sub>2</sub>O flux at the coverage of O<sub>v</sub> around 0.05 ML on rutile TiO<sub>2</sub> (110) surface.

other hand, also the coverage of OH hydroxyls depends on the arriving H<sub>2</sub>O molecules; when the H<sub>2</sub>O flux arrived at surface increases, the production of OH hydroxyls increases and reaches a maximum at 0.7 ML for H<sub>2</sub>O flux around 0.4 ML, despite, for H<sub>2</sub>O flux takes value more than 0.4 ML and filling all the surface leading to no production of OH hydroxyls on the surface which is occupied only with H<sub>2</sub>O molecules.

From Eq. (16), the curve of the coverage of O<sub>b</sub> for different concentrations of O<sub>v</sub> and H<sub>2</sub>O flux arrived on surface is shown in Fig. 7.

Figure 7 (a) illustrates the variation of  $\theta_{O_b}$  as a function of  $\theta_{O_v}$  for the H<sub>2</sub>O flux taken 0.4 ML. The graph clearly shows that  $\theta_{O_b}$  decreases when the concentration of O<sub>v</sub> grows. Besides, in Fig. 7(b) the coverage of O<sub>b</sub> decays exponential-like with increasing the H<sub>2</sub>O flux for the concentration of  $\theta_{O_v}$  equals 0.05 ML.

Figure 8 is plotted using Eq. (16); it is interesting to note some common relations; the coverage of O<sub>b</sub> decreases exponential-like with increasing the coverage of O<sub>v</sub> and

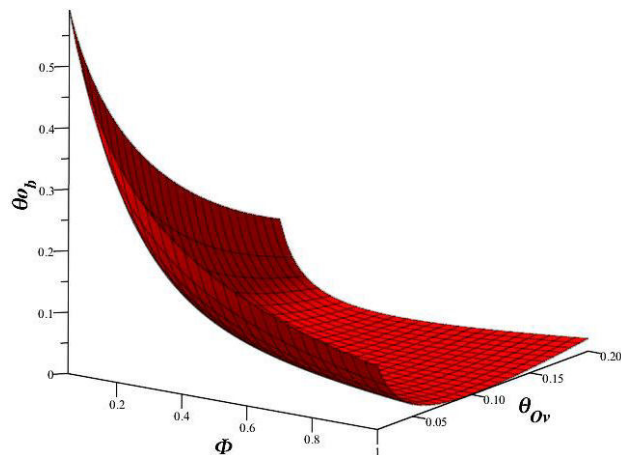


FIGURE 8. The coverage of O<sub>b</sub> as a function of H<sub>2</sub>O flux and O<sub>v</sub> defects on rutile TiO<sub>2</sub> (110) surface.

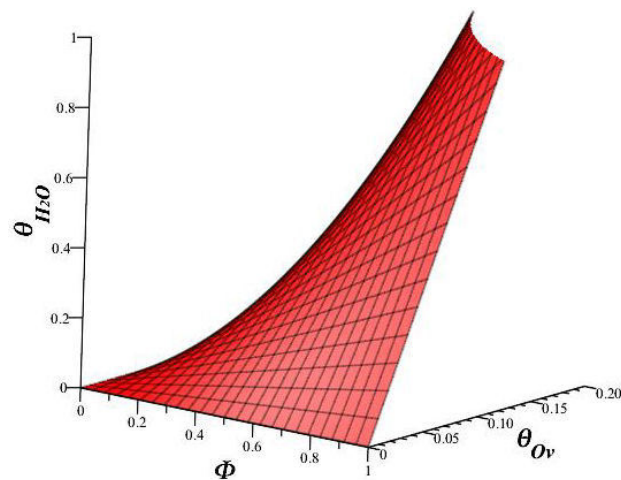


FIGURE 9. The coverage of H<sub>2</sub>O on surface versus H<sub>2</sub>O flux and the coverage of oxygen vacancies O<sub>v</sub>.



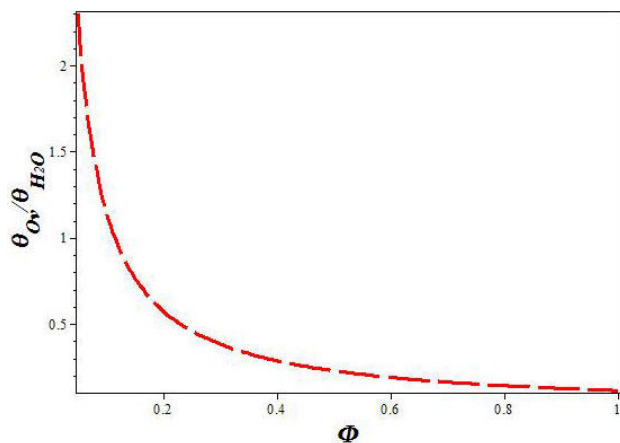


FIGURE 10. The ratio of  $(\theta_{O_v} / \theta_{H_2O})$  on rutile  $TiO_2$  (110) surface versus  $H_2O$  flux.

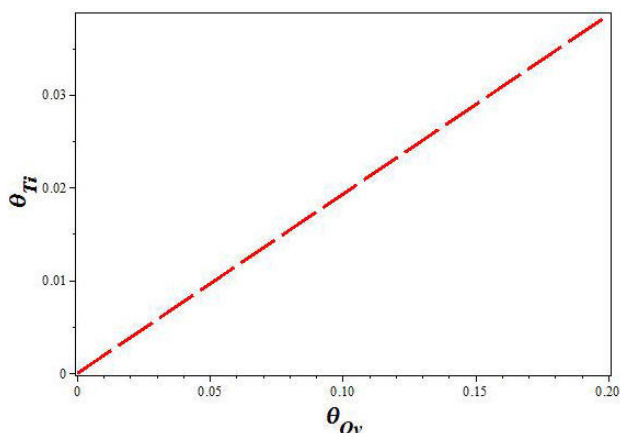


FIGURE 11. The coverage of  $Ti_{5c}$  on rutile  $TiO_2$  (110) surface as a function of the concentration of oxygen vacancies ( $O_v$ ).

tends to a small value for large value of  $O_v$ , also at high value for the  $H_2O$  flux, the coverage of  $O_b$  decreases.

This figure demonstrates that the  $O_b$  is a key factor in the dissociation and the adsorption of  $H_2O$  molecules.

The Eq. (15), variation of water coverage versus the rate of oxygen vacancies and the  $H_2O$  flux, indicating, the coverage of  $H_2O$  takes small values almost plateau when the  $H_2O$  flux and the concentration of  $O_v$  on surface is very small, afterward, the coverage of  $H_2O$  increases steadily with  $H_2O$  flux and the concentration of  $O_v$ , as illustrated in Fig. 9.

Figure 10 shows the ratio of  $(\theta_{O_v} / \theta_{H_2O})$ , from Eq. (15), versus the  $H_2O$  flux; indicating that the fraction of  $(\theta_{O_v} / \theta_{H_2O})$  decreases with increasing the  $H_2O$  flux. This can be explained that increasing the coverage of  $H_2O$  at the surface is caused by the filling of oxygen vacancies sites.

From these results, the interactions of  $H_2O$  with rutile  $TiO_2$  (110) surface were heavily affected by the  $O_v$  and  $H_2O$  flux. This was expected, since the  $H_2O$  flux arrived on rutile  $TiO_2$  (110) surface,  $H_2O$  molecules take up to  $Ti_{5c}$  sites (which is positively charged) rendering its able to bind  $H_2O$  molecules via electrostatic interactions. Many authors

[52, 54] have studied the effect of  $H_2O$  flux and the coverage of  $O_v$  on the behavior of  $H_2O$  molecules on rutile  $TiO_2$  (110) surface. First, at low values of  $H_2O$  flux, is expected the mobility of  $H_2O$  molecules to be high which is helpful for the  $H_2O$  molecules to diffuse on the surface on direction [001] which dissociate at oxygen vacancies firstly to heal the vacancies and defect-free sites as well as a strong attractive of H proton to near bridging oxygen due to transfer the H proton and formed another OH hydroxyls, because dissociation at bridging oxygen vacancies is more favourable than  $H_2O$  adsorption on the  $Ti_{5c}$  sites [55], as the  $H_2O$  flux increases the OH hydroxyls continue to increase till reach the maximum at 0.7ML for 0.4 of  $H_2O$  flux, this is in good accordance with the prediction by Lindan and Zhang [56]. At a high  $H_2O$  flux, water may be adsorbed molecularly with a small fraction adsorbed dissociative on  $O_v$  because (i) at least one or two  $H_2O$  molecules uptake on  $Ti_{5c}$  sites and form a chains of  $H_2O$  molecules (ii) when the amount of  $H_2O$  molecules are large, hinders the diffusion of  $H_2O$  molecules and remains in molecular forms, therefore,  $H_2O$  molecular adsorption is more favourable at high coverage [30]. As it is seen, the coverage of  $O_v$  affects on the adsorption of water, however, the amount of OH hydroxyls formed on rutile  $TiO_2$  (110) surface increases at low concentration of vacancies because the  $H_2O$  favours the dissociation at oxygen vacancies [54] reach to the maximum around 0.7 ML because the repulsive interaction between the functional groups, afterward, when the coverage of  $O_v$  increases beyond to 0.05 ML, the OH groups coverage decreases, because at high concentration of  $O_v$  affects on the structure properties, which lead to  $(2 \times 1)$  reconstruction surface [40], additionally, and we know the  $O_v$ 's created from the bridging oxygen, this implies that the coverage of  $O_v$  increases due to decrease the bridging oxygen as illustrated in Fig. 8. In noting, when  $(N_{O_b} < N_{O_v})$  deficient the dissociation in  $O_v$  and the defect-free sites, this is in a good agreement with previous works reported in [57]. Exists due to the fact, the dissociation of  $H_2O$  molecules in either terminal hydroxyl or OH in vacancy need a neighbouring oxygen atoms for the H proton creates the second OH hydroxyls on  $O_b$ , besides, the coverage of bridging oxygen decreases with  $H_2O$  increases as Fig. 7(a) improved that clearly. The formation of these radical groups is active to promote the charge separation process as well as the oxidation of organic substances and several applications (self-cleaning, pharmaceutical...) [49] and references therein]. This inhibit the production of OH hydroxyls, meanwhile the molecular adsorption will be the predominant as Fig. 9 illustrates that; where the vacancies increasing the asymmetry for titanium atoms near vacancies that leads to enhance the water adsorption further the  $H_2O$  adsorbed molecular at high and low coverage [38, 53]. From the Eq. (14) it is clearly shown that the coverage of  $Ti_{5c}$  is independent to the flux, it depends only on the concentration of the surface  $O_v$ . Many authors overbalanced the increase to transfer the  $Ti_{6c}$  coordinate underneath the  $O_v$  to  $Ti_{5c}$  [52, 58]. In other hand,  $H_2O$  adsorbed molecular on  $Ti_{5c}$  meanwhile diffuses

toward the vacancy site where the dissociation takes place, thus, H<sub>2</sub>O let behind a Ti<sub>5c</sub> site, however, the coverage of Ti increases as illustrated by Fig. 11. Several literature papers conclude that mixed molecular/dissociate is the most stable configuration on rutile TiO<sub>2</sub> (110) surface [59], besides, the behavior of the water (molecular or dissociative) can change dramatically even for the same materials as the structure and termination of the surface changes.

## 6. Conclusion

The interactions H<sub>2</sub>O / rutile TiO<sub>2</sub> (110) are intriguing subjects; therefore, several experimental and theoretical methods were used to understanding the reaction mechanisms. In terms of theoretical studies, the proposed model presented in this research, a system of coupled differential equations, described and solved in the steady state case taking into account the different reactions of H<sub>2</sub>O / rutile TiO<sub>2</sub> (110). The findings strongly indicate that the interactions H<sub>2</sub>O- rutile TiO<sub>2</sub> (110) have a crucial impact on the production of OH groups at the surface. As one might expect, the coverage of OH hydroxyls increases in the presence of O<sub>V</sub> which can be applied to enhance the performance of the purification of waste water from organic and inorganic materials plus others applications, but when the concentration of O<sub>V</sub> increases up to 0.05 leads to reduce the production of OH hydroxyls. This behavior is believed to be a good reason of a modification on surface structure, as well as the H<sub>2</sub>O flux. By way of outlook for future challenge given a presence of chemically adsorbed water at rutile TiO<sub>2</sub> (110) interface and intriguing behavior, this shows the importance of understanding both the structure of rutile TiO<sub>2</sub> (110) surface and dynamics of H<sub>2</sub>O molecules on them. Indeed, knowing the mechanism behavior of water molecules on metal oxides under deferent conditions is very important due to its applications in catalysis.

## Nomenclature

variables	
H <sub>2</sub> O	Water
Ti <sub>5c</sub>	Titanium five coordinate
Ti <sub>6c</sub>	Titanium six coordinate
O <sub>2c</sub>	Oxygen two coordinate (bridging)
O <sub>3c</sub>	Oxygen three coordinate
O <sub>V</sub>	Oxygen Vacancy
OH	Hydroxyl group
$\Phi$	Water flux density per surface site
$\theta$	Coverage
$\theta_{Ti}$	Coverage of undercoordinated titanium
$\theta_b$	Coverage of oxygen bridging
$\theta_v$	Coverage of oxygen vacancies
$\theta_{H_2O}$	Coverage of water molecules on surface
$\theta_{OH}$	Coverage of hydroxyls groups
$K_i$	The rate constant (s <sup>-1</sup> )
$K_0$	Attempt frequency (s <sup>-1</sup> )
$E_a$	Activation energy (Kj/mole) or (eV)
$T$	Temperature (K)
$R$	Universal gas constant (K j/mole. K)
$ML$	Monolayer
$n_a$	The concentration of the adsorption sites
$n_s$	The concentration of all the atoms in the surface

## Acknowledgement

We gratefully acknowledge financial support of this work from the ministry of higher education and scientific research in Algeria (MESRS).

1. M. Elahifard, H. Heydari, R. Behjatmanesh Ardakani, P. Bijan and S. Ahmadvand, A computational study on the effect of Ni impurity and O-vacancy on the adsorption and dissociation of water molecules on the surface of anatase (101), *J. Phys. Chem. Sol.* **136** (2020) 109176, <https://doi.org/10.1016/j.jpccs.2019.109176>.
2. U. Diebold, The surface science of titanium dioxide, *J. Surf. Sci. Rep.* **48** (2003) 53, [https://doi.org/10.1016/S0167-5729\(02\)00100-0](https://doi.org/10.1016/S0167-5729(02)00100-0).
3. U. Diebold, Perspective: A controversial benchmark system of water-oxide interfaces: H<sub>2</sub>O/TiO<sub>2</sub> (110), *J. Chem. Phys.* **147** (2017) 040901, <https://dx.doi.org/10.1063/1.4996116>.
4. B. Wei, F. Tielens, M. Calatayud, Understanding the role of rutile TiO<sub>2</sub> surface orientation on molecular hydrogen activation, *J. Nanomaterials (Basel)*. **9** (2019) 1199, <https://doi.org/10.3390/nano9091199>.
5. M.A. Shaheed, F.H. Hussein, Preparation and applications of titanium dioxide and zinc oxide nanoparticles, *J. Environ. Anal. Chem.* **2** (2014) 1000e109, <http://dx.doi.org/10.4172/jreac.1000e109>.
6. M.L. Weichman *et al.* Dissociative water adsorption on gas-phase titanium dioxide cluster anions probed with infrared photodissociation spectroscopy, *J. Top. Catal.* **61** (2018) 92, <http://dx.doi.org/10.1007/s11244-017-0863-4>.
7. L. Jiang, Y. Wang, C. Feng, Application of photocatalytic technology in environmental safety. *Procedia Eng.* **45** (2012) 993, <https://doi.org/10.1016/j.proeng.2012.08.271>.
8. B.G. Obeid, A.S. Hameed, H.H. Alaaraji, Structural and optical properties of TiO<sub>2</sub>, *Digest Journal of Nanomaterials and Biostructures.* **12** (2017) 1239-1246, <https://www.researchgate.net/publication/322399704>.

9. C. Zhao, Y. Yang, L. Luo, S. Shao, Y. Zhou, Y. Shao, F. Zhan, J. Yang, Y. Zhou,  $\gamma$ -ray induced formation of oxygen vacancies and  $Ti^{3+}$  defects in anatase  $TiO_2$  for efficient photocatalytic organic pollutant degradation, *J. Sci. Total Environ.* **747** (2020) 141533, <https://doi.org/10.1016/j.scitotenv.2020.141533>.
10. A. Khataee, G.A. Mansoori, Nanostructured materials titanium dioxide: properties, preparation and applications, World Scientific Publishing Company, London, 2012.
11. Y. Lan, Y. Lu, Z. Ren, Mini review on photocatalysis of titanium dioxide nanoparticles and their solar applications, *J. Nanoen.* **2** (2013) 1031, <http://dx.doi.org/10.1016/j.nanoen.2013.04.002>.
12. H. Tributsch, T. Bak, J. Nowotny, M.K. Nowotny, L.R. Shepard, Photoreactivity models for titanium dioxide with water, *J. Ener. Mat.* **3** (2008) 158, <https://doi.org/10.1179/174892409x435770.P>.
13. P. Krüger, J. Jupille, S. Bourgeois, B. Domenichini, A. Verdini, L. Floreano, A. Morgante, Intrinsic nature of the excess electron distribution at the  $TiO_2$  (110) surface, *J. Phys. Rev. Lett.* **108** (2012) 126803, <https://doi.org/10.1103/physrevlett.108.126803>.
14. T. Minato, M. Kawai, Y. Kim, Creation of single oxygen vacancy on titanium dioxide surface, *J. Mat. Res.* **27** (2012) 2237, <https://doi.org/10.1557/jmr.2012.157>.
15. C. Di Valentin, G. Pacchioni, A. Selloni, Reduced and n-type doped  $TiO_2$  nature of  $Ti^{3+}$  species, *J. Phys. Chem. C* **113** (2009) 20543, <https://doi.org/10.1021/jp9061797>.
16. X. Chen, S.S. Mao, Titanium dioxide nanomaterials: Nanomaterials: Synthesis, Properties, Modifications and Properties, *J. Chem. Rev.* **107** (2007) 2891, <https://doi.org/10.1021/cr0500535>.
17. S. Wendt *et al.*, The role of interstitial in the Ti 3d defect state in the band gap of titanium, *J. Sci.* **320** (2008) 1755, <https://doi.org/10.1126/science.1159846>.
18. F. Han, V.S.R. Kambala, M. Srinivasan, D. Rajarathnam, R. Naidu, Tailored titanium dioxide photocatalysts for the degradation of organic dyes in wastewater treatment, *J. Appl. Catal. A* **359** (2009) 25, <http://dx.doi.org/10.1016/j.apcata.2009.02.043>.
19. M.A. Henderson, The interaction of water with solid surfaces: fundamental aspects revisited, *J. Surf. Sci. Rep.* **46** (2002) 1, [http://dx.doi.org/10.1016/s0167-5729\(01\)00020-6](http://dx.doi.org/10.1016/s0167-5729(01)00020-6).
20. P.A. Thiel, T.E. Madey, The interaction of water with solid surfaces: fundamental aspects, *J. Surf. Sci. Rep.* **7** (1987) 211, [http://dx.doi.org/10.1016/0167-5729\(87\)90001-x](http://dx.doi.org/10.1016/0167-5729(87)90001-x).
21. C. Sun, L.M. Liu, A. Selloni, G.Q. Lua, S.C. Smith, Titania-water interaction: a review of theoretical studies, *J. Mater. Chem.* **20** (2010) 10319, <http://dx.doi.org/10.1039/c0jm01491e>.
22. L. Largette, R. Pasquier, A review of the kinetics adsorption models and their application to the adsorption of lead by an activated carbon, *J. Chem. Eng. Res. Des.* **109** (2016) 495, <http://dx.doi.org/10.1016/j.cherd.2016.02.006>.
23. N.H. Turner, Kinetics of chemisorption: An examination of the Elovich equation, *J. Catal.* **36** (1975) 262, [http://dx.doi.org/10.1016/0021-9517\(75\)90035-4](http://dx.doi.org/10.1016/0021-9517(75)90035-4).
24. K.A. Connors, Chemical Kinetics: The Study of Reaction Rates in Solution, VHP Publisher, United States of America, 1990.
25. A.G. Makeev, M.M. Slinko, D. Luss, Mathematical modeling of oscillating CO oxidation on Pt group metals at near atmospheric pressure: activity of metallic and oxidized surfaces, *J. Appl. Catal. A: General* **571** (2018) 127, <http://dx.doi.org/10.1016/j.apcata.2018.11.015>.
26. M. Ohman, D. Persson, C. Leygraf, In situ ATR-FTIR studies of the aluminium/polymer interface upon exposure to water and electrolyte, *J. Prog. Org. Coat.* **57** (2006) 78, <https://doi.org/10.1016/j.porgcoat.2006.07.002>.
27. E.D. Revellame, D.L. Fortela, W. Sharp, R. Hernandez, M.E. Zappi, Adsorption kinetic modeling using pseudo-first order and pseudo-second order rate laws, *J. Clean. Engin. Tech.* **1** (2020) 100032, <https://doi.org/10.1016/j.clet.2020.100032>.
28. S. Wendt *et al.*, Oxygen vacancies on  $TiO_2$  and their interaction with  $H_2O$  and  $O_2$ : A combined high-resolution STM and DFT study, *J. Surf. Sci.* **598** (2005) 226, <https://doi.org/10.1016/j.susc.2005.08.041>.
29. D. Brinkley *et al.* A modulated molecular beam study of the extent of  $H_2O$  dissociation on  $TiO_2$  (110), *J. Surf. Sci.* **395** (1998) 292, [https://doi.org/10.1016/s.0039-6028\(97\)00633-x](https://doi.org/10.1016/s.0039-6028(97)00633-x).
30. R. Mu, Z. Zhao, Z. Dohnálek, J. Gong, Structural motifs of water on metal oxide surfaces, *J. Chem. Soc. Rev.* **46** (2017) 1785, <https://doi.org/10.1039/c6cs00864j>.
31. N. Kumar *et al.* Hydrogen bonds and vibrations of water interaction on (110) rutile, *J. Phys. Chem. C* **113** (2009) 13732, <https://doi.org/10.1020/jp901665e>.
32. A. Fahmi, C.A. Minot, Theoretical investigation of water adsorption on titanium dioxide surfaces, *J. Surf. Sci.* **304** (1994) 343, [https://doi.org/10.1016/0039-6028\(94\)91345-5](https://doi.org/10.1016/0039-6028(94)91345-5).
33. J. Zhang, R. Zhang, B. Wang, L. Ling, Insight into the adsorption and dissociation of water over deferent  $CuO$ (111) surfaces: the effect of surface structures, *J. Appl. Surf. Sci.* **364** (2016) 758, <https://doi.org/10.1016/j.apsusc.2015.12.211>.
34. P. Scheiber *et al.* (Sub) Surface mobility of oxygen vacancies at the  $TiO_2$  anatase (101) surface, *J. Phys. Rev. Lett.* **109** (2012) 136103, <https://doi.org/10.1103/PhysRevLett.109.136103>.
35. O. Dulub, C.D. Valentin, A. Selloni, U. Diebold, Structure, defects, and impurities at the rutile  $TiO_2$  (011)-(2 x 1) surface: A scanning tunnelling microscopy study, *J. Surf. Sci.* **600** (2006) 4407, <https://doi.org/10.1016/j.susc.2006.06.042>.
36. Z. Zhang, O. Bondarchuk, B.D. Kay, J.M. White, and Z. Dohnalek, Imaging water dissociation on  $TiO_2$  (110): Evidence for inequivalent geminate OH groups, *J. Phys. Chem. B* **110** (2006) 21840, <https://doi.org/10.1021/jp063619h>.



37. H. Heydari, M.R. Elahifard, R. Behjatmanesh-Ardakania, Role of oxygen vacancy in the adsorption and dissociation of the water molecules on the surfaces of pure and  $N_i$  doped rutile (110): A periodic full-potential DFT study, *J. Surf. Sci.* **679** (2019) 218, <https://doi.org/10.1016/j.susc.2018.09.014>.
38. S. Malali, M. Foroutan, Dissociative behavior of water molecules on defect free and defective rutile  $TiO_2$  (101) surfaces, *J. Appl. Surf. Sci.* **457** (2018) 295, <https://doi.org/10.1016/j.apsusc.2018.06.275>.
39. F. Bouzidi, M. Tadjine, A. Berbri, A. Bouhekka, The impact of temperature and  $H_2O$  flux on the adsorption of water on rutile (110), *Inter Conf.* **95** (2022) 652, <https://doi.org/10.51582/interconf.19-20.01.2022.073>.
40. N. Bundaleski, A.G. Silva, U. Schröder, A.M.C. Moutinho, O. Teodoro, Adsorption dynamics of water on the surface of  $TiO_2$  (110), *J. Phys. Conf. Ser.* **257** (2010) 012008, <https://doi.org/10.1088/1742-6596/257/1/012008>.
41. K. Sebbari *et al.*, Investigation of hydrogen bonds and temperature effects on the water monolayer adsorption on rutile  $TiO_2$  (110) by first-principles molecular dynamics simulations, *J. Surf. Sci.* **605** (2011) 1275, <https://doi.org/10.1016/j.susc.2011.04.015>.
42. M.B. Hugenschmidt, L. Gamble, C.T. Campbell, The interaction of  $H_2O$  with a  $TiO_2$  Surface, *J. Surf. Sci.* **302** (1994) 329, [https://doi.org/10.1016/0039-6028\(94\)90837-0](https://doi.org/10.1016/0039-6028(94)90837-0).
43. M.F. Calegari Andrade, H.Y. Ko, L. Zhang, R. Car, A. Selloni, Free energy of proton transfer at the water- $TiO_2$  interface from Ab initio deep potential molecular dynamics, *J. Chem. Sci.* **9** (2020) 2335, <https://doi.org/10.1039/c9sc05116c>.
44. Z.T. Wang *et al.*, Probing equilibrium of molecular and deprotonated water on  $TiO_2$  (110), *J. Proc. Nat. Acad. Sci.* **114** (2017) 1801, <https://doi.org/10.1073/pnas.1613756114>.
45. G. Fazio, D. Selli, L. Ferraro, G. Seifert, C. Di Valentin, Curved  $TiO_2$  nanoparticles in water: Short (chemical) and long (physical) range interfacial effects. *J. ACS Appl. Mater. Interfaces.* **35** (2018) 29943, <https://doi.org/10.1021/acscami.8b08172>.
46. R. Schaub, N. Lopez, E. Laegsgaard, J.K. Nørskov, F. Besenbacher, Oxygen vacancies as active sites for water dissociation on rutile  $TiO_2$  (110), *J. Phys. Rev. Lett.* **87** (2001) 266104, <https://doi.org/10.1103/PhysRevLett.87.266104>.
47. J.V. Barth, H. Brune, B. Fischer, J. Weckesser, K. Kern, Dynamics of surface migration in the weak corrugation regime, *J. Phys. Rev. Lett.* **84** (2000) 1732, <https://doi.org/10.1103/PhysRevLett.84.1732>.
48. U. Aschauer *et al.*, Influence of subsurface defects on the surface reactivity of  $TiO_2$ : water on anatase (101), *J. Phys. Chem. C* **114** (2010) 1278, <https://doi.org/10.1021/jp910492b>.
49. X. Pan, M.Q. Yang, X. fu, N. Zhang, Y.J. Xu, Defective  $TiO_2$  with oxygen vacancies: Synthesis, properties and photocatalytic applications, *J. Nanoscale* **5** (2013) 3601, <https://doi.org/10.1063/1.4967520>.
50. S. Banerjee, D.D. Dioysiou, S.C. Pillai, Self-cleaning applications of  $TiO_2$  by photo-induced hydrophobicity and photocatalysis, *J. Appl. Catal. B: Environ.* **176** (2015) 396, <https://doi.org/10.1039/c2ee03390a>.
51. Z. Futera, N.J. English, Oscillating electric-field effects on adsorbed-water at rutile- and anatase- $TiO_2$  surfaces, *J. Chem. Phys.* **145** (2016) 204706, <https://doi.org/10.1063/1.4967520>.
52. M. Menetrey, A. Markovits, and C. Minot, Reactivity of a reduced metal oxide surface: hydrogen, water and carbon monoxide adsorption on oxygen defective rutile  $TiO_2$  (110), *J. Surf. Sci.* **524** (2003) 49, [https://doi.org/10.1016/s0039-6028\(02\)02464-0](https://doi.org/10.1016/s0039-6028(02)02464-0).
53. L. Huang, K. Gubbins, L. Li, X. Lu, Water on titanium dioxide surface: A revisit by reactive molecular dynamics simulations, *J. Langmuir.* **30** (2014) 14832, <https://doi.org/10.1021/la5037426>.
54. A.V. Bandura *et al.* Adsorption of water on the  $TiO_2$  rutile (110) surface: a comparison of periodic and embedded cluster calculations, *J. Phys. Chem. B* **108** (2004) 7844, <https://doi.org/10.1021/jp037141i>.
55. L.-Q. Wang *et al.*, Interactions of liquid and vapor water with stoichiometric and defective  $TiO_2$  (100) surfaces, *J. Surf. Sci.* **440** (1999) 60, [https://doi.org/10.1016/S0039-6028\(99\)00677-9](https://doi.org/10.1016/S0039-6028(99)00677-9).
56. P.J.D. Lindan and C. Zhang, Comment on molecular chemisorption as the theoretically preferred pathway for water adsorption on ideal rutile  $TiO_2$  (110). *Phys. Rev. Lett.* **95** (2005) 029601, <https://doi.org/10.1103/PhysRevLett.95.029601>.
57. Z. Dohnálek, I. Lyubintsev, R. Rousseau, Thermally-driven processes on rutile  $TiO_2$  (1 1 0)-(1x 1): A direct view at the atomic scale, *J. Prog. Surf. Sci.* **85** (2010) 161, <https://doi.org/10.1016/j.progsurf.2010.03.001>.
58. K.P. Gopinath, N.V. Madhav, A. Krishnan, R. Malolan, G. Rangarajan, Present application of titanium dioxide for the photocatalytic removal of pollutants from water: A review, *J. Environ. Manag.* **270** (2020) 110906, <https://doi.org/10.1016/j.jenvman.2020.1110906>.
59. L.J.D. Lindan, N.M. Harrison, M.J. Gillan, Mixed dissociative and molecular adsorption of water on the rutile (110) surface, *J. Phys. Rev. Lett.* **80** (1998) 762, <https://doi.org/10.1016/j.susc.2005.06.021>.